Stable Isotope Analysis of Anthropogenic Compounds in Aquatic Systems

Marcin Fiedziukiewicz

A thesis submitted in partial fulfilment of the requirements of Nottingham Trent University for the degree of Doctor of Philosophy

September 2024

Copyright Declaration

To all unborn potentials

Abstract

Isotopic fractionation can be very specific, based on initial isotopic composition, the type of reaction, and ambient conditions. Therefore, stable isotope techniques are frequently applied to environmental studies. However, the compounds of interest in the environment are often in trace concentrations. Any extraction steps following can be lengthy, making routine analysis impractical. Wide screening of compounds has not been explored either.

A focus was made on phthalates as a group of common pollutants with negative health effects not only to the environment but also humans as well. DEHP $\delta^{13}C$ value results ranged between -28.8 ‰ to -27.1 ‰ and measured at 0.14 to 0.22 µg L^{-1} in surface waters. The quantification was done through the combined and simultaneous measurement using GC-C-IRMS. This makes it the first report of a compound specific isotope analysis at trace levels in surface water combined with quantification of that compound.

By examining the ratios of individual datapoints from individual chromatogram channels (44 m/z, 45 m/z, and 46 m/z) allows to verify if there is any interference in the underlying signal. Such practice expands the application scope of compound specific isotope analysis to all heavily

gradient programmes, elevated baselines, and closely eluting peaks which is currently limited to fully separated peaks with stable baseline only. The above approach was applied to the surface water samples and published in an international journal in 2021.

The extent of chromatographic isotope effects was indirectly correlated with the molecule size, something that has not been done before. In addition, a little unknown isotope effect on chromatographic peak width was better defined and quantified. DEP and DBP standards had almost up to 6% difference between isotope peaks widths at different GC programme conditions. Those were linked to the structural differences between heavy and light isotopologue.

Results demonstrated that it is possible to perform a trace quantitative analysis, and measure the $\delta^{13}C$ value of the selected compound simultaneously using only the GC-C-IRMS. Typical approach can include the ratio of the 45 m/z and 44 m/z. The new approach is compensated for oxygen. An integration of chromatogram signals with common slope threshold for peak detection was shown that it might be insufficient due to chromatographic effects introduced. Depending on the approach taken to the integration of the same peak shifted the $\delta^{13}C$ by over 1.2 ‰.

Acknowledgments

This has been a work of many years. In the first instance, I would like to take this opportunity to thank my wife, Susy, who put up with me during this time. All the absent days were not only when I was in the lab or office, but even sat next to you at home, my mind was often somewhere else. You have sacrificed a lot for me to be able to do this.

My thanks go to Dr Quentin Hanley and Dr David Kilgour who advised me and stuck with me throughout. Your unwavering dedication to your students is only to be admired.

I would like to thank Dr Golnaz Shahtahmassebi, and Dr David Boocock who helped me get over the line in these last but important stages.

Last but not least, I would like to thank my family and friends who always believed in me.

Contents Page

Nomenclature

$\delta^{13}C$	– Carbon-13 Isotope Delta Notation
ACN	– Acetonitrile
ACT	– Acetone
BBP	– Benzyl butyl phthalate
CRS	– Certified reference standard
CSIA	– Compound specific isotope analysis
DBP	– Dibutyl phthalate
DEHP	– Diethyl hexyl phthalate
DEP	– Diethyl phthalate
DI	– Deionised water
EI	– Electron ionisation
FDA	– Food and Drug Administration
GC	– Gas chromatography
IAEA	– International Atomic and Energy Agency
ICE	– Isotope chromatographic effect
IRMS	– Isotope ratio mass spectrometer
KIE	– Kinetic isotope effect
MS	– Mass spectrometry
NIE	– Normal isotope effect
NTIA	– Non-targeted isotope analysis
PAE	– Phthalic acid esters
PVC	- Polyvinyl chloride

RIE – Reverse isotope effect

SPE – Solid phase extraction

SSH – Santrock – Studley – Hayes oxygen compensation

VISMOW – Vienna international standardised mean ocean water

VPDB – Vienna Pee Dee Belemnite

WS – Working standard

WWTP – Waste water treatment plant

List of Figures

List of Tables

Publication Arising from this Thesis

M. Fiedziukiewicz, Q. Hanley, Compound specific isotope analysis (CSIA) of phthalates and non-targeted isotope analysis (NTIA) of SPE-extractable organic carbon in dilute aquatic environments, Environmental Advances, 2021, 4, 100050.

Conferences Attended

MERCIA Annual Meeting at Keele University

Keele 19 December 2017

Attended as a poster presenter

Latest Advances in the Analysis of Complex Environmental Matrices at the Royal Society of Chemistry

London 22 February 2019

Attended as a participant

Science and Technology Annual Research (STAR) Conference Nottingham Trent University

Nottingham 16, 17 May 2019

Attended as participant and oral presentation

1. Introduction

Isotope analysis can have a wide range of applications. Isotope led methodologies are widely used in the environmental studies, drug testing and the authentication of different products.

All of these techniques are possible because of the phenomenon of isotope fractionation. Isotopes are atoms with an equal number of protons and electrons but a different number of neutrons. This causes them to have different masses and in turn, this mass difference causes the atoms to behave slightly differently in chemical physical processes. One manifestation of this effect is observed when the proportion of the isotopes start changing during a kinetic based process. This is called kinetic isotopic fractionation.

1.1 Anthropogenic compounds in waste water treatment plants

There are many compounds that, *via* numerous environmental cycles, end up in the environment. Those pollutants are frequently harmful or toxic and cause measurable and negative effects on many organisms.[1] For example, within the pharmaceutical industry, the US Food and Drug Administration (FDA), on average, approved 26 new chemicals a year between 1998 to 2022.[2] This demonstrates growth of the pharmaceutical industry; however, medicines can also affect other animals, not just

humans. Since the 1990s such compounds of anthropogenic origin are referred to as emerging pollutants.[3]

Some of the medicines, once taken, can be excreted unchanged or as metabolites. Through domestic sewage they end up being processed in waste water treatment plants (WWTPs). These plants remove many polluting and potentially hazardous compounds before they are discharged into the environment. Unfortunately, many of the polluting compounds are not removed with 100% efficiency. The typical removal can be anywhere between 70 – 100%.[4–6] There are a number of different factors affecting the efficiency of the extraction and almost all waste water treatment plants still discharge trace amounts of various organic compounds into the environment.[7]

Some of the earliest reports about anthropogenic pollution were first brought to light in the early 1960s.[8,9] For some the compounds responsible for the pollution were commonly referred to as emerging pollutants (EPs). Phthalates, specifically, have been detected and measured in rivers in early 1970's.[10] In 2005, an Italian group determined trace levels of an illicit drug – cocaine – and back calculated it onto average drug use in the area.[11] The result revealed that 4 kg of cocaine were passing through the river Po, every day. This illicit drug, being present in the water, is then absorbed by other organisms living in within the water. This has a range of effects such as tachycardia (increased

heart rate) in fish; affected swimming patterns in *Daphnia magna,* and it also affects the physiological processes in marine muscle *Perna perna*.[12–14]

Over the past few years, the media has put a spotlight on such pollution.[15,16] Many waste water treatment plants overflow and release untreated sewage to rivers and seas and, consequently, excessive pollution can affect industries relying on the aquatic environment or its products.[17,18]

1.2 Application of IRMS in a range of studies

Analysis of isotope ratios is used in many fields such as geology, archaeology, physics, biology, environmental sciences, zoology and chemistry.[19–23] The fractionation of the hydrogen and oxygen isotopes in arctic ice can indicate atmospheric temperature.[24,25] T combination of isotopes in bones can indicate the type of the diet an organism followed.[26,27] The ratio can indicate the origin of compounds or certain processes that they have undergone. In sport there are compounds that can occur naturally but taking them to boost performance is illegal. For example, testosterone occurs naturally in the body but taking it as a steroid might be indicated by the isotope ratio.[28,29] A study of cannabis seized by police was linked to a specific growing plantation in Brazil thanks to unique isotope composition.[30,31]

The work presented in the following chapters will focus on the application of stable isotope measurements in the environment.

The challenge for any environmental study using IRMS is the trace concentrations of the analytes. The instrumentation can require as little as 42 ng carbon equivalent of material.[32] For example, this would require to 85 ng of caffeine to be introduced to the system to be analysed. Concentrations of caffeine in the WWTP effluent can be as little as 30 ng · L^{-1}.[33] Concentrations of other compounds such as illicit drugs can be lower even still, below nanogram per litre concentrations. Therefore, quantities required for accurate and precise results may require in excess of 10 L.[34]

Previous work concerned with isotopes in surface waters studied oxygen isotopes in phosphate to gain insights into the isotopic fractionation of phosphates.[35] The sample size, was reported to be 1 – 10 L to enable sufficient conversion of phosphate to silver phosphate (the final analyte). The study sample size was similar to the expected theoretical sample size.[36] The study suggested that the oxygen present in the phosphate molecule might be undergoing oxygen exchange with surrounding water by an unspecified biological process. Therefore, the selection of the element to study and the matrix can play a vital role in the interpretation of the data.

1.3 Compound specific isotope ratios in the environment

Stable isotopes are widely used to study pathways of compounds through various eco-systems.[37–40]

For the purpose of CSIA, the sample size can be quite large due to the trace concentrations of the analytes in the matrix. Targets of interest may often reside at levels in a range of part per billion or even trillion.[11,41,42] Hence, in a surface water context, a sample can be expected to be in a range of 10 L.[43,44]

Extraction and purification are commonly considered to be the Pre-analysis steps of primary importance.[44–47] The perfect analyte would be separated from the remainder of the matrix by either purification such as solid phase extraction or liquid extraction, solid liquid extraction or by chromatography. That means only a small number of analytes can be targeted at a time. A large sample size can only be used to analyse a few selected compounds. This is very time consuming and therefore not suitable for large scale routine monitoring.

1.4 Isotopes – Theoretical perspective and background

The mass of atoms bound with a bond affect certain properties of this bond and the molecule they form such as bond length and dissociation energy. Bond length is inversely proportional to reduced mass (represented as μ) of the diatomic structure. The mass and bond length

relation is presented as per Equation 1-1

Equation 1-1: Reduced mass

$$\mu = \frac{m_1 m_2}{m_1 + m_2}$$

Here m_1 and m_2 stand for mass of two bonded atoms.[48]

Equation 1-2: Intermolecular distance between two bonded atoms.

$$R = \sqrt{\frac{h}{8\pi^2 c\mu B}}$$

In the Equation 1-2 above *h* represents Planck's constant, c is the speed of light μ is reduced mass obtained from Equation 1-1, and B stands for rotational constant.[49]

Heavier isotopes have a lower zero-point energy increasing the difference between the zero point energy and the dissociation energy as was shown in Figure 1-1.[50–52] Conversely, the lighter isotopes will create longer bonds. The implication of this is well described and studied and gives rise to the phenomena of isotope fractionation and enrichment.

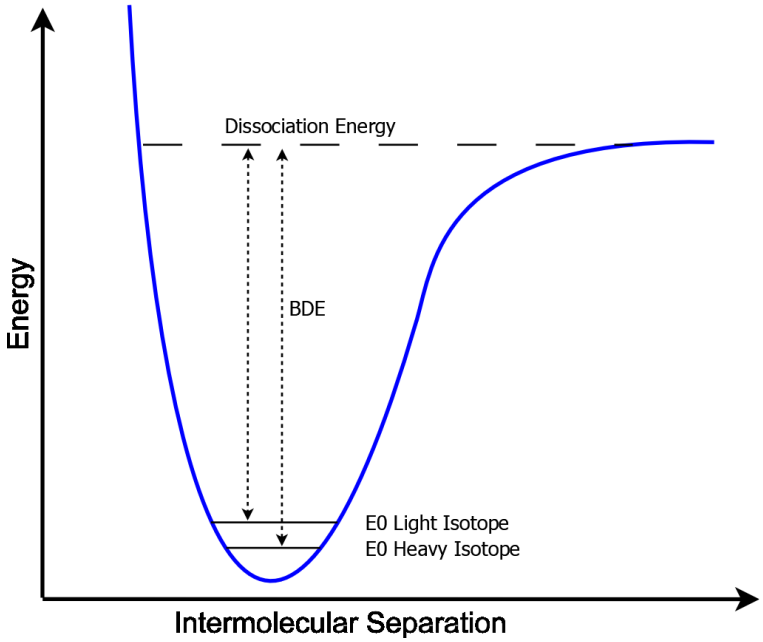

Figure 1-1: The relation between the zero point energy (E0) and dissociation energy in context of isotope. Bond dissociation energy (BDE) is represented by vertical dotted lines.

From the explanation in the previous paragraphs, isotopic effects are greater for smaller atoms and molecules. For example, relative the ratio of molecular mass between deuterium and hydrogen is 1.998 but is 1.083 between ^{13}C and ^{12}C.

Differences in molecular mass between isotopes are usually small, but result in enrichment and depletion of isotopes during a reaction and this is referred to as fractionation[53–57]. A level of separation in the stable isotopic composition between isotopologues can also occur based on their properties and the effect can be referred to as a kinetic isotope effect (KIE).[51,53,56,58–61]

The KIE affects all the types of reactions, such as, but not limited to synthesis, replacement and decomposition. All of these occur in the environment or are carried out anthropogenically by our activities. Depending on the type of the reaction there can be changes in the isotopic composition in the pool of substrates and products. As the reaction progress the proportion of heavy isotopes in the substrates tend to increase. The opposite is true for the products. This is the fractionation result due to the KIE as explained earlier. Chemical reactions and processes can have a very specific and unique rates. This often can result in a specific isotope composition.

1.4.1 Stable isotopes instrumentation and methods

The following sections will present further theoretical details and principles of the isotope analysis, starting with a description of carbon, and oxygen isotopes, a description of isotope ratio mass spectrometers (IRMS), calculation of the isotopic ratio and isotopic scales. The main difference is that in CF-IRMS the analyte is combusted to a gas which is then ionised on the entry into a mass spectrometer. This is in contrast to techniques that ionize molecules directly without a combustion or other thermal conversion step. There are two main ways IRMS utilise the thermal conversion, it is combustion and pyrolysis. Both processes occur with aid of high temperature. The main difference between the processes is in the presence of oxygen in combustion process and pyrolysis does

not involve oxygen in the process. Products of the combustion process are carbon dioxide and water. In comparison products of pyrolysis are carbon monoxide and gaseous hydrogen. Intending to analyse the carbon isotopes make the combustion process more suitable to this purpose and therefore the reference gas used is CO_2.[62]

After the molecules elute from a GC column, they undergo a process of combustion and oxidation in a reaction chamber.[63,64] The chamber itself is either a ceramic or quartz glass tube.[63] Inside the chamber, there are wires made of oxides of copper, platinum and nickel. Combustion is done at the temperatures over 800 °C, under excess of oxygen fed into the chamber from external source.[63,64] Metal oxides present in the chamber can get reduced as result the combustion reactor needs to be flushed with oxygen and re-oxidised.

The isotope analysis presented in the following chapters was done at 1020 °C.[65,66] This was in accordance with the Once combusted, organic sample will be reduced down to C, CO and CO_2. For accurate data all the carbon must be combusted to CO_2. To ensure complete conversion free carbon atoms and CO must undergo an oxidation reaction to CO_2. This is achieved by reducing the copper oxide to copper and CO_2.

The oxidation of carbon and CO for IRMS analysis usually happens by transporting the gases through an oxidation reactor (throughout this

study reactor used was Thermo Scientific part number 1255321).[67]

1.4.1.1 Isotope ratio mass spectrometer

IRMS instruments work on the same principle as ordinary sector mass spectrometers and can be coupled to chromatographic techniques. The initial heterogenous ion beam is split to isotopologues with the same masses as the ions progress through the electromagnetic field. The isotopologues with the same mass are separated into geometrically different beams allowing for them to be measured at different spots by a detector (Figure 1-2).

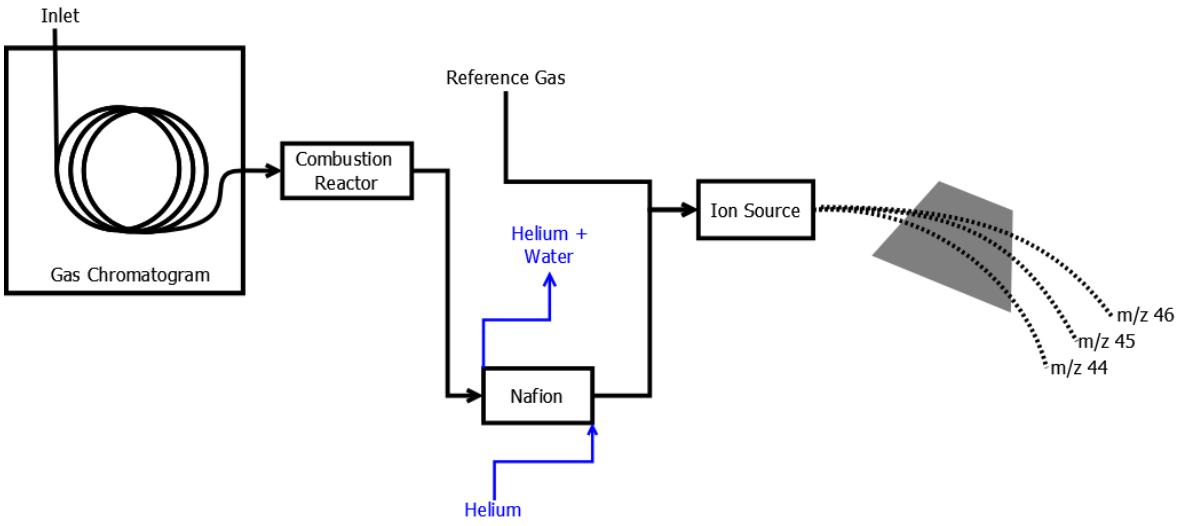

Figure 1-2: A diagram of GC-C-IRMS

The IRMS consists of three main sections: the ion source, the electromagnetic field where the ions are separated, and the detector. Each of these will be further discused in the following sections. This will

give context to the explanantions for certain practices and limitations of the technique.

The IRMS measures the signal of an isotopologue of the corresponding simple gas and not of an analyte. The reason for this is, even with small molecules, it is necessary to eliminate interfering isotopes from the structure like those introduced by nitrogen or hydrogen that may be forming a part of the molecule and yet are not subject of the analysis.

IRMS instruments are typically built with three or five faraday cups. Three cups are used to measure the majority of the isotopes. The remaining two are used for hydrogen and deuterium isotope measurement as, by design it only measures an ion current and is not able to distinguish between the isotopes. Each cup is calibrated to measure an isotope beam. Therefore, the instruments have multiple cups placed in an array.

1.4.1.1.1 Ionization and the ion source

IRMS employs electron impact ionisation also referred to as electron ionisation (EI). Term electron ionisation is preferable, as word impact indicates that the electrons generated in the source make contact with a molecule being ionised. The electron source in EI produces the electrons through thermionic emission.[68] The electrons come from a charged filament labelled with number 3 on Figure 1-3. Heat within the system is generated by the halogen lamps indicated with a number 2 on the Figure

1-3.

The ion source consists of an ionisation chamber and a set of ion lenses. In the chamber, there are parts consisting of a filament and an electron trap. They are set opposite to each other across the ionisation chamber. The filament generates an electric field which has high energy typically of 70 eV. About 0.01-0.03% molecules entering the field become positively charged by losing an electron (in positive ionisation mode). The EI works by transporting a molecule through vaccuum and through a beam of electrons. A beam of elecrons interacts with a molecule and removes an electron from a valence shell of an atom in the molecule. It therefore functions predominantly in the positive mode. This ionisation pattern within the EI is as follows $M + e^- \rightarrow M^+ + 2e^-$.[69–72]

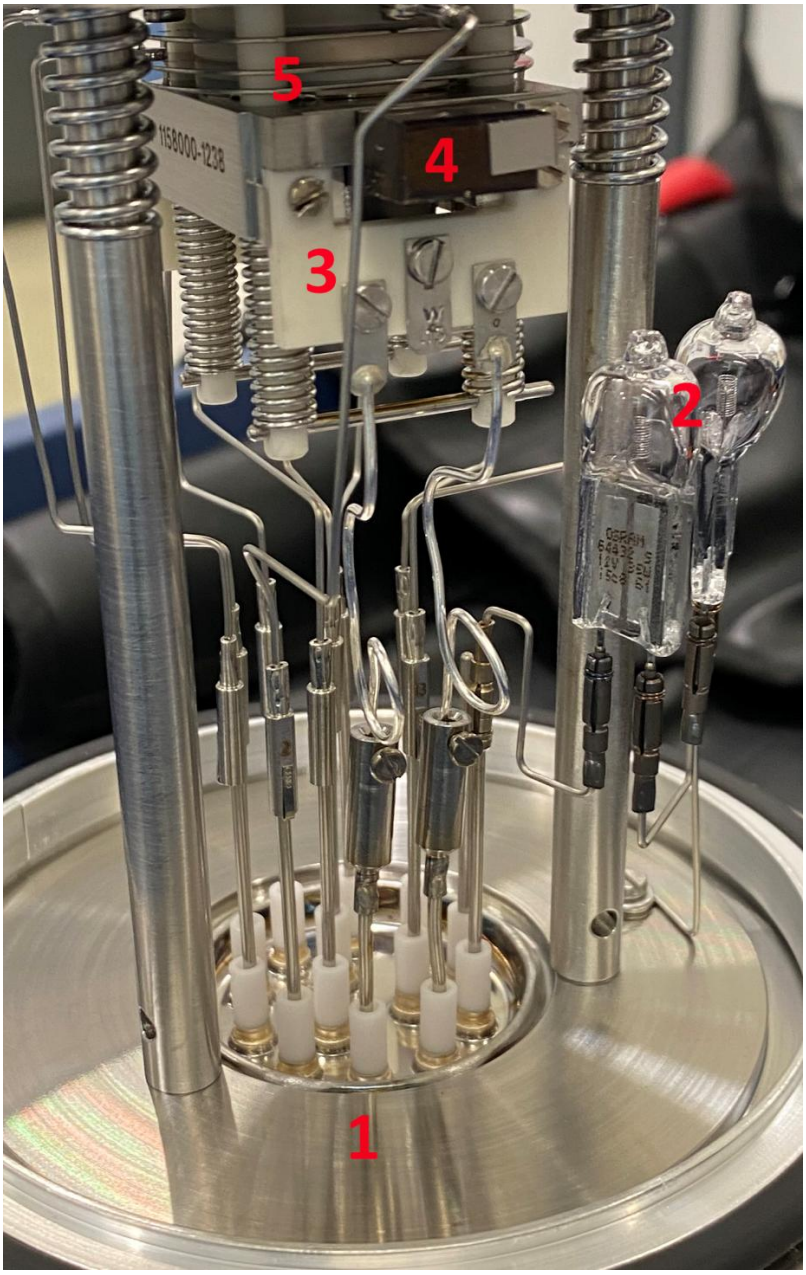

Figure 1-3: The figure shows the electron ionisation ion source used. The elements visible are 1 - power source feed throughs; 2 - two halogen lamps, 3 - a cathode filament plate (the collector is located on the opposite side); 4 - magnet; 5 - extraction plates and ion lenses. (Photo: M. Fiedziukiewicz, photo taken during filament replacment).

An IRMS measures signals created by CO_2 for carbon, CO for oxygen, N_2

for nitrogen and H_2 for hydrogen isotopes.[73,74] The work presented here focuses primarily on isotopes of carbon. Isotopes of oxygen are discussed in the following chapters as an interference to carbon dioxide, which is the gas carbon isotopes are measured as. The ionisation energy is typically 70 eV however some instruments can deliver range of 50 – 150 eV. Either moderate or excessive ionisation energy will result in inefficient ionisation or multiple charged ions respectively. The analysis in this thesis will focus on carbon analysis. The corresponding reference gas is CO_2, and the predominant ions generated through the EI are CO_2^+. The other ions are CO^+, O^+, C^+.[75] Figure 1-3 presents a photographs of the ion source installed in the Delta Advantage V IRMS.

1.4.1.1.2 Flight path and ion separation

Resolution of the analysis is affected by a three main factors: difference in kinetic energy, difference in the point of origin of the ion, difference in trajectories.

"Trap" and focusing lenses provide necessary control over the angular and time dispersion of an ion and improve the resolution.

Once the ion enters into the flight tube, it travels along it in a vacuum. Isotopes are separated by a magnetic field due to their mass to charge ratio (*m/z*). If an ion is travelling in the direction (x) perpendicular to the direction of the magnetic field (y), this ion will be subject to a force

working towards direction (z). As isotopes of the same molecule have different mass the m/z value will also be different. The basic principle of mass spectrometry using electro-magnetic field is described in Equation 1-3.

Equation 1-3: Relationship between mass to charge ratio and radius

$$\frac{m}{z} = \frac{r^2 B^2}{2V_s}$$

The parameters of the equation are represented by *m* representing ion mass, *z* is ion charge, *r* is radius of the flight path, B is magnetic force and V_s is voltage applied to accelerate ions in the ionization chamber

Heavier isotopes, for example, ^{13}C, will have a greater kinetic energy than ^{12}C and the difference in mass affects the flight path. Therefore, when the magnetic force is applied equally on both isotopes, heavier isotope ^{13}C will be less affected than ^{12}C.

Once the molecule is ionised it will be propelled towards the vacuum tube - the flight path. In the IRMS the flight path is situated in the electromagnetic field as opposed to typical charged electric field. IRMS relies on the Lorentz Force Law which can be expressed with Equation 1-4: Lorentz Force Law with non-perpendicular *v* and *B* vectors. Equation 1-4.

Equation 1-4: Lorentz Force Law with non-perpendicular *v* and *B* vectors.

$$F_L = qvB(\sin\alpha) = \frac{M_i v^2}{r_m} = F_c$$

In the equation parameters are represented by the following symbols: *q* is a charge of an ion, *v* is velocity, *B* is magnetic field, *a* is an angle between vectors *v* and *B,* F_c is Centripidal force, M_i is ion mass, and finally r_m is radious of the ion motion

After rearranging the above formula it can be presented in the following form:

Equation 1-5: Rearranged Lorentz Force Law

$$r_m = \frac{M_i}{q} \times \frac{v}{B \times (\sin\alpha)}$$

From the Equation 1-4 rearranged to above Equation 1-5 it can be deduced that the radius of the path is dependant on the mass to charge ratio.[72,76,77] The mass to charge ratio is equal to three parameters the radius of the ion path, magnetic field and voltage applied to accelerate the ions. Both magnetic field and acceleration voltage are constant through out the analysis. Threfore the change in mass to charge ratio will be proportional to the radius of the ion path.

1.4.1.1.3 Detection

Once isotopes are separated, they are collected by Faraday cups. IRMS instruments use Faraday cups because of their accuracy.[78,79] Within the IRMS typically three Faraday Cups are placed in an array to detect electromagnetically separated signals. Additional cups can be present depending on the purpose of the analysis.

When an ion makes contact with a faraday cup, its charge causes a small electric current to flow through the detector. Faraday cups are positioned on the flight path of a selected isotope, a simplified diagram can be seen in the Figure 1-4.

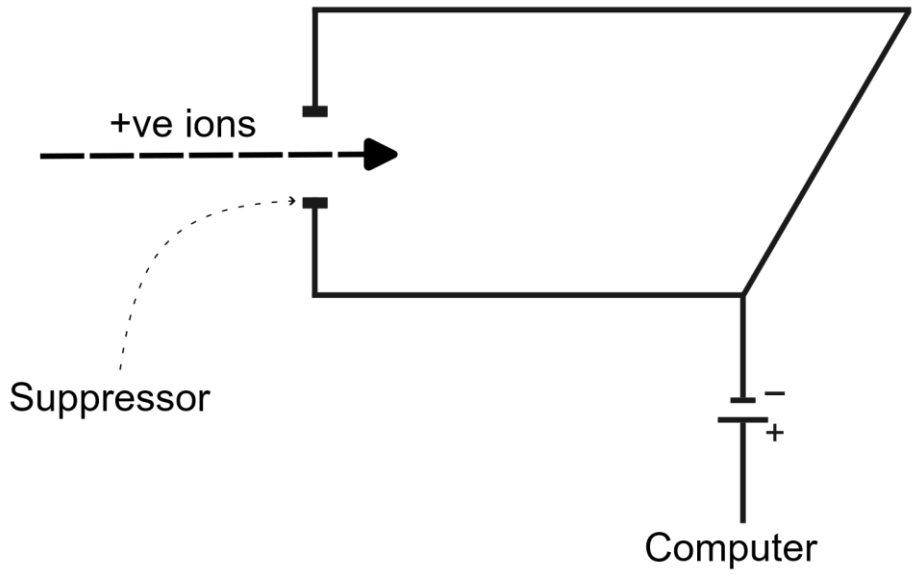

Figure 1-4: Faraday cup diagram

Each cup is connected to a resistor matching its magnitude with the

natural abundance of the isotope. For example, the cups positioned to measure the CO_2 gas isotopologues (*m/z* 44, m/z 45, and m/z 46) are followed by a resistor 300 MΩ, 30 GΩ and 100 GΩ, respectively. The electrical current is then amplified and converted to frequency using voltage to frequency converter (VFC). The frequency is counted and passed to a digital signal processor and then recorded on a computer.[80]

1.4.1.1.4 Oxygen compensation

For the purpose of carbon isotope analysis, the IRMS measures combusted compounds in the form of CO_2. It is important to note that the IRMS does not measure R $^{13}C/^{12}C$; it measures R $^{45}CO_2/^{44}CO_2$. The latter is affected by the oxygen isotopes and the exact mass of those is presented in Table 1-1. Some carbon and oxygen isotope combinations will form isotopologues of the same mass to charge ratio, interfere with carbon measurements and introduce inaccuracies on the analysis.

Table 1-1: Isotopologues of CO_2 with ^{12}C, ^{13}C, ^{16}O, ^{17}O, and ^{18}O.

CO_2 Isotopologues	**Mass (Da)**
$^{12}C^{16}O^{16}O$	43.989830
$^{12}C^{17}O^{16}O$	44.994047
$^{12}C^{17}O^{17}O$	45.998264
$^{12}C^{18}O^{16}O$	45.994075
$^{12}C^{18}O^{17}O$	46.998292

$^{12}C^{18}O^{18}O$	47.998320
$^{13}C^{16}O^{16}O$	44.993185
$^{13}C^{17}O^{16}O$	45.997402
$^{13}C^{17}O^{17}O$	47.001619
$^{13}C^{18}O^{16}O$	46.997430
$^{13}C^{18}O^{17}O$	48.001647
$^{13}C^{18}O^{18}O$	49.001675

To improve the accuracy of the results there are two main ways of compensation for oxygen Santrock – Studley – Hayes, and Craig.

1.4.1.1.4.1 Santrock – Studley – Hayes (SSH)

One way to convert R $^{45}CO_2/^{44}CO_2$ to R $^{13}C/^{12}C$ is through (SSH) calculation.[81] It is one of the two models used in oxygen compensation in IsoDat v3.0 and it was used in this work.

The SSH model to solve the correction calculation was presented in an IUPAC Technical Report.[82] The calculation is an iterative procedure and is still an approximation, however, with multiple cycles of calculations to generate a R $^{13}C/^{12}C$ the value becomes stable and surpasses the accuracy of the instrument measurement. The calculation with four cycles can result with the ratio with no change down to 59 decimal places in comparison with the previous cycle. The formula uses two constants λ and K. There are a few references that dispute the exact value of these

quantities.[81–83] The calculations used in IsoDat are λ = 0.516 and K = 0.0099235 based on comparison with manual manually calculated values. When values were identical to 7 decimal places when compared between the manual calculation and from IsoDat. This is the maximum precision reported by the IsoDat.

This method was used for data processing presented in this thesis unless otherwise stated. Appendix A includes an R script that was used to manually calculate ratios of $^{13}C/^{12}C$ during this project. It can be adapted and used to calculate the R $^{13}C/^{12}C$ from a large data set.

1.4.1.1.4.2 Craig

The second method used is to estimate the compensation for ^{17}O.[84] The estimation can be calculated by the following equation. This method is only an estimate and therefore is not widely used during data processing.

Equation 1-6: Craig's estimation for oxygen compensation

$$\delta^{13}C \approx 1.0676 * 45\delta - 0.0338 * \delta^{18}O$$

Further discussion and a critique of both approaches may be found in the literature.[82,84]

1.4.1.1.4.3 Others

Since the development of the two main methods presented in previous sections, literature does not report any other numerical methods that are routinely used with data analysis.[85]

1.4.1.1.5 Calibration

The signal intensities are arbitrarily calibrated. Therefore, each chromatogram can have two typical strategies to deal with it.

First, each chromatogram can have a series of gas reference pulses that are compared to a standard and then the same gas is injected to the mass spectrometer during the sample analysis. Once the values are calculated they will be on the reference gas scale, for example CO_2 for carbon analysis. To express them on an international scales reference standard must be used to create a conversion plot with $\delta_{\text{Reference Gas}}$ and $\delta_{\text{International Scale}}$ on each of the axis.

An alternative strategy is to use an internal standard. This approach allows direct comparisons between the standard and the sample.

In addition to the above strategies, the analysis sometimes considers only one standard.[86] This can be done, however, if possible multiple standards should be used such as standard bracketing approach. Single standard calibration makes an assumption that the correlation will happen in a

perfectly linear fashion. This limits the results in a way that if the correlation is not perfect the error can be magnified the greater the difference between the analytes and standards.

There are certain good practices that can be followed to improve the accuracy of the isotope results. The ideal approach towards the calibration would involve three or more standards with delta values spanning a wide range (enough to cover the expected values during the analysis), the CRSs and laboratory working standards (LWS) would be identical to the analyte in their molecular structure.

Using multiple standards will enable correction of the slope and accuracy. One standard can introduce error when converting onto an international scale. Two standards correct for the slope inaccuracy however the precision error still remains. For these reasons three or more standards is recommended.[86]

Using standards which span the range of δ values expected in the set of samples. Interpolation is preferred; however, such standards may not always be available therefore extrapolation is accepted.

The ideal approach is identical treatment of standards and analytes. Whenever available the standards should be the same compound as the analyte. This way, the combustion process will be the same.[82] However,

it is worth pointing out that currently all the standards are expressed on a scale anchored to a single compound like VPDB, VSMOW2, or SLAP. Transition from the scale has to be made to the remaining compounds. Standards or LWS are used with every analysis to correct for any instrument internal calibrations.

1.4.2 Isotope calculation process

During measurement of reference gas isotope ratios there are isotopologue combinations present in the gas. In such a case the ratio calculated would be of the combined effect like in CO_2. To correct for such effect, it is necessary to perform a mathematical procedure. Isotope data processing can consist of several stages.

First stage, is to obtain the signal peak areas and calculate the ratio between the heavy and the light isotope.

Next, the signal ratio needs to compensated for the oxygen in the measured CO_2.[87] This can be achieved by applying the Santrock – Studley - Hayes (SSH) or Craig compensation method.[81,84] The SSH approach is the more accurate of the two as the Craig method is an estimation as it includes assumptions based on the natural oxygen distribution and should not be applied for high accuracy measurements.[36,81,84] Calculations in RStudio using both approaches are presented in the Appendix A for future use. Thirdly, once the ratio is compensated for oxygen, it can be calculated as a $\delta^{13}C_{Zero}$. This is an arbitrary value specific to the analysis entity and the instrument.

For the above reason the $\delta^{13}C_{Zero}$ value needs to be expressed on the VPDB scale using certified standards. This is achieved *via* a simple XY calibration graph.

Software as provided with the installation of the IRMS does not analyse the individual data points from a chromatogram and it is not routinely done. Most contemporary analysis involves taking the data from the commercially available software which uses a ratio of a peak area obtained from chromatogram integration.

1.4.3 The δ Scale

For historical and ease of reporting the IRMS results are expressed on a δ scale - Equation 1-8.[86,88,89]

Equation 1-7: Stable isotope ratio definition.

$$^{13}R = \frac{^{13}C}{^{12}C}$$

Equation 1-8: Delta notation of the carbon isotope ratio.

$$\delta^{13}C = \left(\frac{^{13}R_{\,Sample}}{^{13}R_{\,Standard}} - 1\right) * 1000$$

The ^{13}C and ^{12}C are respective signals of the isotopic counterparts. The ratio of those signals is also interchangeably abbreviated to a ratio following Equation 1-7.

The delta notation as presented in Equation 1-8 is relative to an international standard. The initial values are a ratio of signals between $^{13}CO_2$ and $^{12}CO_2$. Therefore, a raw ratio scale could be applied, however, due to the small changes between values a relative scale is more practical and convenient.[90]

The standards have to be traceable to an agreed international standard to be compatible. Historically the scales have been updated and the scales are not equivalent, making the comparison of historical data difficult.[91]

1.4.4 The isotope scales and primary standards

Currently, standards are maintained by IAEA (Table 1-2).

Table 1-2: Scales and reference standard for isotope analysis of most common elements.

Element	Calibration Scale	Ratio	Gas
Carbon	Vienna Pee-Dee Belemnite (VPDB)	0.011180 [82]	CO_2
Hydrogen	Vienna Standard Mean Ocean Water (VSMOW)	0.00015576 [90]	H_2
Oxygen	Vienna Standard Mean Ocean Water (VSMOW)	0.0020052 [92]	CO
Nitrogen	Air	0.0036765 [93]	N_2

Well defined secondary standards are also available with certificates of analysis provided with the material. Work presented here is

predominantly focused on the carbon isotope. Therefore, all the results will be expressed in relation to VPDB. The oxygen isotopes are also of interest since carbon is measured against CO_2. The instrument is not able to distinguish between $^{13}C^{16}O^{16}O$ and $^{12}C^{17}O^{16}O$ since the molecular mass is almost identical: 44.9932 u and 44.9940 u respectively.[94]

The standards above are of limited supply. The most practical way is to select a material easily available and measure it against a set of certified reference standards (CRS). This selected material is referred to as working standard (WS). WS are used with every analysis therefore it is critical there will be a sufficient amount to last for practical amount of time. The WS isotope ratio is measured alongside every unknown sample. The WS can be used as an internal standard and mixed with the analyte. This way the analyte can be measured against the WS directly. An alternative way is to inject the WS and the analyte separately within a short period of time. The common practice is to use reference gas pulses providing a link between analytes and standards. Those are injected in every chromatogram. This requires the gas to be uninterrupted and the environmental conditions to stay as constant as possible. Once the data is collected the laboratory working standards and the analytes are initially expressed relative to the reference pulse which is collected during the injection. A reference pulse is pure CO_2 gas injected directly into the mass spectrometer. Since it is the same molecule as an analyte after combustion, it enables the unknown sample to be referenced to the VPDB

scale. The sample is measured against the reference pulse the same as the WS. The WS has a known δ ^{13}C value as was measured against certified or primary reference standards - CRS. CRS standards are provided with a δ $^{13}C_{VPDB}$ values assigned to them. Having a known δ $^{13}C_{VPDB}$ value and a δ $^{13}C_{Zero}$ value (measured during the analysis against the reference pulse), these can be plotted against each other on a calibration graph with the two data sets on corresponding axis. Form the graph the zero scale can be converted onto the VPDB scale.

1.4.5 Isotope chromatographic effect

As much as different isotopes can affect the reaction rates they can also have an effect on interactions between the analyte and stationary phase in chromatography. This is known as the isotope chromatographic effect (ICE) and it is most pronounced in isotopically substituted analytes.[95–99] Some of the earliest mentions of the ICE date back to late 1950's.[97]

In the study of Wilzbach and Riesz, deuterated and tritiated counterparts had reduced retention times compared with the non-substituted counterparts, referred to as reverse isotope effect. It is also one of the first reports of ICE on the chromatographic peak width. However, the only detail provided was that peak width due to radioactive isotope can be twice as much of the non radioactive counterpart. The chromatographic effects are often referred to as "S" shape. This refers to a shape formed across a peak when looking at ratio between the heavy and light signal

ratio as shown in Figure 1-5.

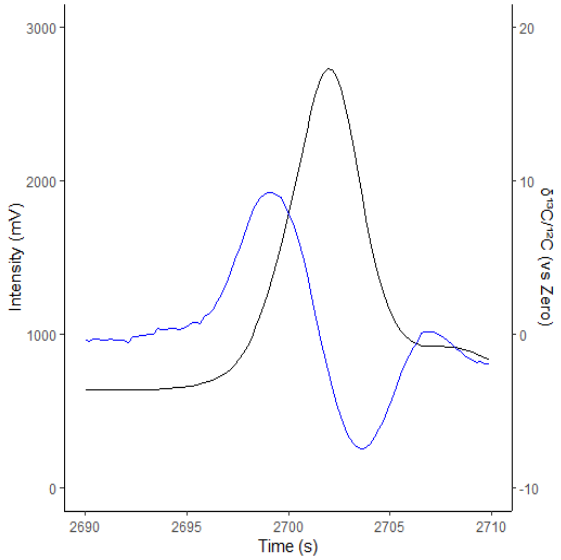

Figure 1-5: Chromatogram of DEHP peak (black) and ratio chromatogram compensated for oxygen using SSH calculation (blue).

Isotope effects were observed in and a much more recent study, which also presented a link between the polarity of the chromatographic column and the type of isotopic effect.[100] Some compounds were presented on the same GC chromatographic columns, and other combinations can be paired by the compound on different columns. Compounds on different polarity stationary phase do not always have to exhibit the same isotope chromatographic effect. This study presented a number compounds with either no deuterium or some atoms being substituted with this heavy isotope. The observed trend was that the less polar the stationary column the reverse isotope effect is more frequent. This trend reverses with decreased polarity number. It also demonstrated that the isotope effect can be switched for the same compound depending on the type of column

being used and presents a link between the chemical interaction and isotope effect.

Another aspect that affects the isotope effect relate to the shape of the molecule. This is demonstrated trough a substitution of isotopes in the sp^2 and sp^3 positions there are retention differences based on such substitution. The difference between the minimum and maximum geometrical cross section of the sp^2 orbital is greater than the sp^3. This means that the peak broadening of the sp^2 substituted isotopologue should be greater than the sp^3.[101]

The articles published by Thakur and Aslani are probably the biggest contribution to understanding the isotope effects to date however they do not discuss the peak width. To date, no discussion appears to be present according to literature review that comprehensively explains the cause of the ICE or any further detail about peak widths due to different isotopologues. Majority of data is done through the substituted compounds.[97,100–104]

1.5 Project rationale and hypothesis

The majority of studies have concentrated on quantifying and identifying compounds mainly found in rivers.[105–107] However, interest has spread to other, larger ecosystems, like lakes [108], seas and oceans.[109,110]

Some studies have started looking for the origin of contaminants in aquatic systems using stable isotope analysis.[111–113] Kim studied stable carbon isotope signatures of compounds and compared the results of samples obtained from different marine environments.[111] The reported result was that PAHs analysed in an urban lake had a unique isotopic composition. A different study analysed phosphates found in rivers and reported differences in $\delta^{18}O$ values obtained for PO_4^{3-} measured in water from two WWTPs, although they were not able to determine the origin of the phosphates analysed.[112] Inorganic nitrogen was studied in a river and it was reported that the main sources of nitrogen pollution were agriculture and domestic waste from residential release.[113]

To the best of knowledge, there are not many attempts to combine these two areas, or tried to trace the origin and understand the future of the organic pollutants in rivers by measuring the ratio of stable isotopes. Little is known about the isotopic composition of the trace compounds from rivers lakes and oceans.

Typical sample amounts required for an IRMS analysis need to be > 10 nMol.[36] Therefore, 3.9 µg of DEHP would be required for analysis *via* GC-C-IRMS. DEHP is not expected to be found in concentrations greater than 1.3 µg · L^{-1} in the discharge of the WWTP.[114] Considering the extent of dilution of the WWTP effluent when it enters the river the biggest technical challenge will be to extract sufficient sample size to determine the stable isotope ratio of a target. Papakosta conducted a study determining the isotopic composition of extracted lipids from samples < 100 mg.[115] This study determined the isotope ratio of samples at relatively high concentrations of 0.1 µg · L^{-1} per compound. Obtaining this kind of concentration from a water sample will be one of the biggest challenges for this project. The reported concentrations of DEHP in WWTP effluent can range from 0.3 to 8.2 µg · L^{-1}.[116–118] This translates onto approximate range of 0.5 – 13.0 L of WWTP effluent required.

Isotopes of the same element have different masses. This mass effects the zero-point energy of the bond with heavier isotopes forming a bond with a lower zero-point energy.[119] The difference between the zero-point and dissociation energies is the amount of energy required to break the bond (see Figure 1-1). Therefore, the heavier isotopes form fractionally more stable bonds. Therefore, due to the BDE value being slightly greater for bonds with heavier isotope they react and decompose at a slower rate. As a result, the final product of an incomplete reaction or one reaching its equilibrium will result in a different ratio of heavier to lighter isotopes.

Kinetic isotope effect favours the lighter isotope due to its lower BDE, however thermodynamic effect is dependant if the analyte is a substrate of a reaction or a product, skewing the equilibrium towards the heavier isotope. Overall, this process is known as isotopic fractionation and relative isotopic compositions are often expressed as a δ value in ‰.[120] Fractionation is of compounds is omnipotent in the environment and occurs in plants depending on the way that they fic CO_2 during photosynthesis and local environmental conditions. This results in a carbon isotopic composition that differs between plants from different areas and by virtue of their photosynthetic pathways.[30,53] A hypothesis tested will be if there is any observable fractionation or difference in compounds at trace level. Knowing the $\delta^{13}C$ value compounds extracted from a river may give an indication of their origins and testing this hypothesis will contribute towards this knowledge.

IRMS instruments have low sensitivity when compared to other mass spectrometry techniques, especially ones that utilize a type of signal multiplier. However, isotopic information related to environmental pollutants can provide invaluable data about their origin. Trace concentrations of target compounds often prove to be difficult and laborious to extract. Challenge that will be undertaken is to extract analytes from aqueous sample at low concentrations that material still be analysed by IRMS. The complexity of environmental samples carry a large amount of information, most of which is related to unknown compounds.

The following section will explore additional information that can be extracted from IRMS chromatograms.

Isotopes have some known effects on chromatography. Most notable are differences in transfer through a chromatographic column between individual isotopes of an analyte. Considering the complexities of the chromatographic interactions those differences should be measurable. The key metrics of a peak are peak height, retention time and peak width, amongst others. Those are expected to affect the accuracy of δ values and therefore will be further explored under context of non-targeted isotope analysis (NTIA).

2 Experimental

2.1 Materials

The materials which follow are as described in Fiedziukiewicz *et al.*[120]. The general-purpose filter paper grade 601 was purchased from CamLab. Di-ethylhexyl phthalate (DEHP) (Tokyo Chemical Industries; GC grade), benzyl butyl phthalate (BBP) (Sigma; 98%), dibutyl phthalate (DBP) (Sigma; 99%) and diethyl phthalate (DEP) (Sigma; 99.5%) and hexane (Arcos; Extra Pure 95+%) were used as received to prepare samples, standards and secondary reference materials. Two certified standards were used, caffeine (IAEA600) and glucose (BCR-657) to calibrate everyday working standards of the phthalates on the VPDB scale.[121]

2.2 Standards

Two certified standards were selected and used to create working standards. Those were caffeine (IAEA-600) and glucose (IRMM-BCR 657). For laboratory working standards compounds selected were phthalates used to make the mixed reference were: diethyl phthalate, dibutyl phthalate, benzylbutyl phthalate, di-(2-ethylhexyl) phthalate.

2.2.1 Preparation of standards - Considerations

The analysis of the caffeine LWS was carried out using EA–IRMS. This is in contrast to usual analysis using GC–IRMS. The reason for the choice of

elemental analyser was the solid form of primary standards. EA was a better choice to compare non-volatile compounds with the selected standards. For this reason, the preparation is unique as opposed to the rest of the analysis presented in this thesis. Below steps describe the preventative actions taken to ensure minimum contamination, accurate and precise results.

2.2.1.1 Area and equipment

Aluminium foil ~5 × 5 cm was placed onto balance pan, a sheet of aluminium foil was placed on the bench next and around the balance. The sheet of foil should be big enough to make a comfortable working space (this will be working area to prevent unintentional contamination from any deposits and residues left on the bench surface). This was to prevent any potential contamination of the outside of the weighing boat. Tweezers were cleaned with methanol and air dried before every analysis. From this point on the tweezers were only keep within the work space.

2.2.1.2 Blank Preparation

For analysis, two of empty capsules were prepared using tweezers by flattening and folding a capsule onto itself. Those were the blank measurements.

2.2.1.3 Sample

Approximately 0.1 mg sample or standard was weighed into tin capsule.

The capsule was closed in the same manner as the blank and all the sample and standard capsules were placed into sample tray and analysed. The EA-IRMS details are present in the suggested order of analysis that was used during this study: blank, laboratory working standard, international certified standard.

2.2.2 Laboratory working standards

The use of primary standards may not always be feasible. For the purpose of this study a caffeine reagent was prepared and stored for routine analysis and comparison to any further standards. The preparation of the LWS material is described in detail in the following sections. Phthalates that were used to make the mixed reference solution were also analysed using EA-IRMS for the isotopic ratio of the individual phthalates.

2.2.3 Laboratory working standard preparation process

A solid bulk standard was mixed with a clean metal spatula. A small approximately 1 mL vial was filled with 0.10 g of the standard. Melted sealing wax was used to seal the lit and the material. Label the standard with standard details. Ensure the details on the label will be traceable to the analysis and individual weights. This can be achieved by recording the batch being prepared, this will provide the isotopic values. It is also encouraged to keep the record of the specific bottle. This number in conjunction with the batch number will allow to access both specific weights dispensed and the isotope value. Once sealed the randomly

selected bottles and the stock material were analysed and compared to each other to verify that the process did not introduce any contamination nor fractionation of the material.

2.3 Sampling and sampling sites

Sampling methodology is reproduced here from Fiedziukiewicz *et al.* Samples were collected in 2.5 L amber borosilicate glass bottles, using a stainless steel bucket for sampling. The bottles were cleaned with methanol then deionized water prior to sample collection. Effluent samples were collected from the drain from the Stoke Bardolph Sewage Treatment Works (What3Words reference: conducted.reference.thigh; GPS: 52°58’24”N , 001°02’15”W), as it enters the River Trent. The river water samples were collected from the river banks. The sample from the River Trent was collected 750 m downstream from the WWTP drain on the same side (What3Words reference: croaking.traffic.comments; GPS: 52°58’48”N , 001°02’18”W). The sample from the River Foss was collected on the east side of the Palmer Street footbridge 1050 m from where it enters River Ouse (What3Words reference: engine.local.dose; GPS: 53°57’30”N , 001°04’24”W).[121] Locations are presented in Figure 2-1.

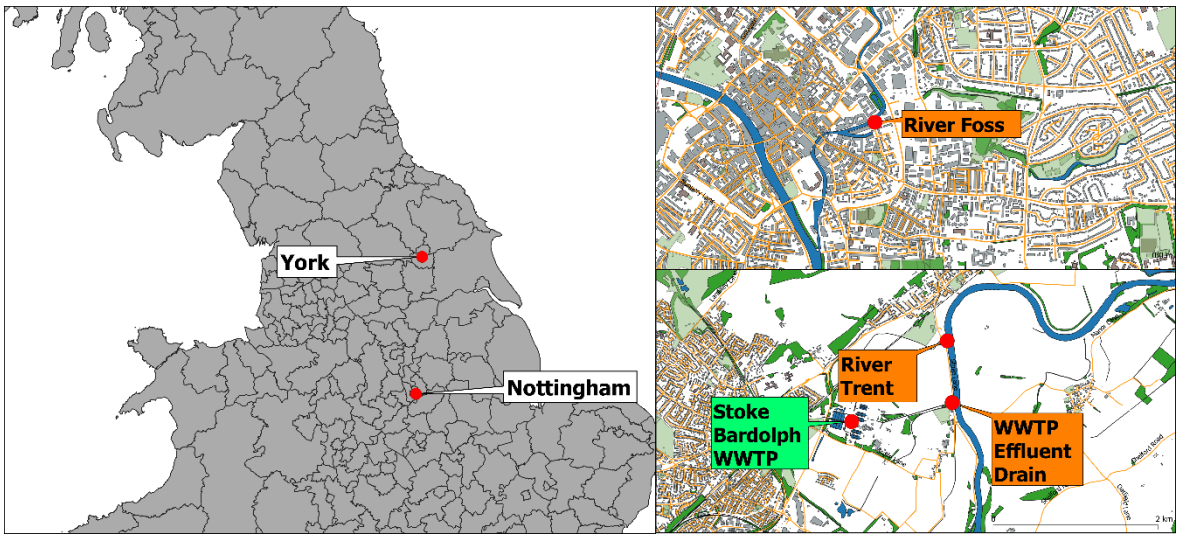

Figure 2-1: Location of the sampling sites in Nottingham and York.

SPE extraction was completed within 6 hours on the day of collection. Both rivers were at high flow (River Foss 4.5 $m^3 \cdot s^{-1}$ and River Trent 203 $m^3 \cdot s^{-1}$) at the time of collection. The average flows of the Rivers Foss and Trent are 1 $m^3 \cdot s^{-1}$ and 90 $m^3 \cdot s^{-1}$, respectively [122]. Flows reported were based on the Huntington (station reference F2470) and North Muskham (station reference 4022) measuring stations (2020).[121]

2 L samples were extracted using a set of eight 6 mL Oasis MCX SPE cartridges (Waters, UK) containing 500 mg of sorbent. The cartridge was first conditioned with 6 mL of MeOH and deionized (DI) water then 250 mL of sample was extracted with a flow rate of 3-5 mL $\cdot$ min^{-1}. Following extraction, the cartridges were rinsed with DI water and eluted with 6 mL of pure MeOH. The aliquots were combined and dried on a hot plate set to < 75 °C under a nitrogen stream. Once dry, the samples were

transferred to GC vials using hexane and dried again. The choice of hexane is discussed later in the chapter. The samples were then resuspended in 5 µL of hexane for analysis. The vials were wrapped in Al foil during any storage to prevent sample degradation through the UV radiation.[121,123]

2.4 Sample preparation and analysis

The samples were collected into 1 L borosillicate glass bottles directly from the wastewater treatment water treatment plant effluent discharge. Sample extraction was done as soon as possible with Water Oasis MCX SPE cartridge (item number 186000776). The cartrige works in mixed mode cation exchange and has three main groups attracting cataions, polar compounds and reverse phase attracting hydrophobic compounds. The limitation of this approach was that it excludes acidic compounds.

The functional group cartridge was selected based on reported use to analyse similar sample.[124] The cartridge was first conditioned with 6 ml of MeOH and deionized (DI) water. Next, no more than 1 L of sample was loaded onto a single 6 cm^3 cartridge with 500 mg sorbent. The flow was kept at an average of 5-6 mL · min^{-1}. The sample was then washed with DI water. The water was discarded and sample was extracted from the cartridge with pure MeOH, then with 2 % ammonia solution in MeOH. Further, multiple aliqiots were combined together. The collected extract was dried on a hot plate set to no more than 70 °C.[121]

2.5 GC-C-IRMS

The conditions below were reproduced from the from paper by Fiedziukiewicz *et al* for completeness as per section publication arising from this thesis.

The analysis was performed using an Agilent GC 7890 coupled to a Thermo Delta V Advantage isotope ratio mass spectrometer. GC parameters were: injector port: 280 °C; oven: 50 °C; ramp: 3 °C/min to 300 °C and hold time of 8 min; column stationary phase (5%-phenyl)-methylpolysiloxane (Agilent DB-5); column length: 30 m; internal diameter 0.25 mm; film thickness 0.25 μm. The GC-C-IRMS combustion reactor was preconditioned at 1000 °C for 1 h before the analysis.[121]

IRMS combustion reactor was preconditioned at 1000 °C for 1 h before the analysis.

2.6 SSH Correction

Where stated the data were manually corrected for oxygen using SSH oxygen compensation calculation. Calculations were performed using RStudio and R programming. Calculations were adapted from papers by Santrock, Studley, Hayes (1985) and Brand, Assonov, Coplen, (2010).

Value for ^{18}R is an iterative process and to calculate it starts by an approximation of this value with Equation 2-1. Then the iteration follows

the Equation 2-2, Equation 2-3, and Equation 2-4.

Equation 2-1: SSH calculation first step

$$^{18}R = \frac{^{46}R}{2}$$

Here ^{18}R represents ratio of ^{18}O and ^{16}O. ^{46}R represents ratio of *m/z* 46 and *m/z 44.*

Equation 2-2: Calculation of first intermediate to ^{18}R represented by ^{18}fR.

$$^{18}fR = \left(-3K^2 * {}^{18}R^{2\lambda}\right) + \left(2K * {}^{45}R * {}^{18}R^{\lambda}\right) + (2{}^{18}R - {}^{46}R)$$

^{18}fR is a first intermediate value, K is a constant equal to 0.0099235, λ is also constant equal to 0.516. ^{45}R represents ratio of *m/z* 45 and *m/z 44.*

Equation 2-3: Calculation of second intermediate to ^{18}R represented by ^{18}ffR.

$$^{18}ffR = \left(-6K^2 * \lambda * {}^{18}R^{2\lambda-1}\right) + \left(2K * {}^{45}R * \lambda * {}^{18}R^{\lambda-1}\right) + 2$$

Equation 2-4: Final fourth step of ^{18}R iteration.

$$^{18}R = {}^{18}R - \frac{^{18}fR}{^{18}ffR}$$

This iteration is performed four times and once complete the process if

finished by following Equation 2-4 again and then Equation 2-5, and Equation 2-6 below.

Equation 2-5: Calculation of ratio ^{17}O / ^{16}O .

$$^{17}R = K * {}^{18}R^{\lambda}$$

^{17}R represents ratio of ^{17}O and ^{16}O.

Equation 2-6: Final expression of ^{13}C ratio.

$$^{13}R = {}^{45}R - 2K{}^{18}R^{\lambda}$$

Here ^{13}R represents ratio of caron ^{13}C and ^{12}C.

A result from Equation 2-6 is ^{13}C / ^{12}C ratio excluding impact from oxygen isotopes present in CO_2 molecule. This process was applied to individual data points across chromatogram signals resulting in individual values that are oxygen corrected. The entire process is presented in Appendix A for RStudio.

3 Screen experiment of an aqueous matrix

I

3.1 Introduction

The first stage of the project was to select compounds of interest. The approach used during this work was to collect multiple samples and from a selection of different places.

The initial goal of the project was to measure the isotope value of an analyte in the complex sample. The purpose of this measurement was to find a link between a potential contaminant and its source.

3.2 Experiment rationale

The purpose of this first experiment is to identify compounds that repeatedly occur in a number of different WWTP effluents. It is to be expected to find a greater number and higher concentration of compounds in the effluent samples compared to the river water samples

---

[I] The information and the some of the content of this chapter has been adapted from published peer reviewed article "Compound specific isotope analysis (CSIA) of phthalates and non-targeted isotope analysis (NTIA) of SPE-extractable organic carbon in dilute aquatic environments". All the work presented here was performed by me with supervision and guidance from Dr Quentin Hanley.

from the where the effluent discharges into the river. This initial experiment was designed to match mass spectra obtained using gas chromatography – mass spectrometry to the NIST database. GC-MS was the prefered method of analysis due to the same chromatographic technique used by the isotope ratio mass spectrometer, which is planned to be used in future studies. Analytical methods were selected and followed so that they could also be used for stable isotope ratio analysis using GC–C-IRMS. The aim of this experiment was to establish a list of copounds that could be the target coumpounds for IRMS analysis.

3.3 Methodology

Methods presented below were described and/or adapted in a paper published as outcome of this work in later chapters. [121]

3.4 GC-MS

The analysis was performed using an Agilent GC 7890 coupled to a single quadrupole mass spectrometer. GC parameters were: injector port: 250 °C; oven: 50 °C; ramp: 10 °C · min^{-1} to 300 °C and hold time of 10 min; column stationary phase (5%-Phenyl)-methylpolysiloxane (Agilent DB-5); column length: 30 m; internal diameter 0.250 mm; film thickness 0.25 µm.

3.5 Results and discussion

A screening experiment using GC-MS was performed on six samples

collected from three different sites (four from Nottingham, one from York and one from Retford). The water samples were collected across a period of time from 09 Dec 2016 to 17 Jul 2017. The samples were collected from waste water treatment plants and directly from rivers. As the main aim of the study was to measure selected compounds in a river the approach adopted was a collection of the single point in time for the entire study. The approach was the best balance of the timing and practicality. The timing and extraction of the samples was prioritised to avoid any decomposition and / or fractionation.

As the samples were analysed by GC-MS there were total there were 1082 compounds that were matched to NIST v2.0 database across all samples. The factor used to find those matches was minimum match factor of 80. According to the AMDIS software manual this is a good match to use for identification.[125] The list of compounds (as presented in an appendix C) was compiled based on sampling from different location the ranking was organised based on the frequency the compounds occurred. There are five compounds that were found in all samples; eight compounds were found in five samples and 13 of the compounds were found in four samples. The list of the most frequent compounds can be found in Table 3-1. None of those compounds were detected in corresponding blank samples which were extracted and run at the same time.

Table 3-1: List of selected compounds previously identified by GC-MS and NIST database in all analysed samples with their structure, CAS number and brief information on use and origin.

Name	CAS No.	Structure	Origin
Bis(2-ethylhexyl) ester 1,3-benzenedicarboxylic acid	137-89-3	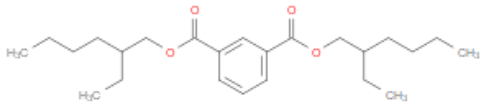	This compound is a plasticiser. It is used in food containers [126,127]
2-Propanol, 1-chloro-, phosphate (3:1)	13674-84-5	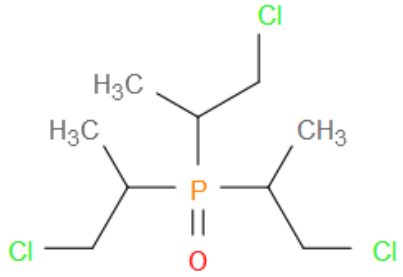	This compound and derivatives are used as common flame retardants [128]

N-ethyl-2-methyl-benzenesulfonamide	1077-56-1	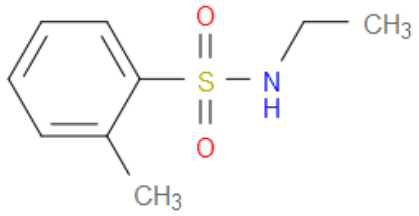	Compound is used as fungicide, plasticizer, and in pharmaceutical production processes [129](Richter et al., 2008)
2,6,10-Dodecatrien-1-ol, 3,7,11-trimethyl-, (E,E)-(Farnesol)	106-28-5	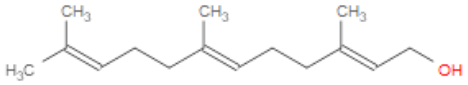	Farnesol presents antibacterial and animicrobial properties [130]. For that it is used in perfumery and wide range of dermatological products [131].

7,9-Di-tert-butyl-1-oxaspiro(4,5)deca-6,9-diene-2,8-dione	82304-66-3	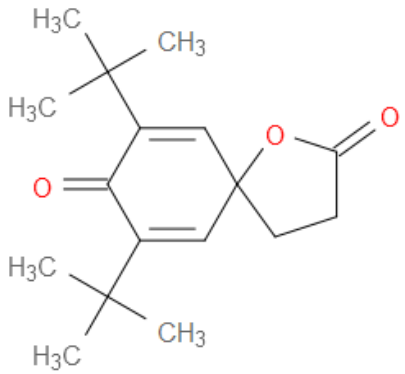	Compound is detected in sheep fat. It is reported to be a product of 2,6-di-t-butylphenol oxidation [132]. The compound also has been found in landfill leachates [133].

Compounds of most interest were those that frequently appear in effluent and river water based on the screen study. A list of all the compounds was created with a number of how many samples those were detected in. The most frequent compounds were listed and presented in Table 3-1. Out of the compounds in the table above the one that was selected for future study was the phthalate ester. Some phthalates are known endocrine disruptors, and others are commonly used as plasticisers. Those two factors make phthalates of potential interest. In addition, phthalates have been measured at higher concentrations than the other compounds from the list.[42,118,134–137]

Some of the more frequent compounds encountered were phthalates, an ethyl hexyl and di-ethyl hexyl esters of phthalic acid– plasticisers. Other frequently observed compounds were short chain fatty acids, sterols and carotenoids.

One of the most commonly identified is 1,2-benzenedicarboxylic acid, mono(2-ethylhexyl) ester or mono(2-ethylhexyl) phthalate (see Figure 3-1). This is a hydrolysis product of the common plasticiser – di-(2-ethylhexyl) phthalate (DEHP) – which in acidic conditions can be a product of hydrolysis. Phthalates are present as additives in many types of plastics within the household and they do not bond with those plastics

allowing them to wash out and find their way to waste water treatment plants (WWTP).[138] If the cleaning process of a WWTP is not fully efficient, compounds such this will be present in effluent discharged into rivers.

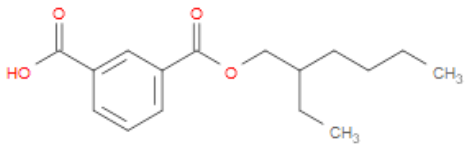

Figure 3-1: 1,2-Benzenedicarboxylic acid, mono(2-ethylhexyl) ester – CAS: 4376-20-9

As an example of the range of compounds found in WWTP, carbamazepine, is a common medication prescribed for conditions such as epilepsy, bipolar, schizophrenia and neuropathic pain.[139] This drug was matched in 4 out of 6 samples tested.

Phenoxyethanol is widely used in cosmetics and is deemed safe at concentrations of less than 1%, however, some concerns about its safety have been raised.[140] Some harmful effects include eye irritation and skin dermatitis.[141]

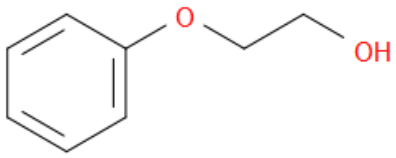

Figure 3-2: Phenoxyethanol – CAS: 122-99-6

Another common compound found in the water samples was squalene (see Figure 3-3). It was identified against the database in all 7 samples. Squalene is a C_{30} hydrocarbon, it is an oily viscous liquid that is immiscible in water. Squalene can have different origins, it is naturally occurring in humans, fish, variety of oils (olive, wheat and rice) and yeast.[142–144] Squalene must be handled with care as it is present in human sweat and makes it very easy to cross contaminate samples. From the point of isotopic ratio this diversity combined with complex reactions that occurred by the point of sampling, makes this compound of potential interest to further project. However, it is outside of the scope of the current work, presented here. A full list of compounds matched with NIST database is attached as Appendix D: Compound screen list.

Figure 3-3: Squalene – CAS: 111-02-4

3.6 Conclusion

Results obtained gave a good insight into the possible list of compounds that can be expected in effluent samples from various WWTPs. Any compounds found in the corresponding blanks were excluded from the list of compounds found in the sample. This was done to avoid listing compounds that were introduced through glassware or equipment. Due to the number of possibilities, it was impractical to be able to verify the identity of all of them and focus was emphasised on the selected few compounds that were verified with standards. The list of the compounds was compiled based on the possible matches with NIST database. Compounds of interest were selected from the list of possible matches based on their frequency and to confirm the identification they were matched with standards.

Diethylhexyl phthalate was selected to be the main subject of the study together with DEP, DBP, and BBP. This compound has a number of biological and environmental effects, this is discussed in the following chapter. It also has pronounced peak and it is of anthropogenic origin.

The next steps to this experiment will be to quantify some of the frequently reoccurring compounds and measure the isotope values of a compound at trace level present in the complex matrix.

4 Phthalates in aquatic systems following compound specific isotope analysis (CSIA) [II]

4.1 Introduction

Anthropogenic polluting compounds in rivers have been widely studied for some time. Examples include drugs, medicines, healthcare products and others.[121,145–148] Phthalic acid esters (PAEs) are common plasticizers and a proportion of those, in their life cycle, find their way into WWTP effluent and rivers *via* a range of sources. Those sources include human excretion after ingestion of food exposed to PAE present in the plastic packaging, cosmetics, and other typically domestic sources.[121,149–151] PAEs are more easily detected in WWTP effluent as opposed to river water due to their presence in higher concentrations.[121,152] Most domestic waste will end up in a WWTP as sludge that is treated and, subsequently,

[II] The information and the content of this chapter has been published in a peer reviewed article "Compound specific isotope analysis (CSIA) of phthalates and non-targeted isotope analysis (NTIA) of SPE-extractable organic carbon in dilute aquatic environments". Fragments of this paper have been used or adapted in this chapter. All the work presented here was performed by the author with supervision and guidance from Dr Quentin Hanley.

discharged into rivers as effluent with any remaining compounds mixing with a wide range of natural and man-made materials.[121]

4.1.1 Phthalates

Based on the considerations in Chapter 3, phthalates were selected to demonstrate CSIA applications in dilute aquatic systems. Phthalates are a group of mostly synthetic compounds used as additives mainly in the manufacture of poly vinyl chloride (PVC) plastics which are used in nearly every aspect of everyday life.

Phthalates are esters of phthalic acid with a generic structure presented in Figure 4-1. Addition of phthalates to plastics makes the material more flexible and elastic and has been used for this purpose since about 1920.[153] The degree of flexibility and elasticity depends on the amount of the phthalate added, hence its wide use in the industry. Currently it is widely considered that the phthalates are mainly synthetic. However, some studies are emerging, reporting biosynthesis of these compounds by certain type of algae and fungi.[154–157]

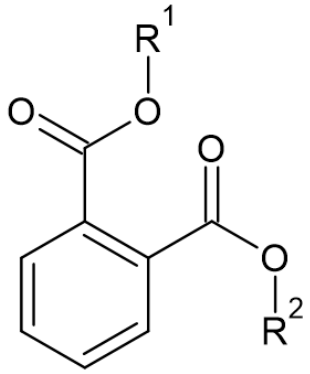

Figure 4-1: Di-ester of phthalic acid. R_1, R_2 are generic organic groups containing ester forming oxygen.

4.1.1.1 Health effects of phthalates

Once mixed with a polymer, phthalates do not chemically bind with the matrix and are free to leach out of plastic.[158] If used in food containers this allows those phthalates to transfer into organisms and then further into environment. Transfer of phthalates to environment and other organisms have wide negative effects since phthalates are thought to be endocrine disruptors, cardiotoxic and a cause of obesity amongst other health effects.[159–161] In children, they are reported to be associated with obesity, ADHD, autism spectrum disorder, neurodevelopment, asthma, and allergies.[162–166] Similar effects are also observed in broader animal kingdom.[167,168] All those negative effects in a wide range of environments stress the importance of studding, controlling and minimising the exposure of phthalates.

4.1.1.2 Restrictions on the use of phthalates

DBP and DEHP are allowed to be used in plastics at concentrations not more than 0.05 % and 0.1 %, but up to 20% of plastics that are in contact with food, might contain plasticisers at concentrations greater than the allowed limit.[169,170] According to the US FDA, dibutyl phthalate (DBP) and dimethyl phthalate (DMP) are used rarely and only DEP is still used in cosmetics manufacture.[171] The European Union restricts the use of certain phthalates such as DEHP, DBP, as well as benzyl butyl phthalate (BBP) in children's toys and other childcare products where concentrations less than 0.1 % are permitted.[172] Some phthalates such as DEHP are banned in cosmetic products by the EU.[173] In the UK, the MHRA recognises and is encouraging all the manufacturers of plastics used in medical items to replace DEHP with alternatives. However, it was decided that no additional measures are required to regulate the use of DEHP.[174]

4.1.1.3 Phthalate exposure

Studies have even presented data showing that phthalates can be detected and quantified in the atmosphere, [175–177] surface waters and soils [178,179]. Phthalates found in domestic households find their way into waste. The compounds are then transported to a WWTP where waste is cleaned. Studies compared the efficiencies of waste water treatment plants.[114,179–181] Any WWTP using more than one technology to purify the influent will increase the purification efficiency from ~65% to ~95

%.[135,182] Once purified, effluent is discharged into rivers, however, effluent is rarely free of pollutants. Once discharged, DEHP levels of about 0.5 μg · L^{-1} can be found in fresh water, as shown by a study conducted in Netherlands.[182]

Babu reported that certain phthalates might be biosynthesised by bacteria.[183] They extracted selected strains of bacteria and observed an increase in concentration of phthalates in bacterial medium. *Spirogyra* sp. gave the highest concentration of MEHP. DEHP was not quantified in this study, however, it was noted that DEHP was detected in all the cultures tested but that it then degraded to MEHP. For comparison of selected phthalates (DMP, DBP, DEHP, and BBP) levels in WWTP effluent were 0–5.95 μg · L^{-1}, 0–0.68 μg · L^{-1}, 0–188 μg · L^{-1}, and 0–0.32 μg · L^{-1}.[179,184]

4.1.1.4 Phthalate decomposition and their metabolites

Majority of di-ester phthalates are metabolized to their mono-ester analogues.[185] and are typically excreted in urine as, for example, mono 2-ethyl-5-hydroxyhexyl phthalate, mono 2-ethyl-5-oxohexyl phthalate, mono-2-ethyl-5-carboxypentyl phthalate, mono-[2-(carboxy-methyl)hexyl] phthalate.[186–189] Phthalates (DMP, DEP, DBP, BBP, DNOP, DPP, DEHP) decompose, to variable degrees yielding benzoic acid, by biodegradation mediated by *Bacillus mojavensis*.[190] *B. mojavensis* was

detected in the WWTP effluent(?).[191,192].

In WWTPs, phthalates have been shown to undergo ~60% decomposition during activated sludge processing.[193] A similar study comparing the efficiency of DEHP removal in two treatment plants [164] revealed that the oxidation pond (OP) process was less effective at purifying the sludge influent than the activated sludge and aeration (ASA) system. The OP WWTP removed 43.3% of phthalate esters while the ASA plant removed 54%. Results also show that DEHP removal on average was 17% and 33% in OP and ASA, respectively.[136]

Decomposition of DEHP in WWTP sludge at 35 °C treated as a first order reaction gave rate constant, k, in a range of 0.03 – 0.07 d^{-1}.[194,195] This study was based on an anaerobic continuous flow stirred tank reactor model, operated at 5 to 20 °C.

4.1.1.5 Phthalate sources in the environment

A study has described the effects of pH and heat on the leaching of DBP from food containers.[196,197] They showed that the leaching of DBP depends on the pH of the food material. Both acidic and alkaline samples leached more phthalate than the neutral pH. This could be due to increased polarity of the solvents however no in depth discussion was provided.

4.1.1.6 Phthalate isotopic fractionation

Lab-based studies have investigated fractionation of phthalates. For example, isotopic fractionation of hydrogen and carbon isotopes in phthalates was observed when decomposed by persulfate oxidation and demonstrates hydroxyl radical.[198] This study demonstrates that isotopic information could distinguish which process are involved in the decomposition of the selected phthalates (dimethyl phthalate, diethyl phthalate and dibutyl phthalate).

For example, it has been shown that the longer the ester chain in a given phthalate, the smaller the carbon fractionation.[60] When decomposed by a single strain bacteria in laboratory controlled conditions. This information indicates that the size of the molecule may have difference in fractionation rate under the same bacterial conditions. Similarly, the size of a molecule can affect the chromatography and separation.

Photolytic decomposition under UV increases the heavy carbon isotope in DMP, DBP and DOP. The smaller the molecule the greater the fractionation.[123] Phthalates in this research were only studied at a laboratory scale of the degradation model using a selection of phthalate esters: di-methyl phthalate, di-ethyl phthalate, and di-butyl phthalate.[199,200] Isotope values reported range was from $\delta^{13}C$ -29 ‰ to

$\delta^{13}C$ -26 ‰. This is comparable to the results presented later in this chapter.

The technical challenge was to extract sufficient sample size to measure isotope ratios. Previous work has determined the isotope ratio of extracted lipids from samples < 100 mg.[115] This study claims to have measured isotope ratio of samples at concentrations of 0.1 mg · mL^{-1} of an individual compound, an unrealistically high concentration for water pollution studies. Obtaining this kind of concentration from a water sample will be one of the biggest challenges of this project. A second big challenge that is expected during this project is to obtain a good chromatographic separation of very complex samples, as well as minimizing the base line noise.

Although several laboratory studies have considered the isotopic composition of phthalates, none have been conducted in dilute aquatic systems and WWTP effluent.

4.1.2 Compound specific isotope analysis [III]

Compound specific isotope analysis (CSIA) in either WWTP effluent or

[III] This section has been reproduced from the article by Fiedziukiewicz *et al.* as per section Publication Arising from this Thesis.

river samples has not been done previously. Such information can help and identify the origin of the pollution if the processes are sufficiently understood. This will not be possible without first being able to measure the isotope compounds in aquatic systems. Furthermore, the understanding of the real life and scale purification might provide a tool to measure the efficiency of the WWTP based on the level of fractionation.

Most studies focus on either spiked samples or lab scale study. Analysis of samples directly from the environment can allow for monitoring of the selected compounds but also for potential links with the sources. However, the field CSIA is commonly used in forensic and environmental studies but it also has applications in sport, geochemistry, food and extraterrestrial chemistry.[199,201–203] It incorporates a separation step followed by combustion, to produce CO, CO_2, N_2, or H_2 prior to measuring the isotope ratios.[121,204] This allows for multiple compounds to be separated and analysed at once making the analysis more efficient. Such aspect very important in routine or larger scale analysis of complex matrices.

The major advantage of CSIA over elemental analysis (EA) IRMS is the application of chromatography to separate complex samples. CSIA was successfully applied to a selection of compounds in the range of 138 - 1389 ng · L^{-1} using 10 - 12 litres of groundwater.[34] It is also used for

laboratory scale studies of isotope behaviour.[199,205,206] CSIA offers the possibility of assessing source and fractionation of anthropogenic material released into the environment.[207,208] Isotopic fractionation of carbon in the environment is affected by, but not limited to, factors such as humidity, temperature, atmospheric pressure and chemical reactions.[31,198,209] Over the past decade, a number of studies have been published presenting model results of the analysis of emerging pollutants in spiked environmental samples using CSIA finding an inverse relationship between the size of the molecule and the level of isotopic fractionation.[121,205,210,211] These combined factors have made it possible to determine the origins of samples.[30,31,63,212]

A linear correlation has also been shown between two GC detectors – the GC-FID and GC-IRMS.[213] This supports the idea to use the GC-IRMS to measure the quantity of analyte in an unknow sample.

4.2 Results and discussion

4.2.1 Measurement of laboratory working standards

Once the working standard was prepared as described in the previous sections, samples were taken from the pool individual aliquots for analysis. Three individual samples were selected at random and tested in triplicate. The aim is to determine the uniformity of the references across the prepared batch and within the individual vial. Delta values in

comparison to the reference peak only are presented within the Table 4-1 below.

Table 4-1: Individual results of the working standards of caffeine expressed on a zero scale (reference pulse ratio is set as zero).

	$\delta^{13}C_{zero}$ value	Average	Average Total
Vial 3	−7.64	−7.77 ± 0.12 n = 3	−7.86 ± 0.13 n = 9
	−7.77		
	−7.88		
Vial 40	−7.79	−7.88 ± 0.13 n = 3	
	−7.82		
	−8.02		
Vial 84	−7.91	−7.94 ± 0.12 n = 3	
	−8.07		
	−7.83		

Above results show that reproducible results can be obtained from the individual reference vial and that randomly selected vials are comparable to each other.

4.2.2 Matrix solvent

Solvents can have a large effect on the sensitivity of the mass spectrometer.[214] The type of ionisation The intention of measuring compounds at very low concentrations required method optimisation. The selection of solvent was done by comparison of three selected solvents:

acetone, methanol, and hexane. The concern was to make sure that during the preparation the analytes would not react with the matrix.

Six solutions of DEHP were prepared at two concentrations and in three solvents each. Each of the solutions was injected 11 times. The runs and injections were expected to be lengthy due to the complexity of the sample. From the previous chapter a environmental sample can include upwards of 300 compounds. Separating every individual compound was unfeasible. Therefore, purpose was to examine chromatographic changes across as long a period as possible. The concern was around degradation of the standards and potential isotope fractionation. The sequence was arranged so that the injections were evenly spread out across 90 hours. There were 11 time points with approximately 8 h intervals. Such an arrangement allows for an evaluation of the solution stability over the given period. This is important consideration especially if a reference solution is used for a prolonged period of time.

Table 4-2: Descriptive statistics of the solvent effect at nominal concentration of 100 µg · L^{-1} (n = 11) The values compare the Peak Area (PA), and the $\delta^{13}C_{Zero}$.

Matrix	Average PA (Vs)	SD PA (Vs)	RSD PA (%)	Average $\delta^{13}C_{Zero}$	SD $\delta^{13}C_{Zero}$
Acetone	3.247	0.393	12.095	3.80‰	0.50‰

Hexane	4.301	0.395	9.179	3.70‰	0.42‰
Methanol	0.095	0.031	32.726	2.51‰	5.42‰

Data presented in the Table 4-2 show the average, standard deviation and relative standard deviation of the peak areas. However, delta values only have average and standard deviation. This is because delta values are expressed as relative ratio of a standard and are not absolute. Similar values of the analyte and the standard can result in very high values of % RSD, even if the variability is within the instrument specification.

Based on the data in the Table 4-2, hexane had the highest peak area, the lowest RSD, and the smallest SD for the $\delta^{13}C_{Zero}$. Hexane was selected as an optimal solvent and used for the remainder of this work.

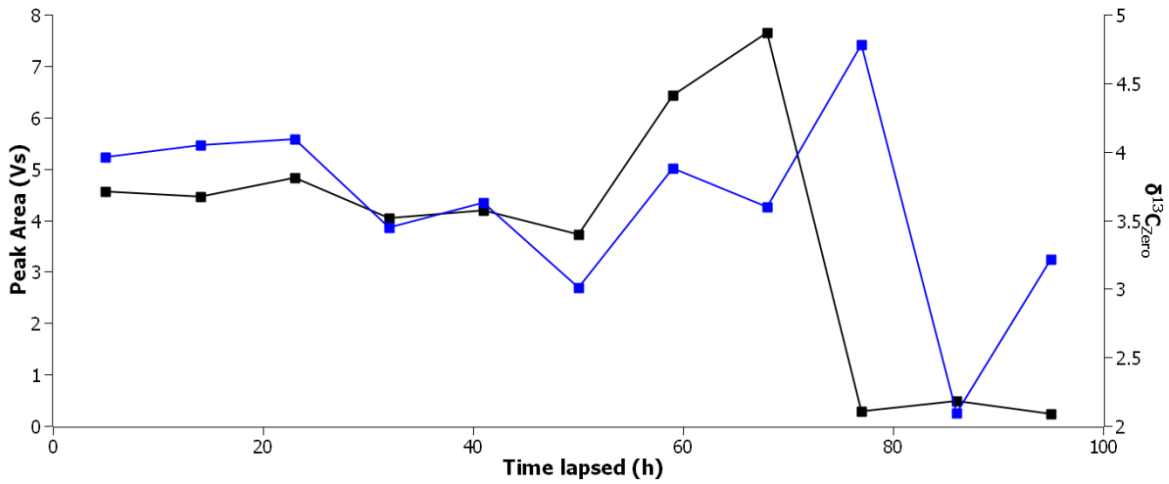

Figure 4-2: Comparison of DEHP in hexane peak area and $\delta^{13}C_{Zero}$ being reinjected over time (black – peak area; blue - $\delta^{13}C_{Zero}$).

From the data presented in the Figure 4-2 it can be concluded that the length of the sequence can be about one day. The peak area does not deviate from the mean by more than 9.2 %. Within the same time frame the delta values standard deviation was ± 0.4 ‰.

4.2.3 Water sample GC-IRMS analysis

Due to the volumes of the preparation process a new extraction is required with every analysis. The presence of di-(2-ethylhexyl) phthalate was confirmed in samples by matching the retention time with a reference run at the same time. For an example of a IRMS chromatogram see Figure 4-3.

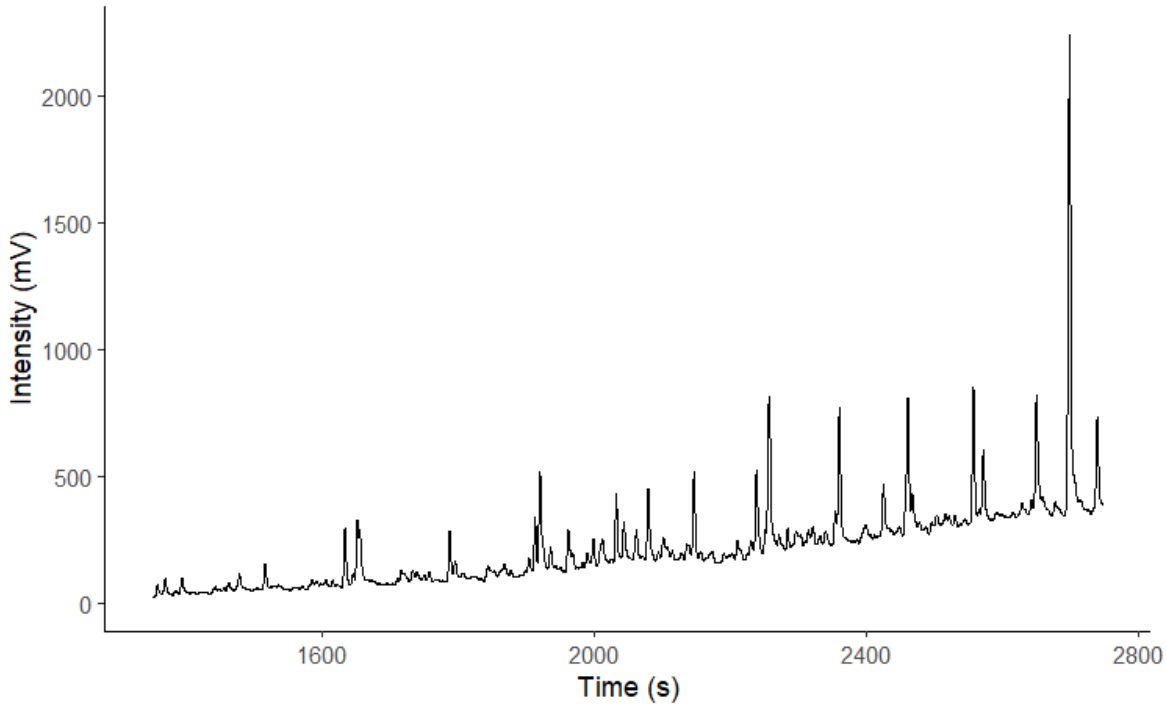

Figure 4-3: A partial gas chromatogram (*m/z* 44) obtained from Nottingham waste water treatment plant effluent.

Phthalate samples were analysed using solid phase extraction sampling techniques.

4.2.4 Compound specific isotope analysis – phthalates from a WWTP [IV]

To evaluate the relationship between signal level and δ ^{13}C values in phthalates, a range of concentrations from 5–100 μg · mL^{-1}. Standards were run at the same time as the isotope analysis. With 1 μL injections this is equivalent to 5–100 ng of compound being introduced into the system. GC-C-IRMS is reported to require 10–100 ng of an analyte for reproducible results [199]. The SD for $\delta^{13}C$ values was ± 0.4‰ across the full range including the lowest standard concentration (5 μg · mL^{-1}). Standard deviation values (n=5), at separate concentrations, ranged between ±0.1‰ and ±0.2‰ for a set of 30 μg · mL^{-1}. The average δ ^{13}C value at each concentration ranged from −26.6‰ to −26.4‰. No significant trends were observed in either the mean values or precision

[IV] Below section has been reproduced from the article by Fiedziukiewicz *et al.* as per section Publication Arising from this Thesis.

throughout the range of concentrations. The minimum concentration considered was 5 μg · mL^{-1} which corresponds to 0.013 μg · mL^{-1} in a field sample when following the extraction procedure. For reference for the 5 μg · mL^{-1} DEHP sample, a signal of 479 arbitrary raw intensity units for *m/z* 44 was obtained.

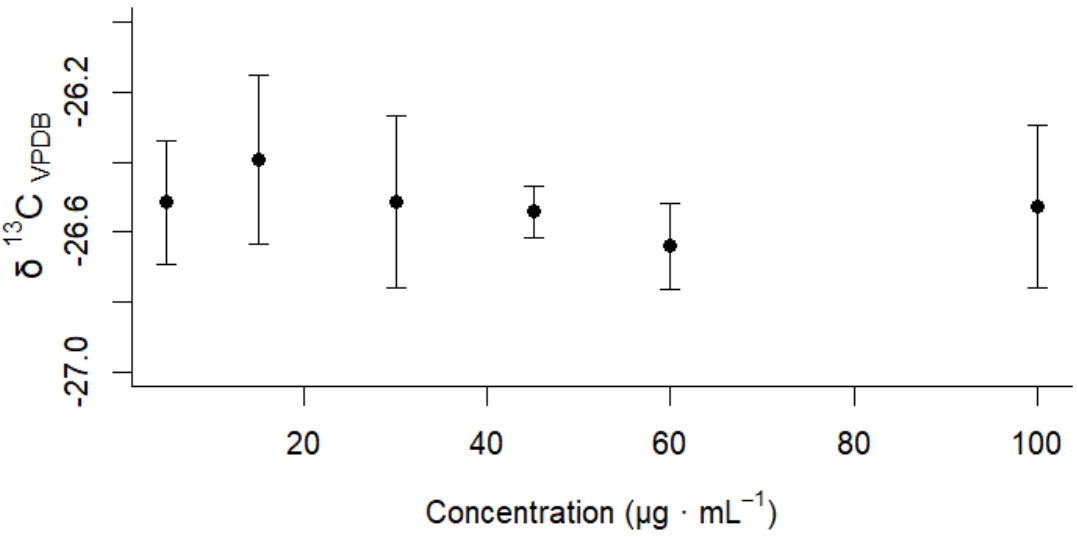

Figure 4-4: DEHP δ ^{13}C values across a range of concentrations with standard error represented by error bars.

Phthalate esters: DEHP, BBP, DBP and DEP, were detected and characterised in waters from WWTP effluent discharge and the two rivers. Figure 4-4 presents the stability of DEHP δ ^{13}C values across a selected range of concentrations. To date phthalates have been studied in model

experiments and spiked samples.[60,200,205,215] To the best of the author's knowledge, this is the first report of CSIA conducted on these compounds extracted directly from real environmental samples. Figure 4-3 depicts a representative GC-C-IRMS chromatogram with a mixed standard superimposed. The presence of the phthalates was confirmed by GC-MS. DEHP was found in all samples analysed. This is consistent with this ester being the most widely produced plasticiser in the world, previous published reports and data presented in

4.2.5 Quantitative compound specific isotope analysis

A range of concentration standards were run at the same time as the isotope analysis. The range of concentration evaluated was 5–100 μg · mL^{-1}. With sample injection size of 1 μL, this range is equivalent to 5–100ng of being introduced into the system. GC-C-IRMS is reported to require 10–100 ng of an analyte for reproducible results.[199] The SD for $\delta^{13}C$ values was ± 0.4‰ across the full range, and the same value for standard at lowest concentration – 5 μg · mL^{-1}. No trending change of accuracy or precision was observed throughout the range of concentrations. The slope value was calculated to be -0.0011. SD values at separate concentrations ranged between ± 0.2 ‰ for set of 45 μg · mL^{-1} standards and ± 0.5‰ for set of 30 μg · mL^{-1} (n = 5). The average $\delta^{13}C$ value at each concentration ranged from −26.6 ‰ to −26.4 ‰ (see below).[121]

4.3 Quantification calibration curve

Different concentrations at which standard solutions were made: 0.5 mg · L^{-1}; 10 mg · L^{-1}; 100 mg · L^{-1}; and 1000 mg · L^{-1} by series of dilution steps. Each solution was injected onto the system five times. Figure 4-5 presents data obtained.

4.3.1 GC-C-IRMS *vs* GC-MS: A comparison of the two techniques in relation of their suitability to quantify the sample amounts

To assess the suitability of the GC-C-IRMS system for quantification purposes and to evaluate $\delta^{13}C$ values at a set of different concentrations. Solutions spanning four orders of magnitude were measured using GC-C-IRMS and GC-MS.

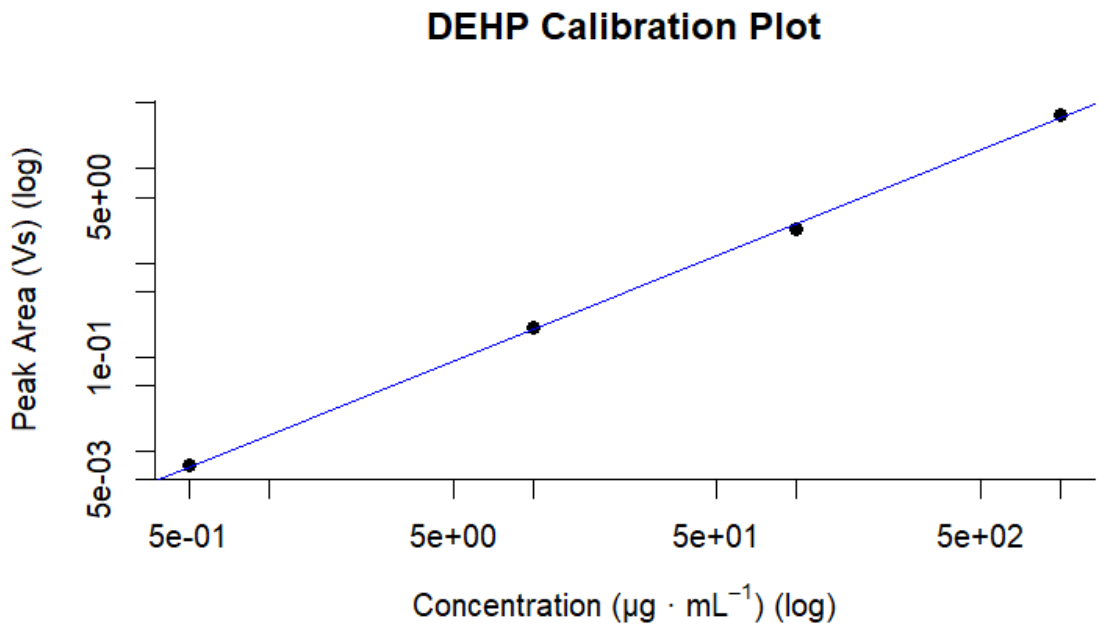

Figure 4-5: Calibration graph for DEHP in the range 0.5– 1000 mg · L^{-1} presented on a log-log scale as obtained by GC-C-IRMS and presented as a sum of the channels.

The exact concentration of the analyte in a sample of surface water could vary. Therefore, it was important to assess the sensitivity of the GC–C – IRMS. This was achieved by measuring solutions of DEHP. Table 4-3 below presents the $\delta^{13}C$ values for the different concentrations.

Table 4-3: Individual results of the calibration DEHP calibration graph used to calculate $\delta^{13}C$ from the effluent sample and DEHP concentration.

mg · L^{-1}	**δ ^{13}C value (‰)**	
1000	−26.647	−26.784 ‰- Average

1000	−26.743	0.1 ‰ – SD
1000	−26.795	
1000	−26.880	
1000	−26.855	
100	−27.083	−26.985 ‰ - Average 0.4 ‰ – SD
100	−26.593	
100	−27.453	
100	−26.663	
100	−27.133	
10	−26.278	−26.576 ‰ - Average 1.3 ‰ – SD
10	−26.070	
10	−28.903	
10	−25.923	
10	−25.706	
0.5	−24.931	−39.629 ‰ - Average 38.0 ‰ – SD
0.5	−73.948	
0.5	−86.033	
0.5	−11.480	
0.5	−1.755	

As expected, the precision presented in the Table 4-3 decreases with lower concentration of the solution analysed. Further information about the relationship between concentration and δ ^{13}C was possible due to the complexity of the chromatograms.

Table 4-4: Table presents average, standard deviation and relative standard deviation data for each concentration on the calibration graph

for each isotopologue

	All DEHP	44	45	46	δ ^{13}C
1000 mg · L^{-1}					
Ave	38.18	37.58	0.48	0.16	-26.78
SD	1.6	1.6	0.02	0.007	0.1
RSD	4.3	4.3	4.4	4.5	
100 mg · L^{-1}					
Ave	2.33	2.29	0.029	0.0098	-26.99
SD	0.06	0.05	0.0007	0.0004	0.4
RSD	2.4	2.4	2.4	4.6	
10 mg · L^{-1}					
Ave	0.21	0.21	0.003	0.001	-26.58
SD	0.008	0.008	0	0	1.3
RSD	3.9	4.0	0	0	
0.5 mg · L^{-1}					
Ave	0.0072	0.007	0	0	-39.63
SD	0.002	0.002	0	0	38.0
RSD	28.5	26.7			

As can be seen (Table 4-4), the most consistent quantitative data were obtained in a range of about 100 mg · L^{-1}. However, the 10 mg · L^{-1} and 1000 mg · L^{-1} were also consistent. The $\delta^{13}C$ values were improve with increasing concentration of the standard solutions up to 1000 mg · L^{-1}.

The same solutions were also analysed by GC-MS. Table 4-5 presents the comparison of the measurements.

Table 4-5: Table presents total peak area average, standard deviation and relative standard deviation data for each concentration obtained by GC-C-IRMS and GC-MS

DEHP	GC-C-IRMS	GC-MS
1000 mg · L^{-1}		
Ave	38.2	569 * 10^5
SD	1.65	457 * 10^4
RSD	4.32 %	8.03 %
100 mg · L^{-1}		
Ave	2.33	161 * 10^5
SD	0.0553	360 * 10^4
RSD	2.38 %	22.3 %
10 mg · L^{-1}		
Ave	0.207	129 * 10^4
SD	0.00811	677 * 10^3
RSD	3.92 %	52.4 %
0.5 mg · L^{-1}		
Ave	0.0072	446 * 10^2
SD	0.0020	372 * 10^2
RSD	28.5 %	83.4 %

Based on the relative standard deviations from the above results GC-C-IRMS shown greater precision than GC-MS. GC-C-IRMS gave consistent accuracy in the range between 10 mg · L^{-1} –1000 mg · L^{-1}. The instrument precision was poor only when a concentration of 0.5 mg · L^{-1} was analysed, however, when in the range between 0.5 mg · L^{-1} to 10 mg · L^{-1} the response was low and was not evaluated.

The precision of GC-MS correlates with the concentration. As the concentration of solutions decreases the precision of the measurement

decreased with it. Based on the values shown in Table 4-5, using the GC-C-IRMS can be used to quantify content DEHP at concentrations of 10 mg · L^{-1} and higher.

4.3.2 Quantification of phthalates with GC-C-IRMS

As already established and demonstrated in an earlier section, a linear response of faraday cups in IRMS is already well-known.[216,217] The excellent precision and good linearity of the GC-C-IRMS indicated, the GC-IRMS data is capable of providing quantitative CSIA (qCSIA) to a low concentration environmental sample. The quantification of DEHP was performed by GC-C-IRMS.[121]

Analysis of the effluent sample gave the following results. DEHP concentration in effluent and river Trent water down the stream from the WWTP drain were in the range of approximately 200 ng · L^{-1}. As per Environmental Quality Standard directive 2008/105/EC the DEHP limit in surface waters is ≤1.3 µg · L^{-1} for annual average. Therefore, the rivers are meeting this standard on the days sampled. This directive does not specify a maximum allowed concentration for DEHP. Concentration values correspond to 3.5 kg of DEHP passing through the river Trent every day. In comparison, only 53.1 g of DEHP passes through the river Foss every day. Slower river flow and therefore daily DEHP retention rates correlate with the observed enrichment of $\delta^{13}C$ values. The slower the river flow

the longer the pollutants are in the river extending the time for any in river decomposition to progress. This can be an indication of DEHP degradation instead of dilution. However, further work needs to be carried out.[121]

The concentrations of DEHP in WWTP Effluent, River Trent and River Foss were 0.20 μg · L^{-1}, 0.22 μg · L^{-1}, and 0.14 μg · L^{-1} respectively. However, as GC-C-IRMS involves a quantitative combustion, it might afford the opportunity to use one set of quantitative standards for multiple known compounds. This concept can work because the signal measured by the MS is from one type of molecule – carbon dioxide when measuring the carbon isotope ratios. By converting a known quantity of an identified compound into corresponding quantity of carbon dioxide and vice versa, it is not necessary to create a calibration graph for each compound. A quantity of CO2 gas assessed can be mathematically converted into corresponding amount of the original molecules. However, standards are still necessary to confirm the identity of the peaks. The GC-C-IRMS does not evaluate the fragmentation of the analytes. Therefore, it will not provide any structural information about the analyte. Alternative can be use of the internal standard. This could be an option in a simple matrix where the internal standard could be isolated. However, adding an internal standard to a complex sample could render the standard unusable. High potential of lack of separation would interfere with the

standard.

4.4 Conclusion

The findings in this chapter have been previously published and document the first time carbon isotopes were measured in the phthalates extracted directly from WWTP effluent and river.

The standard deviations obtained for this CSIA technique were in the range from 0.1‰ – 0.2‰. This precision will be the benchmark for this study. When $\delta^{13}C$ values of the above phthalates were compared, very small differences were observed between pre- and post-purification of the samples. It should be noted, however, that a small ^{13}C enrichment was observed in two of three samples.

The work has been cited by a review article prepared by the French Geological Survey.[218] They stated that this is an early example of CISA presented from surface waters at low concentrations. It was also stated that this was an important step towards large volume SPE for CSIA. The result of the phthalates presented in chapter 4, were also referred to by the Russian Academy of Science. They compared their results to ones obtained from this study and build on the knowledge about the stable composition of phthalates in surface waters.[219] The values presented were comparable to ones presented in these studies. Despite emerging data

showing that the phthalates can be of natural origin, currently the data seem to indicate that the phthalates are more of anthropogenic origin.

5 Non-targeted isotope analysis[V]

5.1 Introduction

The samples collected for CSIA gave chromatograms with over 100 peaks of which only four were used for CSIA. The complex chromatograms provided an opportunity to understand the isotopic behaviour of these unknown compounds. Prior to this work, such material that might be in the river, could be analysed using a range of targeted approaches (GC-MS, LC-MS, etc.) without IRMS or by total organic carbon (TOC).[121] TOC has been combined with IRMS to study organic material in rivers with typical values in the range −25 ‰ to −29 ‰.[220–222] However, almost nothing is known about isotope δ values of the compounds within the complex samples

Therefore, a non-targeted approach was used to examine the isotope ratios in wastewater treatment effluent (WWTE) and river samples using

[V] The information and the content of this chapter has been published in a peer reviewed article "Compound specific isotope analysis (CSIA) of phthalates and non-targeted isotope analysis (NTIA) of SPE-extractable organic carbon in dilute aquatic environments". Fragments of this paper have been used or adapted into this chapter. All the work presented here was performed by me with supervision and guidance from Dr Quentin Hanley.

GC-C-IRMS after solid phase extraction (SPE). NTIA was applied to over 100 unidentified compounds. The aim was to use GC-IRMS and analyse wastewater and environmental samples with analytes at trace concentrations in order to measure the $\delta^{13}C$ in a range of compounds.[121]

5.2 Sensitivity check of IRMS

In Figure 5-1 a range of unknown compounds were compiled together. When $\delta^{13}C$ values were plotted against the corresponding peak intensity there is a clear wide spread of isotopic values at low intensities. This demonstrates that there is an optimum threshold that can be defined for analysis of organic compounds in surface water.

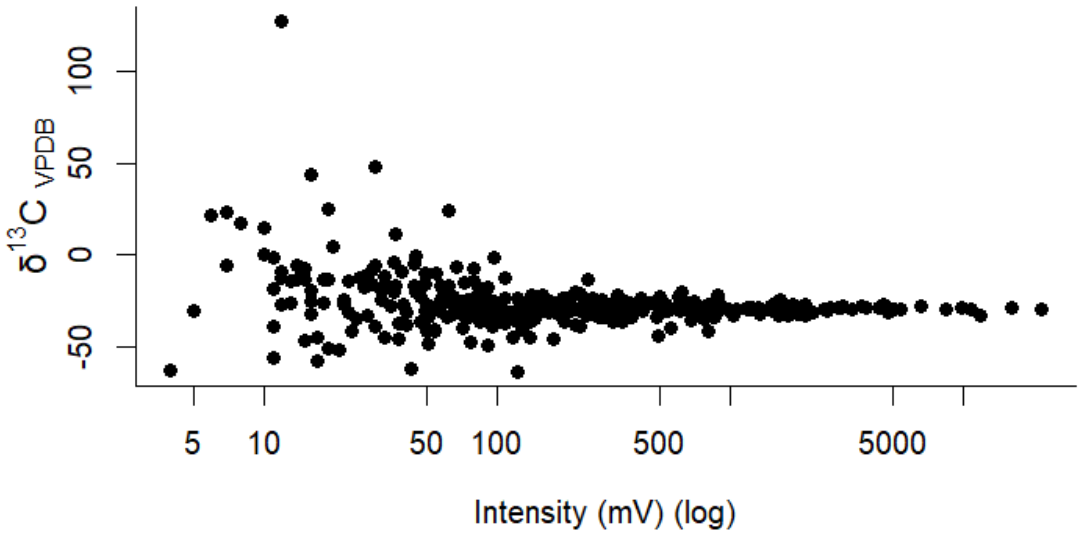

Figure 5-1: Presentation of the precision distribution across a range of intensities. The data presented is of three water samples: river Trent, Foss and from WWTP Effluent.

Results are accompanied by a minimum of four standards analysed at the same time (DEP, DBP, BBP, DEHP). There is to be at least one standard before and after the sample run. All replicates of standards should not deviate from the mean by more than two standard deviations.

5.3 NTIA - Non-targeted isotope analysis [VI]

The GC-C-IRMS analyses produced a large number of peaks corresponding to unknown compounds (Figure 4-3). The signals from these non-targeted unknown compounds can be used to obtain $\delta^{13}C$ values using the phthalate standards as references. It is unrealistic to identify all, prove with authentic standards, and generate appropriate isotope standards before examining isotope ratios. NTIA allows comparison of compounds between samples (e.g. different rivers) and the identification of exceptional compounds for subsequent CSIA. Standards ideally should be chemically close to the sample.[36] Future studies can examine the amount of bias introduced by this

[VI] This section is based and largely adapted from published article by Fiedziukiewicz *et al.* as per section Publication arising from this thesis.

standardisation, but the NTIA results presented here will reflect the use of these standards.[121]

The sample chromatograms were assessed to gain an idea of the scope of pollutants this method can be applied to. After examination of the chromatograms, 56 peaks in effluent sample were considered adequate for isotopic analysis. In the river Foss this number was 26 and in river Trent it was 34. Two factors were identified for the purpose of this assessment: the resolution to be ≥1.0, and the intensity to be of or above minimal stable signal. The resolution ensures almost complete separation between the peaks [223] therefore will minimise isotopic interference between neighbouring peaks. Greater separation threshold can be applied this however will in turn dismiss a greater number of peaks. Examining the IRMS signal ratio across a peak allows for further reassurance of peak purity and potential impact on the isotope results.

As the second parameter, the smallest stable signal identified was 100 mV. The standard deviation of the $\delta^{13}C$ measurements at the said intensity was ≤0.06‰, hence the value was set to be the threshold limit.

5.4 The WWTP, Trent, and Foss samples provided 117, 127, 121 peaks, respectively after SPE extraction. The samples used

were the same as discussed in Materials

The materials which follow are as described in Fiedziukiewicz *et al.*[120]. The general-purpose filter paper grade 601 was purchased from CamLab. Di-ethylhexyl phthalate (DEHP) (Tokyo Chemical Industries; GC grade), benzyl butyl phthalate (BBP) (Sigma; 98%), dibutyl phthalate (DBP) (Sigma; 99%) and diethyl phthalate (DEP) (Sigma; 99.5%) and hexane (Arcos; Extra Pure 95+%) were used as received to prepare samples, standards and secondary reference materials. Two certified standards were used, caffeine (IAEA600) and glucose (BCR-657) to calibrate everyday working standards of the phthalates on the VPDB scale.[121]

5.5 Standards

Two certified standards were selected and used to create working standards. Those were caffeine (IAEA-600) and glucose (IRMM-BCR 657). For laboratory working standards compounds selected were phthalates used to make the mixed reference were: diethyl phthalate, dibutyl phthalate, benzylbutyl phthalate, di-(2-ethylhexyl) phthalate.

5.5.1 Preparation of standards - Considerations

The analysis of the caffeine LWS was carried out using EA–IRMS. This is in contrast to usual analysis using GC–IRMS. The reason for the choice of elemental analyser was the solid form of primary standards. EA was a

better choice to compare non-volatile compounds with the selected standards. For this reason, the preparation is unique as opposed to the rest of the analysis presented in this thesis. Below steps describe the preventative actions taken to ensure minimum contamination, accurate and precise results.

5.5.1.1 Area and equipment

Aluminium foil ~5 × 5 cm was placed onto balance pan, a sheet of aluminium foil was placed on the bench next and around the balance. The sheet of foil should be big enough to make a comfortable working space (this will be working area to prevent unintentional contamination from any deposits and residues left on the bench surface). This was to prevent any potential contamination of the outside of the weighing boat. Tweezers were cleaned with methanol and air dried before every analysis. From this point on the tweezers were only keep within the work space.

5.5.1.2 Blank Preparation

For analysis, two of empty capsules were prepared using tweezers by flattening and folding a capsule onto itself. Those were the blank measurements.

5.5.1.3 Sample

Approximately 0.1 mg sample or standard was weighed into tin capsule.

The capsule was closed in the same manner as the blank and all the sample and standard capsules were placed into sample tray and analysed. The EA-IRMS details are present in the suggested order of analysis that was used during this study: blank, laboratory working standard, international certified standard.

5.5.2 Laboratory working standards

The use of primary standards may not always be feasible. For the purpose of this study a caffeine reagent was prepared and stored for routine analysis and comparison to any further standards. The preparation of the LWS material is described in detail in the following sections. Phthalates that were used to make the mixed reference solution were also analysed using EA-IRMS for the isotopic ratio of the individual phthalates.

5.5.3 Laboratory working standard preparation process

A solid bulk standard was mixed with a clean metal spatula. A small approximately 1 mL vial was filled with 0.10 g of the standard. Melted sealing wax was used to seal the lit and the material. Label the standard with standard details. Ensure the details on the label will be traceable to the analysis and individual weights. This can be achieved by recording the batch being prepared, this will provide the isotopic values. It is also encouraged to keep the record of the specific bottle. This number in conjunction with the batch number will allow to access both specific

weights dispensed and the isotope value. Once sealed the randomly selected bottles and the stock material were analysed and compared to each other to verify that the process did not introduce any contamination nor fractionation of the material.

5.6 Sampling and sampling sites

Sampling methodology is reproduced here from Fiedziukiewicz *et al.* Samples were collected in 2.5 L amber borosilicate glass bottles, using a stainless steel bucket for sampling. The bottles were cleaned with methanol then deionized water prior to sample collection. Effluent samples were collected from the drain from the Stoke Bardolph Sewage Treatment Works (What3Words reference: conducted.reference.thigh; GPS: 52°58’24”N , 001°02’15”W), as it enters the River Trent. The river water samples were collected from the river banks. The sample from the River Trent was collected 750 m downstream from the WWTP drain on the same side (What3Words reference: croaking.traffic.comments; GPS: 52°58’48”N , 001°02’18”W). The sample from the River Foss was collected on the east side of the Palmer Street footbridge 1050 m from where it enters River Ouse (What3Words reference: engine.local.dose; GPS: 53°57’30”N , 001°04’24”W).[121] Locations are presented in Figure 2-1.

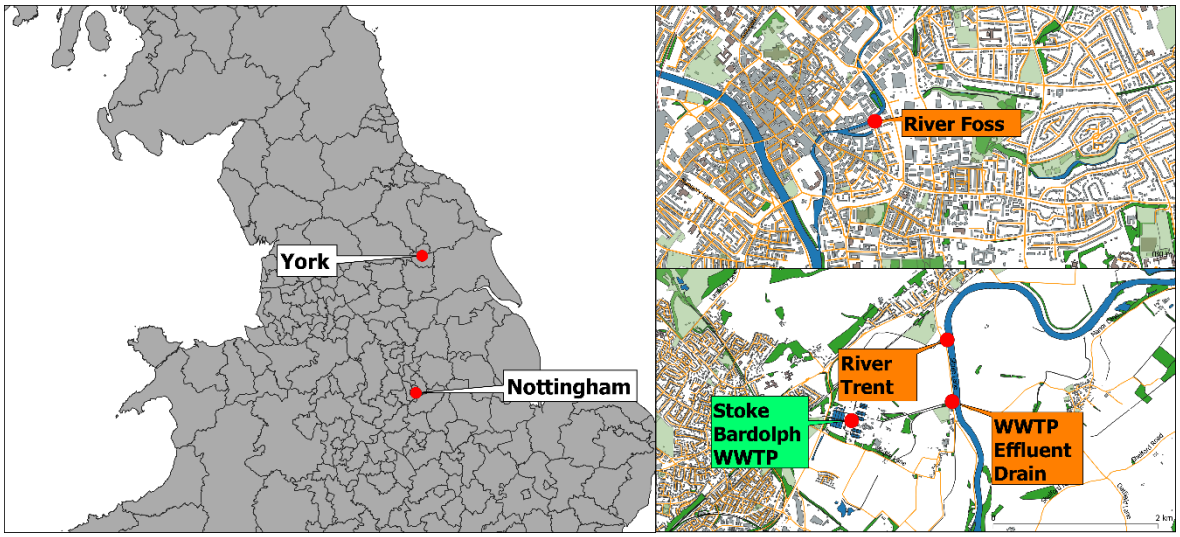

Figure 2-1: Location of the sampling sites in Nottingham and York.

SPE extraction was completed within 6 hours on the day of collection. Both rivers were at high flow (River Foss 4.5 $m^3 \cdot s^{-1}$ and River Trent 203 $m^3 \cdot s^{-1}$) at the time of collection. The average flows of the Rivers Foss and Trent are 1 $m^3 \cdot s^{-1}$ and 90 $m^3 \cdot s^{-1}$, respectively [122]. Flows reported were based on the Huntington (station reference F2470) and North Muskham (station reference 4022) measuring stations (2020).[121]

2 L samples were extracted using a set of eight 6 mL Oasis MCX SPE cartridges (Waters, UK) containing 500 mg of sorbent. The cartridge was first conditioned with 6 mL of MeOH and deionized (DI) water then 250 mL of sample was extracted with a flow rate of 3-5 mL $\cdot$ min^{-1}. Following extraction, the cartridges were rinsed with DI water and eluted with 6 mL of pure MeOH. The aliquots were combined and dried on a hot plate set

to < 75 °C under a nitrogen stream. Once dry, the samples were transferred to GC vials using hexane and dried again. The choice of hexane is discussed later in the chapter. The samples were then resuspended in 5 µL of hexane for analysis. The vials were wrapped in Al foil during any storage to prevent sample degradation through the UV radiation.[121,123]

5.7 Sample preparation and analysis

The samples were collected into 1 L borosillicate glass bottles directly from the wastewater treatment water treatment plant effluent discharge. Sample extraction was done as soon as possible with Water Oasis MCX SPE cartridge (item number 186000776). The cartrige works in mixed mode cation exchange and has three main groups attracting cataions, polar compounds and reverse phase attracting hydrophobic compounds. The limitation of this approach was that it excludes acidic compounds.

The functional group cartridge was selected based on reported use to analyse similar sample.[124] The cartridge was first conditioned with 6 ml of MeOH and deionized (DI) water. Next, no more than 1 L of sample was loaded onto a single 6 cm^3 cartridge with 500 mg sorbent. The flow was kept at an average of 5-6 mL · min^{-1}. The sample was then washed with DI water. The water was discarded and sample was extracted from the cartridge with pure MeOH, then with 2 % ammonia solution in MeOH.

Further, multiple aliqiots were combined together. The collected extract was dried on a hot plate set to no more than 70 °C.[121]

5.8 GC-C-IRMS

The conditions below were reproduced from the from paper by Fiedziukiewicz *et al* for completeness as per section publication arising from this thesis.

The analysis was performed using an Agilent GC 7890 coupled to a Thermo Delta V Advantage isotope ratio mass spectrometer. GC parameters were: injector port: 280 °C; oven: 50 °C; ramp: 3 °C/min to 300 °C and hold time of 8 min; column stationary phase (5%-phenyl)-methylpolysiloxane (Agilent DB-5); column length: 30 m; internal diameter 0.25 mm; film thickness 0.25 μm. The GC-C-IRMS combustion reactor was preconditioned at 1000 °C for 1 h before the analysis.[121]

IRMS combustion reactor was preconditioned at 1000 °C for 1 h before the analysis.

5.9 SSH Correction

Where stated the data were manually corrected for oxygen using SSH oxygen compensation calculation. Calculations were performed using RStudio and R programming. Calculations were adapted from papers by

Santrock, Studley, Hayes (1985) and Brand, Assonov, Coplen, (2010). Value for ^{18}R is an iterative process and to calculate it starts by an approximation of this value with Equation 2-1. Then the iteration follows the Equation 2-2, Equation 2-3, and Equation 2-4.

Equation 2-1: SSH calculation first step

$$^{18}R = \frac{^{46}R}{2}$$

Here ^{18}R represents ratio of ^{18}O and ^{16}O. ^{46}R represents ratio of *m/z* 46 and *m/z 44.*

Equation 2-2: Calculation of first intermediate to ^{18}R represented by ^{18}fR.

$$^{18}fR = \left(-3K^2 * {}^{18}R^{2\lambda}\right) + \left(2K * {}^{45}R * {}^{18}R^{\lambda}\right) + (2{}^{18}R - {}^{46}R)$$

^{18}fR is a first intermediate value, K is a constant equal to 0.0099235, λ is also constant equal to 0.516. ^{45}R represents ratio of *m/z* 45 and *m/z 44.*

Equation 2-3: Calculation of second intermediate to ^{18}R represented by ^{18}ffR.

$$^{18}ffR = \left(-6K^2 * \lambda * {}^{18}R^{2\lambda-1}\right) + \left(2K * {}^{45}R * \lambda * {}^{18}R^{\lambda-1}\right) + 2$$

Equation 2-4: Final fourth step of ^{18}R iteration.

$$^{18}R = {}^{18}R - \frac{^{18}fR}{^{18}ffR}$$

This iteration is performed four times and once complete the process if finished by following Equation 2-4 again and then Equation 2-5, and Equation 2-6 below.

Equation 2-5: Calculation of ratio ^{17}O / ^{16}O .

$$^{17}R = K * {}^{18}R^{\lambda}$$

^{17}R represents ratio of ^{17}O and ^{16}O.

Equation 2-6: Final expression of ^{13}C ratio.

$$^{13}R = {}^{45}R - 2K^{18}R^{\lambda}$$

Here ^{13}R represents ratio of caron ^{13}C and ^{12}C.

A result from Equation 2-6 is ^{13}C / ^{12}C ratio excluding impact from oxygen isotopes present in CO_2 molecule. This process was applied to individual data points across chromatogram signals resulting in individual values that are oxygen corrected. The entire process is presented in Appendix A for RStudio.

Screen experiment of an aqueous matrix Were further analysed Most of the 100+ peaks in these chromatograms are unknown. The $\delta^{13}C$ values from all peaks were plotted against the raw *m/z* 44 signal (Figure 5-1) which indicated low intensity signal correlated with a bigger spread of measured $\delta^{13}C$. If the variability of the 5 µg/mL DEHP standard is considered as a cut off, values can be used down to ~479 intensity units. After imposing the intensity threshold from the 5 $\mu g \cdot mL^{-1}$ DEHP standard 44, 26, and 31 peaks remained providing best quality $\delta^{13}C$ values for the WWTP, Trent, and Foss samples, respectively. Although we used this threshold, the $\delta^{13}C$ and intensity plot suggests that a lower threshold (~150) could be used. The initial wide spread of the data becomes more stable within the range of 80 – 100 intensity units and improves further as intensity rises. For this work, the more stringent intensity threshold was applied; however, future users of NTIA may consider relaxing this as long as the moving standard deviation, standard signal levels and well-resolved peaks justify it. The moving standard deviation is the standard deviation of the moving average (n=10) computed on the intensity rank sorted arrays of $\delta^{13}C$ values for the three sample locations.[121]

Peak resolution is known to influence isotopic analysis [63] and a valley between two peaks of up to 10 % is considered sufficient for GC-IRMS.[224] For inclusion, peak resolution ≥1.0 was required which gives 2.3 %

overlap with adjacent peaks.[121]

Without these criteria, average $\delta^{13}C$ of compounds in both rivers was slightly enriched relative to the effluent. After applying the minimum intensity threshold, the effect inverted (Table 5-1, column 3). The averages were similar to dissolved organic carbon reported in the literature of −26 ‰ to −27 ‰ however with added granularity providing variability, that cannot be achieved by EA-IRMS.[225] Average values of soil organic matter from C_3 type plants are also close with values close to $\delta^{13}C$ −26 ‰.[226] Dissolved inorganic carbon found in rivers is reported to be in a range of −10 ‰ to −12 ‰. [227] These results prove that $\delta^{13}C$ values can be measured on individual compounds composing volatile organic carbon from WWTP and river samples.[121] Such approach provides a screening tool to help identify any abnormalities and target potential compounds of interest.

Table 5-1: Average $\delta^{13}C$ values of the total volatile organic carbon based on individual values measured. Slope (significance) between samples. S: slope; C: correlation coefficient. Values were considered significant if $p < 0.05/6$ to adjust for multiple comparisons. These are indicated with a *. The data in this table were published in the article as mentioned at the beginning of the chapter.

		Average $\delta^{13}C$ ± SD	**WWTP**	**River Trent**
WWTP Effluent	Full intensity range	–28.4 ± 7.6‰ (n=117)		
River Trent		–25.7 ± 20.3‰ (n=127)	S: 0.20 (0.013) C: 0.54 (1.1E-13)*	
River Foss		–24.6 ± 14.0‰ (n=121)	S: -0.062 (0.46) C: -0.093 (0.27)	S: 0.066 (0.37) C: 0.060 (0.42)
WWTP Effluent	Intensity range >479 mV	–28.6 ± 2.2‰ (n=44)		
River Trent		–30.8 ± 4.4‰ (n=26)	S: 0.19 (0.38) C: 0.18 (0.39)	

River Foss		–29.7 ± 3.4‰ (n=31)	S: 0.041 (0.85) C: 0.046 (0.83)	S: 1.1 (1.4E-10)* C: 0.96 (2.1E-12)*

More important than the average is the relationship between matched peaks appearing in the different samples. To investigate this, the $\delta^{13}C$ values were aligned by retention time (Figure 5-2) for peaks with resolution ≥1.0, retention time within ±3 s, and max intensity ≥479 at *m/z* 44. Nearly all $\delta^{13}C$ values from the river Trent were more negative than in the river Foss indicating greater depletion of the heavier isotope. The $\delta^{13}C$ values were significantly and highly correlated with a slope 1.1 between these two rivers (Table 5-1, column 5).[121] Depletion of heavy isotope in compounds in the river suggests that the bacteria present selectively consume ^{13}C, opposite to normal kinetic fractionation effects. An explanation for such results could be that the phthalates have a form of an environmental sink. This has been observed for bacteria degrading asphaltenes in sea water [56] leading to $\delta^{13}C$ values ~1 ‰ more negative in the remaining asphaltenes. This has also been reported for *D. postgatei* and *D. hydrogenophilus* which depleted ^{13}C while degrading acetate. As a result, the $\delta^{13}C$ values became more negative.[228] In addition, radical C-H bond cleavage has shown a reverse isotope effect. The reaction was catalysed specifically under hydrogen peroxide and titanium dioxide.[229]

This suggests that bacteria and / or other process depleting heavy isotopes in their metabolism may also be present in the rivers.

There was no significant correlation in matched compounds between the WWTP effluent and compounds in the river Foss. The strongest correlation was observed between compounds in river Trent and Foss (0.96). There was a tendency for compounds in the rivers to be depleted in ^{13}C relative to the corresponding compounds in the effluent - Figure 5-2. This is specifically based on the intensity range limited to by being more stable. The full range was considered to be in adequate to quantify the data since ratio is based on positive only values the ratio between the two signals was not normally distributed. Therefore, greater relative inaccuracy was observed towards higher values as shown in Figure 5-1. The difference between average $\delta^{13}C$ values was calculated at 1.2‰ and 1.1‰, leaving the river compounds on average depleted from the heavy isotope. The range of differences between compounds in effluent and river Trent was between –3.4‰ to 5.6‰. Notably, three compounds out of twelve changed by less than 1.0‰. Between rivers Trent and Foss (Figure 5-2, bottom), the correlation value was 0.96 and the average difference between them was measured at 1.5‰. This analysis highlighted a pair of compounds with $\delta^{13}C$ values near –35‰ and –43‰ which may offer an intriguing marker of algal-herbivore productivity in tributaries and downstream sites acting as an indicator for further analysis.[230]

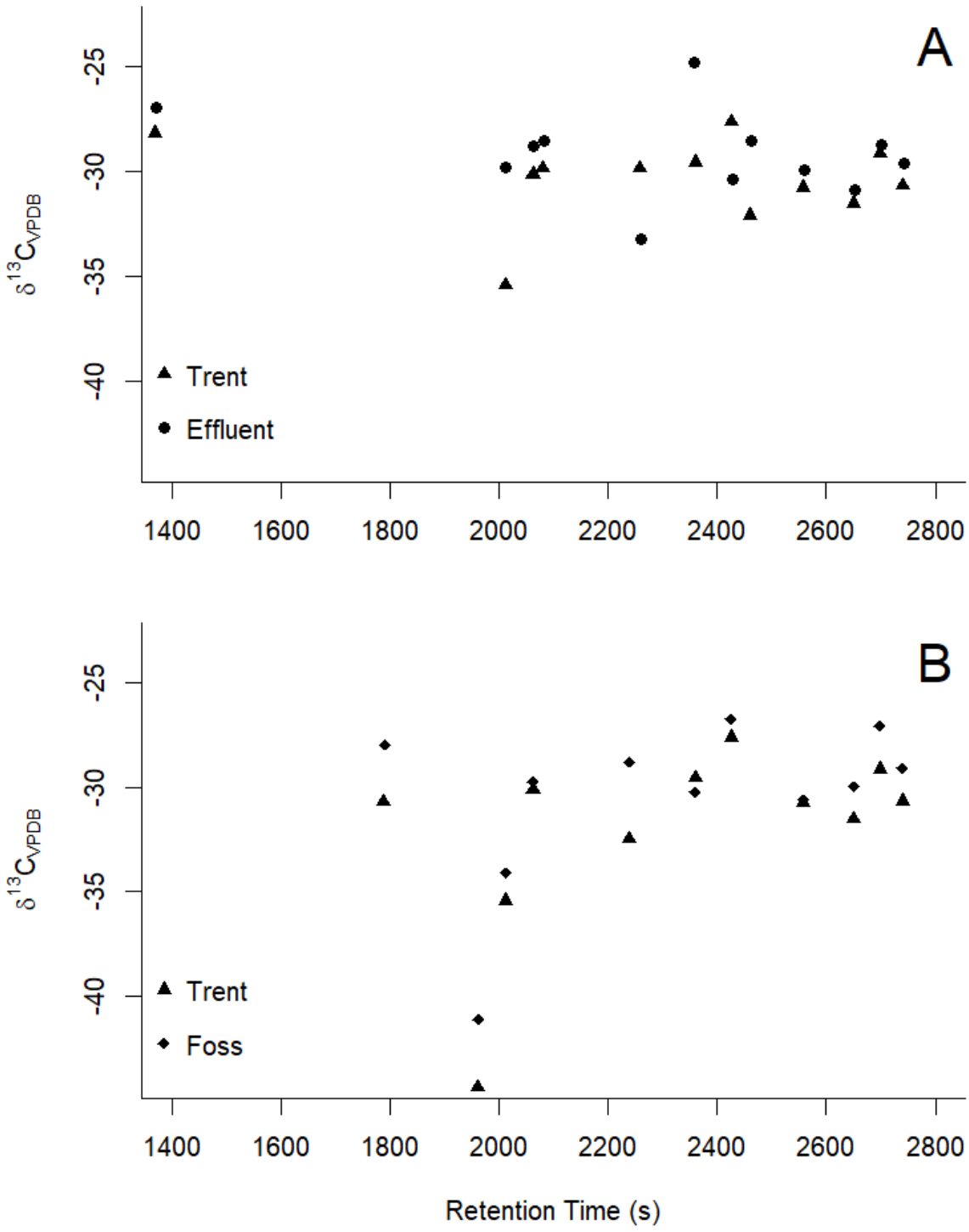

Figure 5-2: $\delta^{13}C$ comparison of distribution of individual compounds in WWTP effluent and rivers. Top graph (A) presents a comparison between WWTP effluent and river, bottom (B) compares between two rivers Trent and Foss.

The strongest correlation coefficient value was observed between the sample from the effluent and the water from river Trent at 0.52. Compounds in the river are being depleted in ^{13}C with respect to the corresponding peaks in the effluent. The difference between average δ values was calculated at 1.6 ‰. Leaving the river compounds on average depleted from the heavy isotope. The range of differences between compounds in effluent and river Trent was between (-) 8.3 ‰ to (+) 5.5 ‰. A study reported the *D. postgatei* and *D. hydrogenophilus* were promoting degradation of acetate with ^{13}C, depleting the remaining pool from the heavy isotope, shifting the $\delta^{13}C$ values more negative.[231] Both types of bacteria mentioned above are sulphate reducing and may contribute to the isotope fractionation.

Between rivers Trent and Foss, the correlation value was only 0.12 and the average difference between them was measured at only 0.4‰. Even though the average values are close the correlation provides a level of distinction between the two samples. Similarly, no correlation has been observed between effluent and river Foss. The correlation coefficient was -0.05 and the average difference 2.3‰. River Foss has smaller amount of heavy isotopes, similarly as river Trent.

T-Scores of the comparisons were as follows: SB WWTP Effluent – river

Trent (0.9); river Trent – river Foss (0.1); and river Foss – SB WWTP effluent (1.4). Two tailed critical values were 2.1, 2.2, and 2.1, respectively. None of the samples were significantly different from each other. However, because the individual compounds in the sample can become either isotopically enriched or depleted during the degradation process, average difference may not change significantly. The limitation of the statistical test applied, is measuring the difference between the average value of the two sets.

Increased correlation and difference of the $\delta^{13}C$ values between the samples can be interpreted as an indication of the different nature of the samples which have a common factor. An example of this deduction is the WWTP effluent and the river the effluent is discharged into. No correlation and little average isotopic difference between the samples has been observed between two independent samples of the same nature. Therefore, it may be possible to distinguish between different bodies of water using stable isotopes form volatile organic compounds found in them.

5.10 Conclusion

This work demonstrated isotope ratio analysis on individual compounds in dilute aquatic samples can be done in a non-targeted way on unknown compounds. The averages obtained are consistent with IRMS done on

TOC while leaving intriguing targets for additional work. This work performed GC-C-IRMS which restricted the analysis to volatile organic compounds. This broadens the existing techniques for the analysis of river systems allowing compound degradation to be better understood.[121,232–236]

The methods described in this chapter can be applied to any dilute water sample compatible with SPE techniques. Such approach will allow an individual compound to be monitored as it progresses through the ecosystem. Carrying out the NTIA on a broad environmental matrices will contribute to understanding the complexity of organic compounds in aquatic systems, even when those compounds are unknown.[121] This was a particularly useful tool for samples of very limited volume where analysis *via* GC – MS as well as GC-C-IRMS may not be possible.

6 Isotope chromatographic effects

Combining gas chromatography with isotope ratio mass spectrometry leads to variation between the readings of the individual isotope signals. The chromatography temperature ramps cause the baseline to drift by increasing the rate of column bleed. A challenge to measuring in a complex matrix is the homogeneity of this background signal. In addition, various compounds can co-elute with the peak of interest. Therefore, complete separation of peaks and minimal baseline is currently deemed a pre-requisite for valid isotope analysis.[237–240] This means that the analysis of complex samples, such as water in rivers or WWTP effluent are not being done routinely and thus environmental studies are limited in their isotopic analysis. This chapter investigates whether differential isotope effects caused by gas chromatographic separations preceding the isotope measurement can allow incomplete separations on drifting backgrounds to be used.

Despite the well-established approach of compound specific isotope analysis [46,47,121,241] more can be achieved with better understanding of the behaviour of peak separation and broadening in complex chromatograms. This chapter will explore further the aspects of isotope analysis. Topics discussed here are intended to supplement the previous chapters and support the non-targeted isotope analysis (NTIA).

6.1 Chapter aims and objectives

The work presented in this chapter attempts to improve the analysis of complex samples, such as the extracts of water from a river, using the GC-C-IRMS chromatogram and the NIE / RIE and related isotope changes across a peak of interest (e.g. in the presence of an unknown background and imperfect resolution). These are expected to subtly affect retention times and peak width giving hints about the number of peaks present. The key is understanding baseline interference and neighbouring compounds and their impact on the signal from the compound of interest. For example, a chromatogram recorded for the heavy and light isotope signal generated by a fully separated compound can be converted to a ratio of the data points of the two signals. A clean 'S' shape is expected when there are no overlapping or underlying peaks.[242] See Figure 6-2 for an example. However, if there are additional compounds, even in the apparently base resolved chromatography, these will be detected in the isotope ratio chromatogram.

This chapter also investigates potential systematic errors introduced by isotope effects on retention times and band broadening. The main consideration is focused on chromatographic detection parameters (the start and end points). The aim was to observe the impact of the complex chromatogram and chromatography parameters on recovered $\delta^{13}C$

values. During the course of the project the isotope calculation process was applied to each individual time point obtaining the δ chromatograms. The goal was to demonstrate methods to robustly verify the interference using GC-C-IRMS chromatograms and assess the impact of overlapping compounds and the matrix. The data collected is expected to support a change of approach allowing complex mixtures of compounds to be more routinely analysed using δ chromatograms.

6.2 Methodology

The data obtained in this chapter were obtained with GC-C-IRMS. The IRMS parameters were the same as presented in the previous sections. The changes were made to the GC programmes as follows. To analyse the changes to the recovered δ values, a set of 11 temperature programmes were used while analysing standard materials (Table 6-1).

Table 6-1: The GC ramp values used to run the isotope changes.

GC Programme	Rate (°C · min^{-1})
P1	0.253
P2	0.5
P3	1.0
P4	3.0
P5	5.0

P6	10.0
P7	20.0
P8	30.0
P9	40.0
P10	50.0
P11	120.0

The GC temperature gradients were adapted from the paper published in accordance with the Table 6-1, above.[121]

6.3 Results and discussion

6.3.1 Chromatographic isotope effect – Molecule comparison

To better describe the temperature effect on isotope behaviour a set of DEP and DBP standards were, under different conditions as described in the Table 6-1, injected and the retention and peak width ratios calculated using a range of different GC oven programmes as described in the Table 6-1, this effect ranges from 0.99994 to 0.99997 for average temperatures ranging from 79.8 to 128.0 °C. Despite the values appearing close to ratio of one (indicating the isotope signals to be the same) they represent multiple conditions and under each the ratio was less than one. Under the same conditions the peak broadening ratio ranges from 1.01961 to 1.06533. The magnitude of the isotope effect is reversed and greater when considering band broadening. This means that

the sorption and desorption effects play fractional role in the band broadening and that longitudinal diffusion happens predominantly in the gas phase. Therefore, they demonstrate a consistent isotope effect on both retention time and peak width that has not been discussed in detail in the literature.

The extent of isotope induced peak width variation has not been discussed in the literature in a quantitative context. Some integration techniques assume the peak widths to be the same between isotopologues.[243] Contrary to this assumption the biggest effect in retention time shift was 0.006% but for band broadening it was 6.5% (Table 6-2).

Table 6-2: Ratios obtained for the retention times and W0.5 for both standards. The repeated values are at different GC temperature programmes. The programmes with temperature gradient of 10 °C · min^{-1} and above did not resolve therefore those are not reported.

GC Programme	DEP		DBP	
	Rt 45/44 (s)	W0.5 45/44 (s)	Rt 45/44 (s)	W0.5 45/44 (s)
1	0.99996	1.065	0.99995	1.048
2	0.99995	1.064	0.99996	1.050
3	0.99996	1.049	0.99997	1.045
4	0.99996	1.020	0.99997	1.021
5	0.99994	1.026	0.99995	1.029

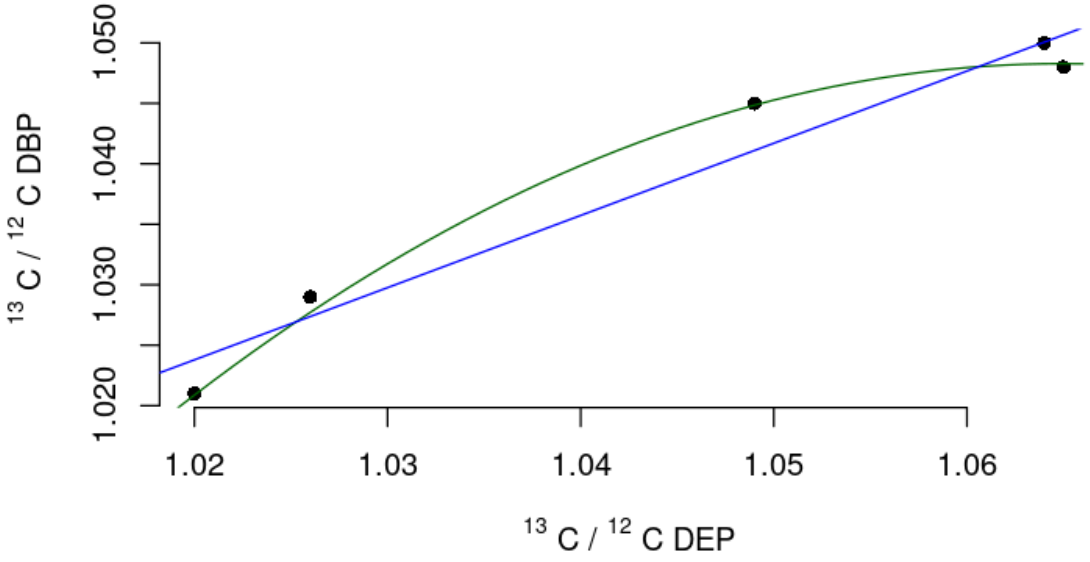

Figure 6-1: Comparison of DEP and DBP peak $W_{0.5}$. Black dots show the datapoints; blue line is a linear correlation; green line represents a two-degree polynomial correlation.

Figure 6-1 shows a comparison of linear and polynomial correlation between $W_{0.5}$ DEP and DBP. The R^2 values calculated were 0.951 and 0.996 for linear and polynomial models, respectively. This is an indication that the two compounds behave in slightly different way to each other.

The data were bootstrapped for the purpose of the evaluation to n = 3000. The retention time datasets failed the Shapiro-Wilks and Kolmogorov-Smirnov tests for normality.[244] Therefore, retention times

and peak widths were compared between the DEP and DBP with the unpaired Mann-Whitney U test. When DEP and DBP Rt data were compared with the obtained p-value was $2.2 * 10^{-16}$ and the U value was 11019120. The peak width comparison was also significantly different with p-value $2.2 * 10^{-16}$ and the U value was 6523613. The statistical testing has been performed on the datasets bootstrapped with random numbers, therefore the exact U values as calculated might differ slightly. The ratios of the metrics were significantly different between the two standards.

For reference, the R programme code for bootstrapping is presented in Appendix B: Statistical bootstrapping (RStudio script).

This means the two compounds have significantly different isotope effects despite both analytes being similar in structure. Both DEP and DBP are di-esters of phthalic acid. They differ by ethyl and butyl chains, respectively. The chain length affects the cross section of the molecule. Also, the size of a molecule affects it's dipole moment and therefore their interaction within a chromatographic system. Therefore, differences between the chains were enough to observe significantly different isotope chromatographic effects.

6.3.2 Peak width and retention time

The empirical data collected through this study shows that compounds separated using a non-polar chromatographic column will result in wider peaks obtained on the channel measuring the heavier isotope – *m/z* 45. The measured sigma and effective FSH diffusion values are presented in the Table 6-3 and Table 6-4. The average measured total diffusion coefficients were calculated as 0.0021 and 0.0023 cm · s^{-2} for light and heavy isotopologues of DEP and respectively 0.0012 and 0.0013 cm · s^{-2} for DBP. The magnitude of the effect between heavy and light isotopes is 10 %. More detailed values are found in Table 6-4.

Table 6-3: Ratios of retention times with corresponding average temperatures based on elution time. The values were obtained from two standards DEP and DBP.

Av temp (˚C)	Standard	Rt (s)	Rt45 / Rt44
79.8	DEP	14527.17	0.999964
97.5	DBP	23022.04	0.999950
86.0	DEP	8870.073	0.999953
104.2	DBP	13242.61	0.999961
92.3	DEP	5318.859	0.999961
110.9	DBP	7540.947	0.999972
103.3	DEP	2367.163	0.999956
122.2	DBP	3124.831	0.999967
108.9	DEP	1644.566	0.999936
128.0	DBP	2104.22	0.999950

The average temperatures were calculated as they are an important element of the diffusion and mass transfer in GC. As the instrument programmes were set up with an incremental temperature ramp. Therefore, two compounds eluting under the same programme will have different average temperatures. Hence, the presentation of average temperatures in Table 6-3.

Table 6-4: Measured / effective diffusions

Standard	°C · min^{-1}	Rt (s)	^{12}C			^{13}C		
			$W_{0.5}$ (s)	σ^2 (s)	D eff	$W_{0.5}$ (s)	σ^2 (s)	D eff
DEP	0.25	14527.17	41.59	313.3	0.0108	44.31	355.5	0.0122
DBP	0.25	23022.04	37.10	249.2	0.0054	38.88	273.7	0.0059
DEP	0.5	8870.07	23.01	95.9	0.0054	24.48	108.5	0.0061
DBP	0.5	13242.61	20.81	78.5	0.0030	21.86	86.5	0.0032
DEP	1	5318.86	12.77	29.5	0.0028	13.40	32.5	0.0030
DBP	1	7540.95	11.51	24.0	0.0016	12.04	26.2	0.0017
DEP	3	2367.16	5.34	5.2	0.0011	5.44	5.4	0.0011
DBP	3	3124.83	4.92	4.4	0.0007	5.02	4.6	0.0007
DEP	5	1644.57	3.98	2.9	0.0009	4.08	3.0	0.0009
DBP	5	2104.22	3.56	2.3	0.0005	3.66	2.4	0.0006
DEP	10	1383.98	2.72	1.3	0.0005	2.72	1.3	0.0005
DBP	10	1621.69	2.51	1.1	0.0003	2.51	1.1	0.0004
DEP	20	1210.98	2.20	0.9	0.0004	2.20	0.9	0.0004
DBP	20	1333.67	2.20	0.9	0.0003	2.20	0.9	0.0003

DEP	30	1138.10	2.09	0.8	0.0003	2.09	0.8	0.0003
DBP	30	1221.68	2.09	0.8	0.0003	2.09	0.8	0.0003
DEP	40	1099.58	1.99	0.7	0.0003	1.99	0.7	0.0003
DBP	40	1164.15	2.19	0.9	0.0004	2.19	0.9	0.0004
DEP	50	1076.11	2.09	0.8	0.0004	2.09	0.8	0.0004
DBP	50	1130.37	1.99	0.7	0.0003	1.99	0.7	0.0003
DEP	120	1038.97	2.09	0.8	0.0004	2.09	0.8	0.0004
DBP	120	1086.41	2.09	0.8	0.0004	2.09	0.8	0.0004

6.4 Introduction

6.4.1 Characteristics of the isotope effect

Gas chromatography causes a slight but observable temporal shift between isotopologues of an analyte.[95,97,237,242] When the chromatographic technique is coupled with the IRMS the ratio can be calculated from the signal channels corresponding to the heavy and lighter isotopologues. When the ratios of individual points are plotted against corresponding time, the pattern resembles a letter 'S'.[237] Modelled and observed 'S' shapes are presented in later in this chapter. The observation of this effect goes back to a study by Wilzbach in 1957.[97] The study presented the separation and retention of cyclohexane with its deuterated and tritiated counterparts. Deuterated and tritiated counterparts had a similar effect of 5 % difference in retention time. Despite the initial observation over 60 years ago, little research has been done subsequently to describe and explain the isotopic effect in gas chromatography.

Recent studies report that the isotope effect can vary between the NIE and RIE. A recent study reported a correlation between the normal and the reverse isotope effects, reported to be dictated by the polarity of the GC column.[100] The data published shows that the more polar the column, more compounds show regular isotope effect (lighter isotope leading). Non - polar columns show the reverse isotope effect. This indicates the

dipole interactions play a key role in the type of isotope effect. The difference in elution times carries information that can be explored drawing conclusions.

It was also demonstrated through the isotope substitution that position of an isotope impacts the isotope chromatographic effect. This is apparent when the isotope is located on an sp^2 or sp^3 orbital. The difference between the minimum and maximum geometrical profile of the sp^2 orbital is greater than the sp^3 This means that the peak broadening of the sp^2 substituted isotopologue should be greater than the sp^3.

The temporal shifts of the isotopologues can be described by either of the two isotope chromatographic effects.[242] The normal isotope effect (NIE) is when the lighter isotope elutes earlier than its heavier counterpart $L_{Rt} < H_{Rt}$. The reverse isotope effect (RIE) is a direct opposite, $H_{Rt} < L_{Rt}$. L_{Rt} represents the retention time of the lighter isotope and H_{Rt} represents retention time of the heavy isotopologue.

The retention time directly correlates to the proportion of time the analyte spends in the stationary and mobile phase (accepting that analytes all spend the same amount of time in the mobile phase). It is frequently described as the partition coefficient - *k* using the following formula:

Equation 6-1: Partition coefficient equation.

$$k = \frac{t_S}{t_M} = \frac{Rt_s - Rt_m}{Rt_m}$$

Where t_S and t_M are the average time analyte spends in stationary and mobile phases, respectively. The Rt_m and Rt_s represent retention time of the mobile phase and sample respectively.

In gas chromatography, there are many factors affecting the isotope dynamics of molecule mobility. The main ones are, temperature, pressure, forces between the analyte molecule and stationary phase, cross section and molecular weights of analyte molecule and the mobile phase. Interaction between analyte and stationary molecule in gas chromatography are typically based on the polarity of both. The polarity of an analyte will depend on the size of the molecule and that is affected by the isotope coordination and substitution in a particular molecule. As presented in Equation 6-2 the polarity depends on two factors the charge and the distance between them. Therefore, as per the Equation 1-2 the distance between the atoms will be affected by the isotopes on either end of the bond. This means a geometry of a molecule will also have an effect. The polarity is proportional to the distance between the charges. Meaning that molecule with heavier isotope will show lesser polarity than its light isotope counterpart.

RIE and NIE effects have been linked to column polarity.[100] Since the apparent prevailing factor is the dipole interaction. The dipole moment was pointed out to be a factor in the switch between the isotope and reverse isotope effect.[57,100] In the studies there is a correlation between NIE and increased polarity of columns and between RIE and decreased polarity. This indicates, polarity interactions play an important role in isotope chromatographic effects. Polarity is characterised by the distribution of charges across a molecule. A simple diatomic molecule can be characterised as per Equation 6-2.

Equation 6-2: Expression of polarity for diatomic molecule

$$\mu = q * r$$

Where q represents a charge, and r is the distance between those charges.

The dipole moment or the polarity of a molecule is calculated by multiplying two factors: the charges and the distance between them. Isotopes ^{12}C and ^{13}C create single bonds with lengths of 1.5312 and 1.5311 Å respectively when bonded to hydrogen in a methane molecule.[245] This means, the polarity of the molecule with ^{13}C is smaller than the corresponding one with ^{12}C and the weak force interactions will

be stronger in a larger molecule (one with only ^{12}C).

For reference, all the data presented in this thesis was performed using a nonpolar capillary column. The gas used in gas chromatography is inert and has not been shown to influence polarity. This leaves the separation to predominantly rely on the dipole moment of the analyte and stationary phase.[100,246] Therefore, chemical interactions are limited in comparison with liquid chromatography and the main separation mechanism can be described as friction: [48]

Equation 6-3: Friction coefficient

$$f = 380Rp\sigma_{12}^2\left[\frac{2}{T}\left(\frac{1}{M_1}+\frac{1}{M_2}\right)\right]^2$$

In the formula above the R is a gas constant, p is the pressure in atmospheres, σ_{12} is a collision cross section in angstroms, T is absolute temperature in Kelvin, M_n are molecular weights of the analyte and mobile phase. Following the above formula there are two main factors distinguishing two isotopologues: the molecular weight, and the size of a molecule. All the other parameters are dependant of the separation conditions and are identical for all isotopologues of an analyte.

Calculated friction coefficients for the phthalate standards used are presented in the Table 6-5 along with the values used for the calculation. DEP and DBP molecules have 12 and 16 carbon atoms using binomial distribution. There is an approximately 0.6 % to 0.7 % chance of having two or more heavy isotopes in a DEP molecule, and approximately 0.9 % - 1.3% chance in DBP molecule. The values were calculated using a binomial distribution function in R (example of the RStudio code is shown in Appendix C. The percentage of ^{13}C used for this purpose was 0.9626 % and 1.1466 %.[247] The Therefore, the values presented in the Table 6-5 are calculated based on no ^{13}C isotope being present in the molecule or just one.

Friction coefficients are inversely proportional to the velocity of the analyte therefore, greater fiction coefficients will result in slower mass transfer into the stationary phase. The calculated frictions are in line with the observed elution orders. The molecule cross sections are not studied frequently. The cross sections of heavy singly substituted isotopologues of DEP and DBP are estimated based on bond length difference of ~0.0001 Å. The value is based on the difference between ^{13}C-^{12}C (0.007738 Å) and ^{12}C-^{12}C (0.007824 Å). [248]

Table 6-5: Theoretical friction coefficients for DEP and DBP ^{12}C ^{13}C

isotopologues

Isotope	**^{12}C**	**^{13}C**
DEP – Friction Coefficient	**2110671**	**2110614**
DBP – Friction Coefficient	**2966116**	**2966037**
DEP cross section	131.9000 Å[249]	131.8999 Å
DBP cross section	156.4000 Å [249]	156.3999 Å
Pressure	1.01 Atm	
Temperature	352.917 °K	

Sorption and desorption ratios will be the same as the *k* value. The relative isotopic effect for sorption and desorption can be estimated by dividing the retention times of the heavier isotope and the lighter one and this predicts a small change in *k* which results in a change in retention time.

Equation 6-4: Relation of equilibrium to chromatography phase volumes, equilibrium values, time spent in corresponding phases and mean adsorption and desorption times.

$$\frac{R}{1-R} = \frac{V_m}{KV_s} = \frac{c_m}{c_s} = \frac{t_m}{t_s} = \frac{t_a}{t_d}$$

R – retention ratio

V_m, V_s – Mobile and stationary phase volume

K – Partition coefficient

c_m, c_s – Equilibrium values in stationary and mobile phase of the

corresponding concentrations.

t_m, t_s – Average time spent in the mobile and stationary phase

t_a, t_d – Average adsorption and desorption times

The ratio V_m/V_s, affects the proportion of the analyte between those phases as presented by the Equation 6-4. In addition, the longer the analytes spend interacting with the stationary phase the greater its elution time. Based on the column dimensions of 30 m long diameter, 250 µm, and film thickness of 0.25 µm the volume of the mobile phase is 1.5 cm^3 and the volume of the stationary phase is 0.006 cm^3, this results in a ratio between the two phases of 250. With this value k can be assessed.

In standard treatments, zone spreading has three main contributing factors: longitudinal diffusion, sorption and desorption of the analyte between the mobile phase and stationary phase and eddy diffusion. In capillary gas chromatography there are no particles and therefore the eddy diffusion is negligible and therefore can be replaced by the Golay equation (Equation 6-5) for capillary gas chromatography.

Equation 6-5: Simplified Golay equation [250]

$$HETP = \frac{B}{v} + C_m v + C_s v$$

B – *longitudal diffusion*

C_m – *mass transfer in the mobile phase*

C_s – *mass transfer in the stationary phase*

v – average velocity of the mobile phase

When B, C_m, and C_s are substituted the above expression becomes the following:

Equation 6-6: Expanded Golay equation [48]

$$HETP = \frac{2D_m}{v} + \left(\frac{(1 + 6k + 11k^2)d_c^2}{96(1+k)^2 D_m} + \frac{2kd_f^2}{3(1+k)^2 D_s} \right) v$$

In the Equation 6-6, the terms D_m and D_s represent diffusion coefficients in mobile phase and stationary phase respectively; d_c is column diameter, d_f represent a film thickness of the stationary phase.

Diffusion in the respective phases is represented by Equation 6-8 and Equation 6-9 later in this chapter. However, both formulas show that diffusion is proportional to the temperature and inversely proportional to the size of a molecule. Therefore, it is to be expected that GC temperature programs appear to have an apparent effect on the isotope δ values and those change depending on the temperature set up.[242] However, no

research appears to have been performed to investigate the chromatographic effect on the isotope distribution across a peak at different temperature ramps.

When the isotopologues fractionate due to temperature on a gradient this causes a small average temperature difference between them. Diffusion models present the temperature factor as $T^{1.75}$.[251] The average temperature for DEP on a 5 °C/min ramp is 127.961 °C for ^{12}C and 127.957 °C for ^{13}C. Such a temperature difference is expected to have only 0.03% effect on diffusion in the mobile phase.

Since a molecule cross section can be smaller for heavier isotopologues [252,253] this contributes to the explanation of the chromatographic isotope effect that can be deduced from chromatography models and approximations.[48,251] The result indicates the following relationship, the smaller the molecular cross section the smaller the friction coefficient and therefore, less resistance to travel through the chromatographic medium.

6.4.2 Peak broadening

The peak broadening is commonly discussed using the following model:

Equation 6-7: Dependence of the peak width, total diffusion and time

$$\sigma^2 = 2D_t t$$

σ refers to the unit of peak width. Peak width at 50% is equal to 2.35σ. D_t is total diffusion or also referred to effective diffusion. Value t expresses time in seconds. The model assumes gaussian distribution of a peak hence the constant associated between the peak width at 50% and σ.

Discussions about the peak broadening involve some kinetic factors. Most are related to instrument parameters, however, two are related to the isotopologues – the molecular weight and a factor related to the collision cross section. The commonly applied diffusion model was developed by Fuller-Shetler-Giddings as presented below: [254]

Equation 6-8: Fuller-Shetler-Giddings diffusion model

$$D_m = \frac{0.00125T^{1.75}\left(\frac{1}{M_1} + \frac{1}{M_2}\right)^{1/2}}{p\left(\left(\sum V_{i\ solute}\right)^{1/3} + \left(\sum V_{i\ mp}\right)^{1/3}\right)^2}$$

Within the equation T stands for temperature; M_1 and M_2 are molecular weights of the analyte and interacting mobile phase; p is pressure; V_i is

molecular volume.

Similarly, to the friction coefficient (Equation 6-3), there are two factors that contribute to differentiating between the isotopologues: the molecular weight and an expression of the size of a molecule.

The stationary phase must be considered to fully introduce the gas chromatography separation dynamics. Commonly, the diffusion can be presented by Stokes – Einstein formula.[255]

Equation 6-9: Stokes Einstein diffusion equation.

$$D_s = \frac{RT}{6\pi r\eta N}$$

In the formula terms are as follows: R is gas constant; *T* is temperature; *r* is solute molecule radius; *η* is viscosity; and N Avogadro's number.

The isotopomers molecular cross section varies with the isotope position [256,257]. This means the heavier isotope will result in greater uncertainty of the measurements. Based on the models presented in this chapter it can be concluded that under adequate conditions and elongated columns, it would be possible to perform a separation of the isotopomers with a regular GC technique.

6.4.3 Baseline and background signal

Chromatographic baselines can shift and change with the temperature ramp, this can be due to column bleed from the stationary phase or can be an indication of unresolved peaks. In the context of NTIA and CSIA unresolved compounds can introduce errors to the values.

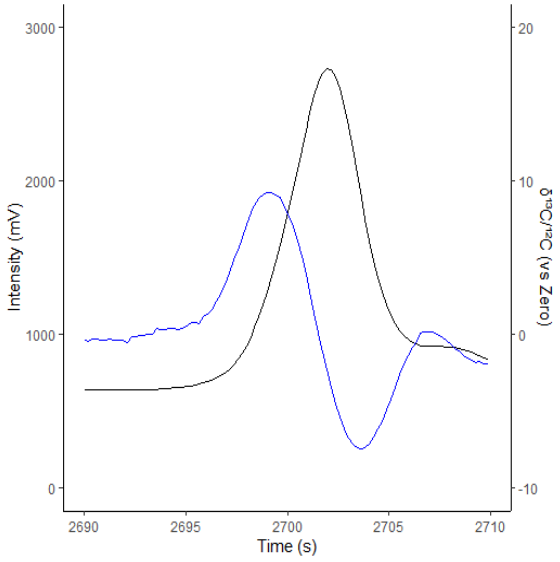

Figure 6-2: Chromatogram of DEHP peak (black) and ratio chromatogram compensated for oxygen using SSH calculation (blue).

Figure 6-2 shows an example of a peak as from a fragment of a complex chromatogram (Figure 4-3) and its corresponding $\delta^{13}C_{zero}$ value across the same time frame. Data shown in Figure 6-2 is a fragment of a full chromatogram depicted in Figure 4-3 and $\delta^{13}C_{Zero}$ value chromatogram in Figure 6-7 which is shown later in this chapter. The chromatographic peak as shown in Figure 6-2 is on a baseline of approximately 700 mV. Typical

analysis would discard such a peak on the basis of the uncertainty of the underlying baseline isotopes and its inhomogeneity. Examining the peak, it is apparent there are minimal / negligible isotopic interferences due to the simple S-shape observed. With support of isotope chromatograms, the peaks on a raised baseline can be used and reported with accurate values as shown on an example in Figure 6-2. Heightened baseline presents to be isotopically homogenous showing negligible effect on the peak.

6.4.4 GC temperature effect on $\delta^{13}C$

As shown previously, the temperature of a GC instrument influences the isotope elution and values, however, the impact has not been previously shown on the underlying isotopic distribution across the peak.

Standards are typically the same compound or very similar chemically to the analyte.[92] However, since all international analysis is done on the VPDB scale, the values are expressed in relation to one compound and by natural consequence there will be comparisons between different compounds. The information about how the compounds compare under different conditions is important, especially as it was demonstrated that chromatographic isotope effects influence isotope results.

To assess this $\delta^{13}C$ values were evaluated across a series of temperature

ramps (Table 6-6, Figure 6-3).

Table 6-6: Isotope effect in relation to the GC temperature ramp.

Ramp °C/min	DEP $\delta^{13}C_{Zero}$ value	DBP $\delta^{13}C_{Zero}$ value
0.253	8.538	3.579
0.5	6.64	3.223
1.0	5.248	1.754
3.0	5.347	1.454
5.0	5.055	0.796
10.0	5.372	1.064
20.0	5.263	0.901
30.0	5.323	0.769
40.0	5.307	1.016
50.0	5.68	1.244
120.0	5.569	1.071

To obtain the values in Table 6-6, all the signals were processed under the same peak start and end conditions, both 0.1 mV · s^{-1}. The GC temperature ramp was tested from 0.253 °C · min^{-1} to 120 °C · min^{-1} respectively. The δ values decreased between 0.253 °C · min^{-1} and 3 °C · min^{-1} indicating an isotope effect related to the temperature programming. The differences between the isotope signals at higher ramp rates were no longer distinguishable due to low data frequency.

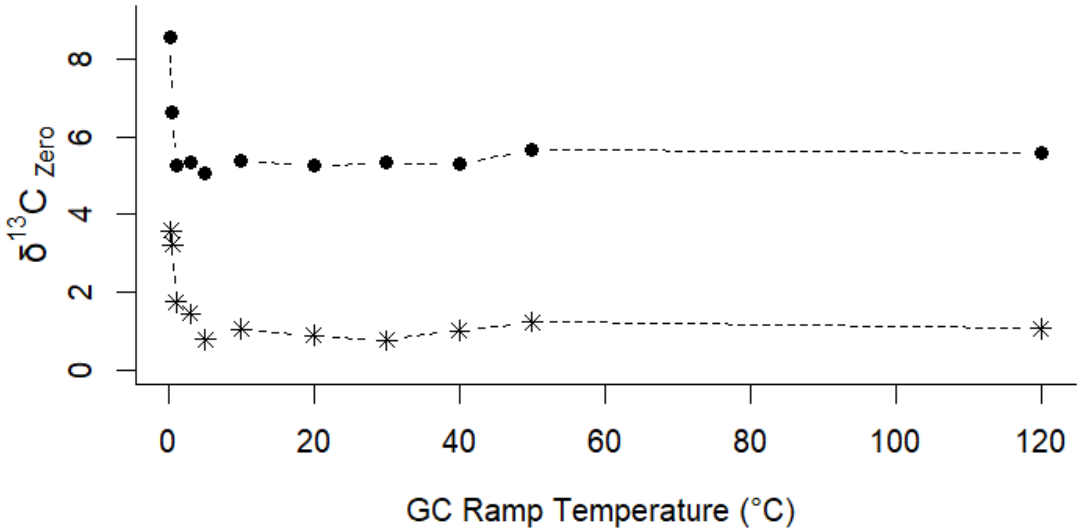

Figure 6-3: Isotope changes of DEP (•) and DBP (*) $\delta^{13}C$ on a zero scale chromatogram (compared against a reference pulse of an IRMS) compensated for oxygen using SSH calculation.

At the ramps of 3 $^{\circ}C \cdot min^{-1}$ and above the isotope values are more reproducible as the standard deviation of the data above that ramp is $\delta^{13}C_{zero}$ 0.2 for both DEP and DBP. The slope of the data from 3 °C/min and above show no significance and slope p-values are above 0.12 (n = 8) for both compounds lacking of statistical significance within this range. This is shown more clearly in a graph of the data in Table 6-6 (Figure 6-3). The R^2 values were calculated as 0.04 and 0.15 for DEP and DBP. Therefore, above 3 $^{\circ}C \cdot min^{-1}$, δ could be considered constant

The data correlate with the changes to the $\delta^{13}C_{Zero}$. Table 6-4 and Table 6-6 present the data of the peak retention time, peak width at 50%, and the corresponding $\delta^{13}C_{Zero}$. This enables calculation of the plate counts – N, and a comparison with the $\delta^{13}C_{Zero}$ value. The results show an initial overall negative correlation between the two parameters. However, the correlation does not meet the statistical significance with p-value of 0.81 (n = 11).

This provides an indication that the excessive column efficiency is detrimental to the isotope values. The largest plate count values correspond to the biggest isotope data spread. When developing a method on GC-IRMS, the temperature ramp needs to be considered. As demonstrated in Figure 6-3, there is a section of rapid change to $\delta^{13}C_{Zero}$ values. Based on the data presented the caution must be taken when comparing data between different GC programmes. This is especially true for low temperatures and long programmes above 1 hour and could vary considerably for different compounds. Although > 3 $^{\circ}C \cdot min^{-1}$ gave constant δ for these compounds and conditions, this is not likely to be general to all compounds and all conditions.

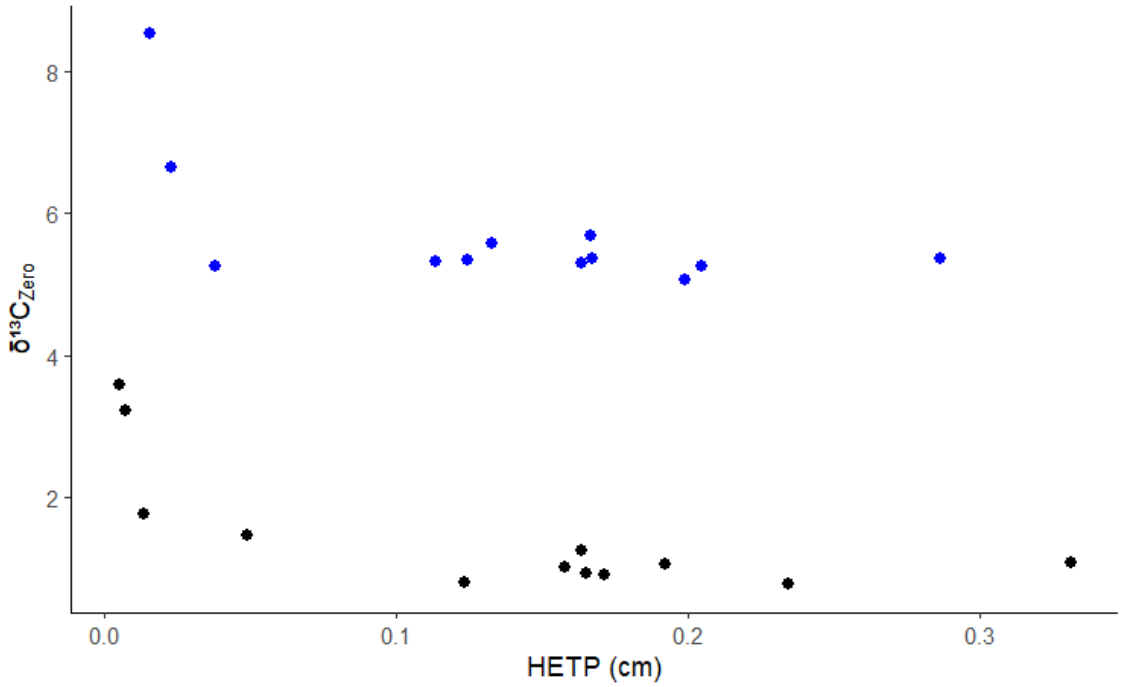

Figure 6-4: Relation between $\delta^{13}C$ and corresponding HETP. Blue markers represents DEP and black are DBP.

The two compounds were taken from the same corresponding manufacturing batches, when measured under different conditions. Therefore, the differences between them were expected to be constant. The δ differences between the DEP and DBP were calculated and expressed as $\delta^{13}C_{zero}$ values, (Figure 6-5) against the GC temperature ramp. Against expectation, the difference in $\delta^{13}C$ value of 1.5 ‰ from 0.253 $^{\circ}C \cdot min^{-1}$ to 3 $^{\circ}C \cdot min^{-1}$. From this point onwards the spread of the data is smaller RSD was calculated as 0.3 $\delta^{13}C$. In this observation, DEP and DBP ($\delta^{13}C$ were shown in Table 6-6: Isotope effect in relation to the GC temperature ramp.) come from the same group of compounds,

solutions were also prepared with both analytes at the same concentration. Therefore, the experimental variability was kept to minimum. This means that a chromatographic bias is being introduced based on the GC temperature parameters and even similar compounds are changing with respect to each other under the same conditions. GC temperature programs used should be of at least 3 °C · min^{-1}.

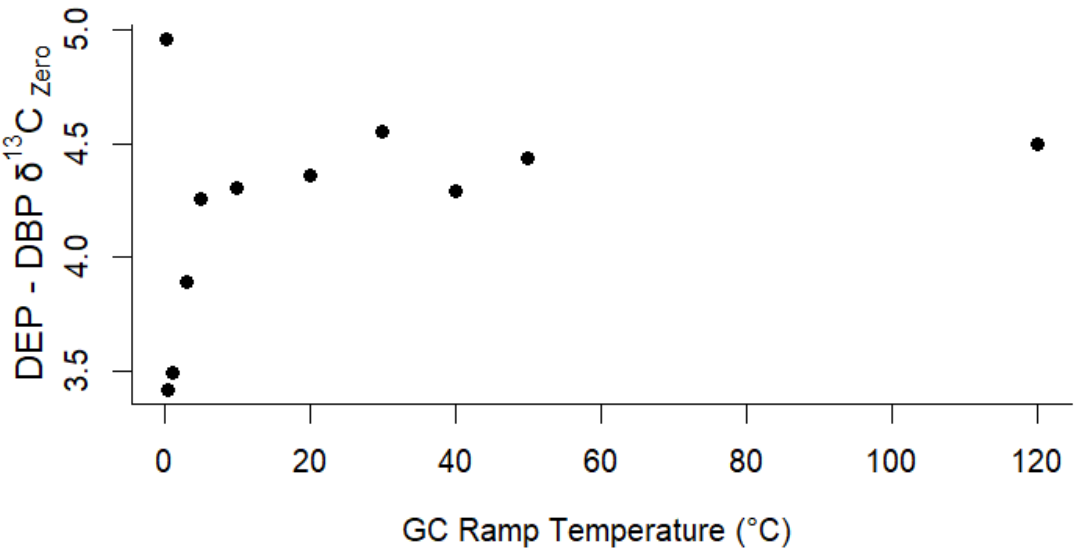

Figure 6-5: Isotope difference changes between DEP and DBP in relation to each other across different temperatures.

As shown above, changing only the temperature may cause chromatographic variability in δ between similar compounds, even when standards are chemically similar. In consequence the comparable

samples may be shifted unless also analysed under the same GC program. This must be taken under consideration whenever GC–C–IRMS results are being compared under different chromatographic conditions.

6.4.5 Complex chromatogram

The previous results discussed the chromatographic effects in the context of standards. The application is intended for challenging complex chromatograms. The following section will discuss isotope effects determined in the complex samples extracted from effluent water from WWTP.

Common practice in isotope analysis does not include examining isotope ratio chromatograms. The primary advantage of changing this is having sight of the individual data points. The specific example would be the analysis of total organic carbon (TOC) determine a bulk $\delta^{13}C$ value. The total content measures the sample as a collective entity disregarding any underlying complexity. The ratio and isotope $\delta^{13}C$ value still contain useful information that is not routinely scrutinised. This section discusses 323 peaks detected, using the software available (IsotDat 3.0), by examining slope changes.

An example of a complex chromatogram can be seen in Figure 1. Using the commercial software (IsoDat 3.0) there were 117 peaks detected with

the start and end slope of 5 mV · s^{-1} and 3 mV · s^{-1}, respectively.

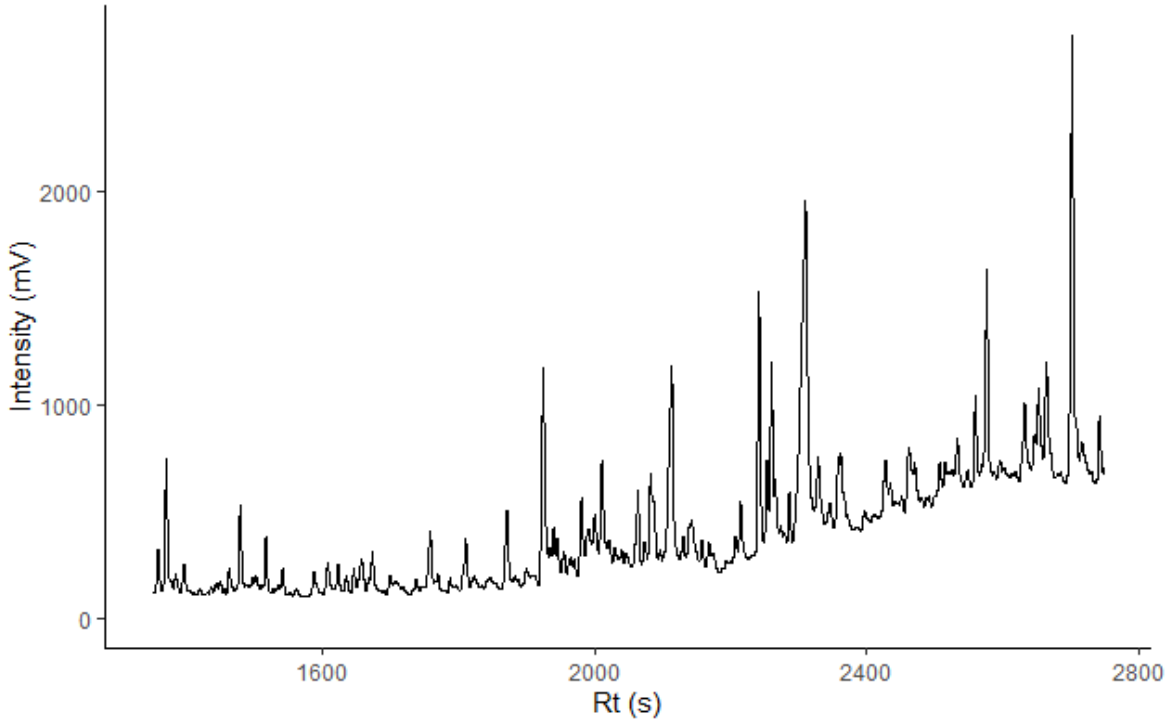

Figure 6-6: An example of a GC-C-IRMS chromatogram – Effluent sample. The reference pulses and the IRMS idle section were removed for simplicity.

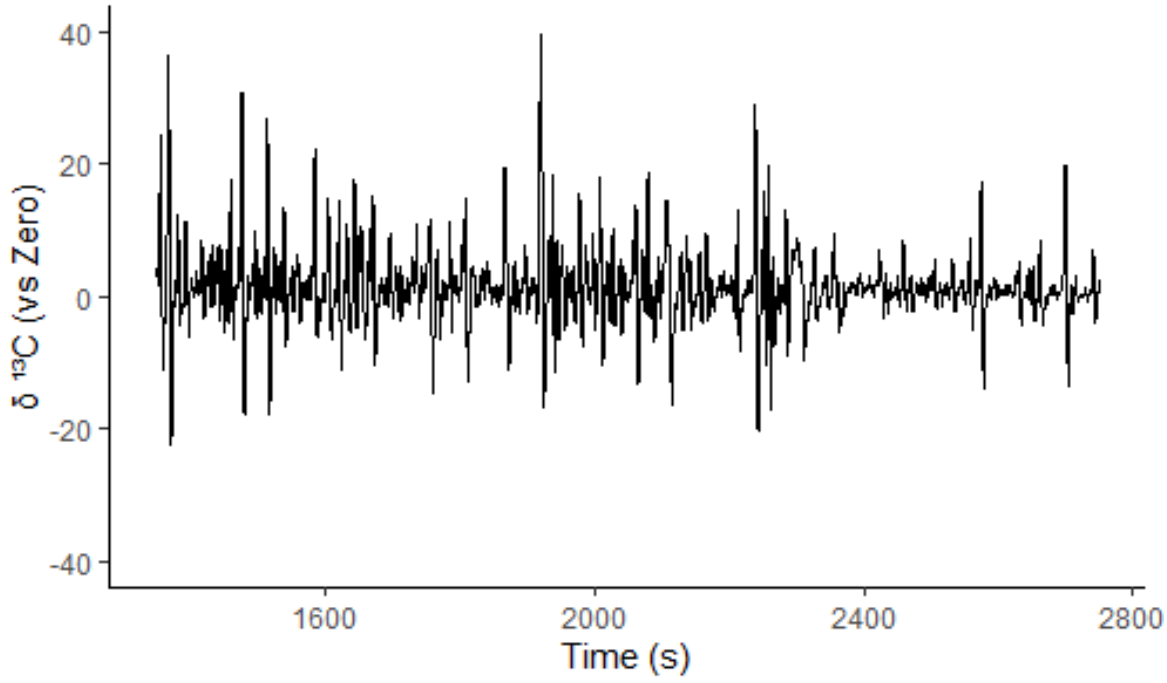

Figure 6-7: Chromatogram of δ $^{13}C_{Zero}$ values.

The above Figure 6-7 presents the delta chromatogram *vs* zero calculated and plotted for every data point of the chromatogram presented in the Figure 6-6. Presentation of data in this way enables examination of the individual peaks through the chromatogram and the $\delta^{13}C_{Zero}$ distribution of complex samples normally represented as homogenised representative number. The approach at this stage does not require the calculating δ against the standards. To examine and express isotope changes within a chromatogram and a peak a zero scale is sufficient. Such non targeted isotope analysis will provide information about the distribution of unknown individual compounds individually and as a wider sample.

Three surface water samples were compared to each other in this manner and tested for isotope drift across the chromatogram (Table 6-7 and Figure 6-8). The drift is represented by the slope calculated between the δ values and retention times. Lack of any significant drift allows to use one standard to measure all peaks. In case of observed drift this can be corrected for.

Table 6-7: Complex sample isotope drift. The samples were performed under the P5 programme.

Sample	**Slope**	**Intercept**	**n**	**SD**	**p-value**
Notts River	-0.000043	0.2987	111	0.48	0.059
Notts Effluent	-0.000028	0.3279	101	0.42	0.185
Foss River	-0.000007	0.2747	111	0.45	0.752

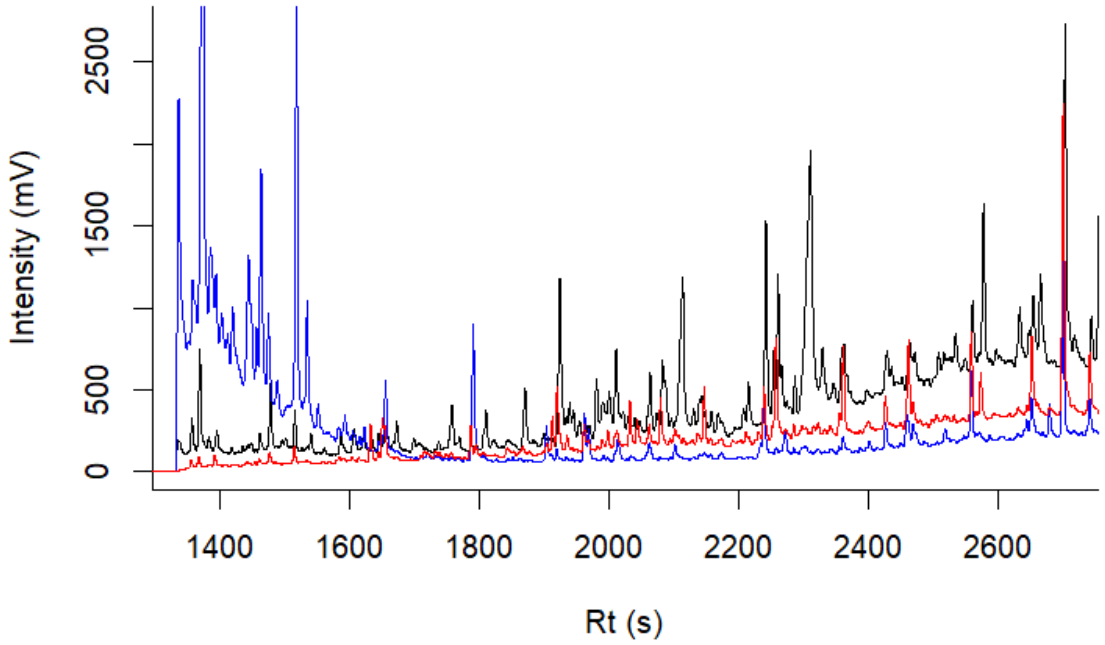

Figure 6-8: An overlay of the three chromatograms. Black – Effluent water, blue – river Foss water, red – river Trent water.

Individually, none of the sample's p-values were below 0.05 indicating lack of 95 % confidence that the slope is significant however any slope can be corrected.[36] Sample collected from the river Trent was measured close with a p value 0.059. Using the peaks on an increased or drifting baseline raises some concerns. A raised baseline would be caused by a multitude of compounds which are not separated. A signal from such unresolved peaks is summed up causing the increased signal. Those underlying compounds, may cause the changes in the chromatographic matrix, this in turn could cause isotopic irregularities across the peak. However, since no slope effect was observed the drifting baseline does

not affect the δ values of compounds.

The real chromatograms can be assessed to determine the extent of NIE and RIE. When all the complex chromatograms were compared using unknown peaks (n=477), three had NIE and 107 peaks showed RIE. The remaining of the peaks could not be determined and may have either effect. The instrument samples data at 5 Hz and this limits the minimum signal differences between isotope channels, below that the difference between the signal are not possible to measure.

When a slope changes from positive values to zero to negative, the centre of the slope measurement window will indicate the centre of the peak. The IRMS sampling frequency is quite low, typically 5–10 Hz. Measuring small changes that would correspond to values below the data collections frequencies is difficult. Using the slope of a peak on either side and their intercept, allows to extrapolate the peak centre.

Therefore Figure 6-9 presents collective retention times that were enhanced by calculating more precise peak maxima based on the inflections of the peak slopes. This was followed by subtracting the *R*t time *m/z* 44 from *m/z* 45. Proportion between the retention times inherently would give a drifting values. The ratio between two values would be greater for higher values than smaller ones (assuming the

difference between them would be the same). Therefore, to expressed the value was expressed as the difference and not a ratio. The difference was divided by the Rt (s) to normalise the data for time. The division was done to because the raw separation can be affected by time over which the separation occurs. The data were obtained by the same gradient GC programme. Therefore, the normalising time also acts as proxy for temperature. The difference above zero (threshold indicate by dashed cut off line) mean the normal isotope effect.

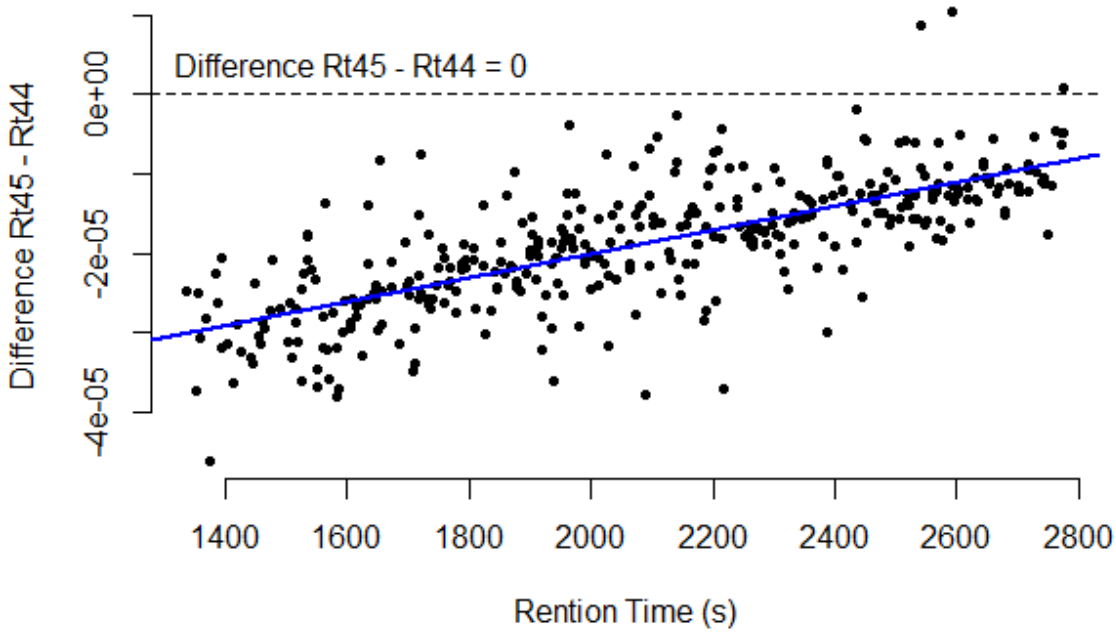

Figure 6-9: Signal differences of the retention times between the signal *m/z* 45 and *m/z* 44. The difference then was divided by retention time in s. Normalised difference < 0 means reverse isotope effect and >0 means normal isotope effect.

This leaves the main factor to be a quality of the molecule itself. The molecular mass and its size correlate with boiling point of the material.[258,259] In the GC analysis longer eluting peaks tend to have higher boiling points and therefore also can have heavier molecular weights. Figure 6-9, presents, for the first time, an indirect correlation of the shift between corresponding signals (isotope effect) and the molecule size. This data shows that early eluting isotope molecules separate more than later ones. Substituting an atom in a small molecule with a heavier isotope has a larger proportional impact on that molecule than a substitution of an isotope on a larger one.

There are three unknown compounds with a positive difference. All of them eluted at higher temperatures also indicating they are of higher molecular weight than the majority. There is a significant relation between the elution time and the extent of an isotopic effect. The normalised slope as demonstrated was calculated to be significant ($p<0.00$; $n=373$).

The same isotopic effect was expected to be observed on the peak width at 50 % parameter. Figure 6-12 presents the ratio of the $W_{0.5}$ between the heavy and light isotope signals. The ratio of 1.0 indicates that there is no observable difference in $W_{0.5}$ between the heavy and light isotope,

ratio of < 1.0 indicate the heavy isotope peak was narrower than the lighter one and therefore showing the reverse isotope effect. Ratios > 1.0 indicate the normal isotope effect.

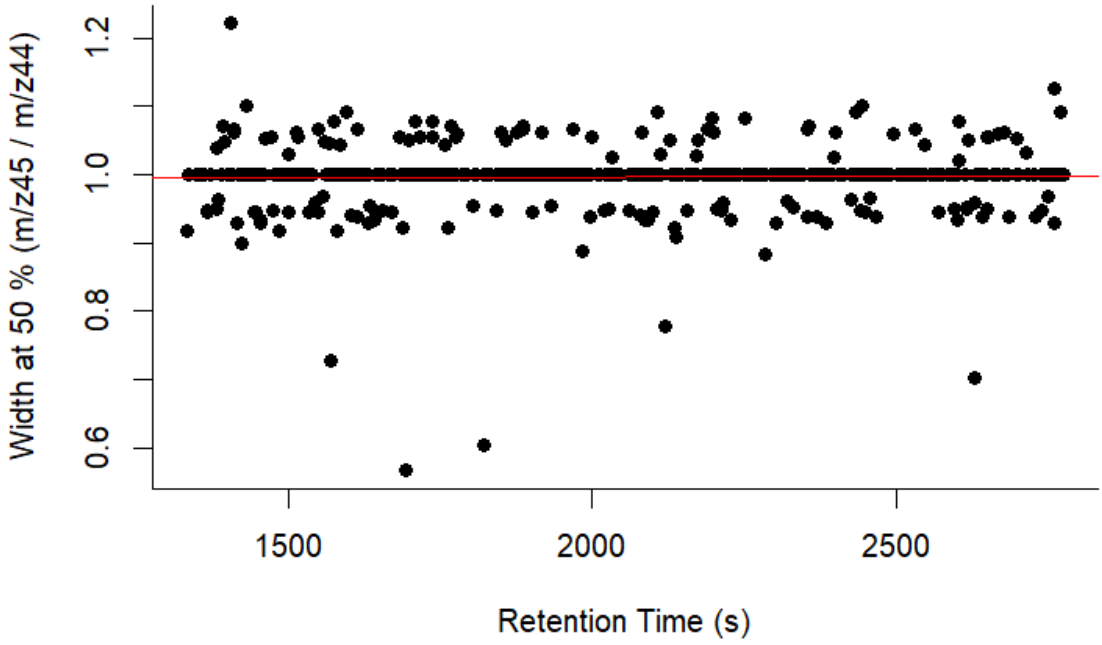

Figure 6-10: Peak width at 50 % ratio between the heavy and light signal. Red line represents slope.

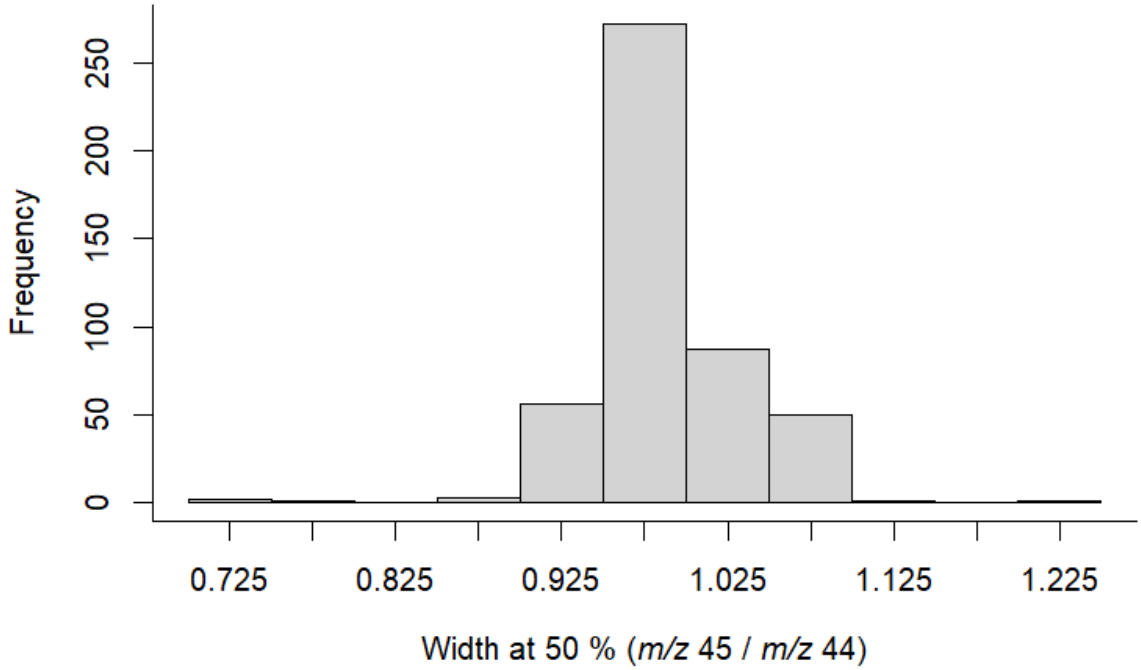

Figure 6-11: Histogram of peak width at 50% ratio between the heavy and light signal.

Figure 6-10 and Figure 6-11 present the ratio of $W_{0.5}$ of the unknown peaks. The average of the ratios is 0.9981345. However no significant trends can be observed. Therefore, this data was bootstrapped using code presented in the Appendix B: Statistical bootstrapping (RStudio script). Because this data is no longer associated with Rt it is presented on a histogram (Figure 6-12).

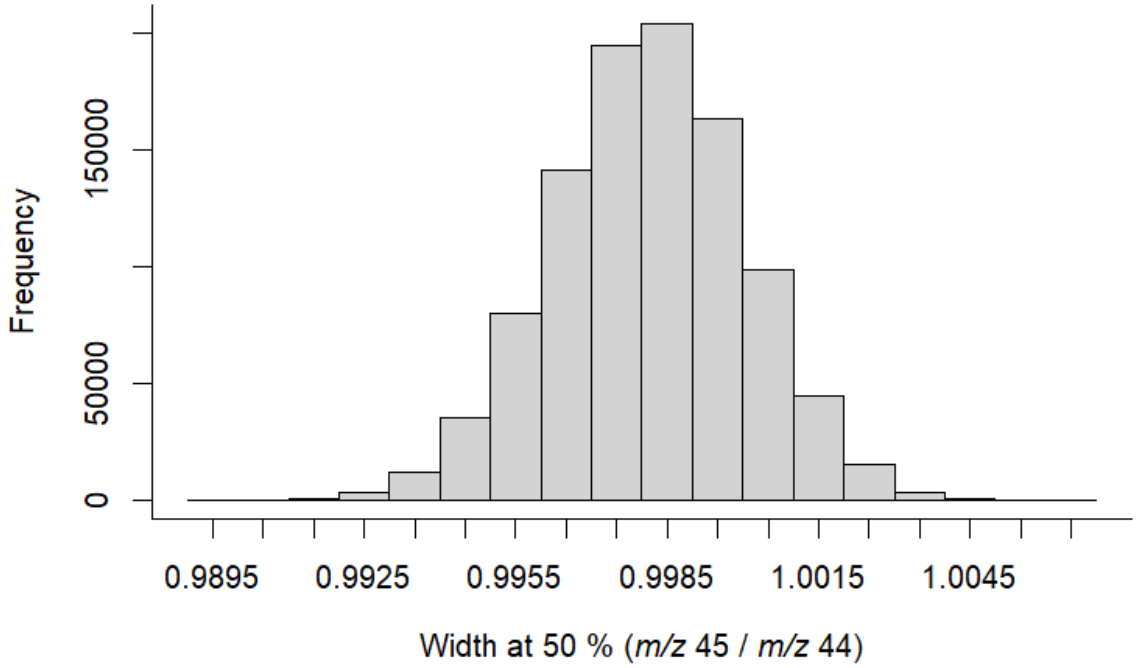

Figure 6-12: Frequency of ratios of peak withs at 50 % presented on a histogram. Initial data bootstrapped to one million datapoints.

When the collective peak width ratios are bootstrapped to n = 1,000,000, the new data set show a significant shift and the ratio is different from 1 according to one sample Wilcox test (p-value is $2.2 * 10^{-16}$). However, the average ratio was 0.9981 with first and third quartile being 0.9969 and 0.9995 (n = 1,000,000), respectively indicate the peak width will affect the accuracy of the results. This means there is a chromatographic effect that affects not only the retention times but the peak broadening as well in both standards and complex sample.

A bond with at least one heavier isotope will have shorter bond length.

Considering molecular cross section contributes to mass transfer terms for both mobile and stationary phases creating difference in retention time and peak width as per Equation 6-6. Combined further with chromatography theory presented in the section 6.4 demonstrates that peak width is dependant on the molecule size. Also, isotopes affect the dipole moment of a bond, further contributing to difference in retention time. There is little discussion in the literature regarding the effects isotopes have on peak widths. This data presented here is new information about chromatographic isotope effect and contributes to the understanding of those effects.

6.4.6 Single vs multi-channel integration

As explained in the earlier section the isotope signals have both retention time and peak dispersion effects. This section presents like for like comparison of the commercial approach and an approach that considers all the channels an individual chromatogram. The goal is to undo clipping of peaks which will differ slightly in retention time and peak width. The commercial approach extends the integration from one channel and projects it onto the remaining ones. However, as shown above, there is an effect on peaks due to the presence of heavy isotopes.

A representative standard was selected to examine the extent of the effect under controlled conditions. Two peaks DEP and DBP were

calculated following the two approaches. The start and end point slope were selected as 2 mV · s^{-1}. The points of interest were selected as the closest datapoint to the nominal value. An example integration is presented in Figure 6-13.

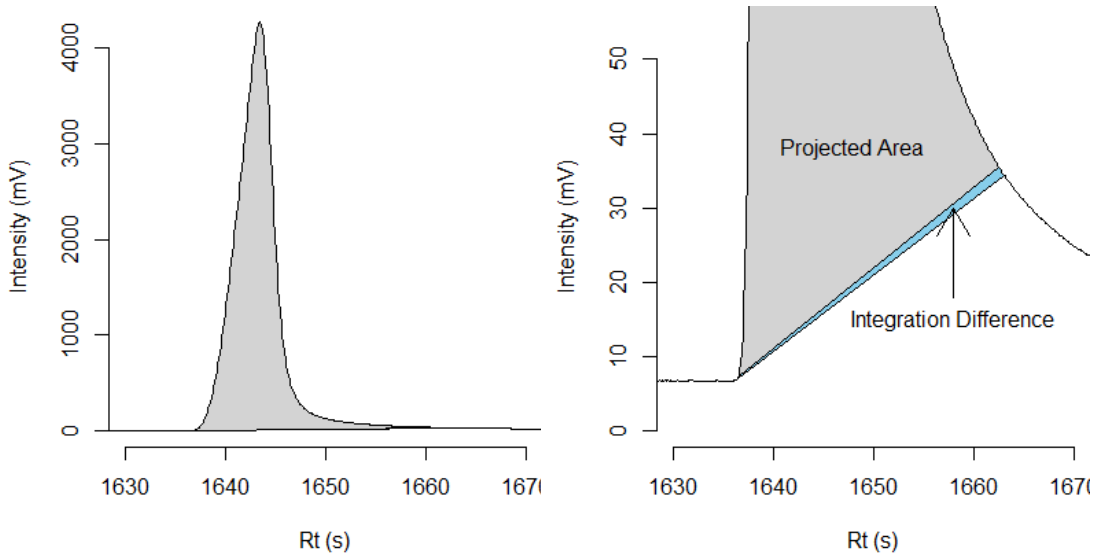

Figure 6-13: Left – an example of DEP peak integration of the *m/z* 45 channel. Start and end points used were projected from channel *m/z* 44 (coloured in grey). Right – zoomed in fragment of the same peak from channel *m/z* 45. Independent integration (was added and highlighted in blue.

The commercial software available used the following approach (grey zone in Figure 6-13). The integration was performed on the peak from the channel *m/z* 44, then the start and end points were considered identical and projected onto channels *m/z* 45 and *m/z* 46. The integration

can be based off any channel however for this purpose the base integration was done on channel *m/z* 44.

Based on the demonstrated differences between peak shapes of heavy and light isotopes an alternative approach is to integrate the channels separately. Figure 6-13 the right side shows a zoomed baseline. The blue area shows the additional space on the channel *m/z* 45 (heavy isotope) after integrating it independently. The exact values of calculated peak areas are presented in the Table 6-8. The extent of the peak area (*m/z* 45) difference is 0.13 % for DEP and 0.18 % for DBP. The difference of the integrations are presented on the channel corresponding to the heavy isotope because the light one was selected as the primary chromatogram. The reason for this selection is related to the lower level of amplification and therefore lower level of noise.

The integrations discussed in this section were applied to the same peak under the same detection conditions. For numerical expression of the effect both approaches were applied to the delta notation substituting the sample with both the commercial approach and standard with independent approach.

Table 6-8: Table presents individual peak areas obtained by two different approaches. *m/z* 45 and 46 start and end point was exactly

the same as the *m/z* 44. The second approach was by integrating the three channels independently. The definition of star and end point was the closest slope point to 2 mV/s.

Peak Areas	**DEP**	**DBP**
m/z 44	16178.8449	14561.0451
m/z 45 (start and end point = *m/z* 44)	18935.8849	16971.5676
m/z 45 integrated independently	18959.9653	17002.5676
m/z 46 (start and end point = *m/z* 44)	21950.4331	19757.5118
m/z 46 integrated independently	22026.3176	19834.4201

The two approaches were calculated using a delta notation with respect to each other. The calculated differences for two standards, DEP and DBP, were 1.26 ‰ and 1.82 ‰ respectively. The values were calculated based on the initial values presented in the Table 6-7. In both cases, applying the same start and end points to all the channels resulted in an increased value for the two phthalates.

This indicates inaccuracies can occur by assuming all isotope chromatograms are chromatographically equivalent. The signals should be treated independently to yield more accurate results. Concluding from the previous sections, the error was inherited from the lack of a better understanding of the isotope effects indicating a need for a reconsideration of how the data is handled.

6.4.7 Slope selection effects

The start and end point are determined by the degree of the slope at the front and tail of a peak expressed as $mV \cdot s^{-1}$. The two points can be determined on one channel and imposed onto the rest of them. Following on the fact that isotopes affect retention time and peak width this aspect of integration needs to be addressed. The signal of the peak presented in Figure 4-3 changes by 54 mV across 3 seconds from 2706 s to 2709s. This is approx. 2.9% of the peak height however the same section of the ratio accounts for 3.0%.

Table 6-9 presents the changes related to the integration aspects of the isotope analysis. The default detection parameter suggestion is start 0.2 ($mV \cdot s^{-1}$) and the end is 0.4 ($mV \cdot s^{-1}$). Therefore, to account for the smaller peaks, the range examined was decided to be from 0.04 mVs and 0.4 mVs. For the start points the difference between the highest and the lowest slope examined is $\delta\ ^{13}C_{zero}$ 0.092‰ and $\delta\ ^{13}C_{zero}$ 0.114‰ for the DEP and DBP respectively. For the same range for the end point slope the result changes $\delta\ ^{13}C_{zero}$ 1.143‰ and $\delta\ ^{13}C_{zero}$ 0.634‰ for the DEP and DBP respectively. The change between the slope detection for the end point and the isotope value is highly correlated (R^2 equals 0.947 and 0.923 for DEP and DBP, respectively). Corresponding R^2 values for the start point were 0.340 and 0.007 indicating very weak correlation. The start and end points changes show that the integration is more sensitive

to end point slope adjustment than the start point. Due to the near linear correlation of the isotope values and the arbitrary slope selection, the isotope chromatogram helps to select both start and end point by applying order of derivatives as a comparable technique that can be used to evaluate both raw chromatogram and isotope ratio.

Table 6-9: Complex sample isotope drift. The samples were performed under the P5 programme.

Start point effect				End point effect			
Start point (mV/s)	**End point (mV/s)**	**DEP (δ $^{13}C_{zero}$)**	**DBP (δ $^{13}C_{zero}$)**	**Start point (mV/S)**	**End point (mV/S)**	**DEP (δ $^{13}C_{zero}$)**	**DBP (δ $^{13}C_{zero}$)**
0.40	0.1	8.717	3.772	0.1	0.40	11.020	5.196
0.37	0.1	8.717	3.545	0.1	0.37	10.780	5.155
0.34	0.1	8.717	3.544	0.1	0.34	10.880	4.832
0.30	0.1	8.771	3.910	0.1	0.30	10.490	4.751
0.27	0.1	8.771	3.916	0.1	0.27	10.210	4.782
0.24	0.1	8.468	3.543	0.1	0.24	10.430	4.691
0.20	0.1	8.625	3.886	0.1	0.20	9.877	4.562
0.17	0.1	8.523	4.076	0.1	0.17	9.265	4.002
0.14	0.1	8.528	3.823	0.1	0.14	9.372	3.456
0.10	0.1	8.538	3.579	0.1	0.10	8.538	3.579
0.07	0.1	8.528	3.823	0.1	0.07	8.552	3.282
0.04	0.1	8.686	3.586	0.1	0.04	8.225	3.109

6.4.8 Peak derivatives

An alternative way to demonstrate the start and end point based on the isotope data is to apply first and second derivatives. Second derivatives are already used in peak detection in chromatographic systems.[260,261] Derivatives can provide a means to compare start and end points for both raw and ratio chromatogram.

The exponentially modified Gaussian (EMG) is commonly used to model real chromatographic data.[262–264] For this work, however, the EMG was selected because it is considered to be one of the most accurate.[265,266] The EMG is defined by μ, σ, and λ. Where μ is the mean, σ is the variance and λ is the exponential rate. In chromatography it will include an intensity adjustment related to peak area and a baseline. The EMG parameters for the model applied are presented in Table 6-10. The model was based on the initial arbitrary sequence from -4, to 5, with increments of 0.05.

Table 6-10: Exponentially modified Gaussian parameters applied to calculate the isotope model.

EMG Parameter	Peak Channel - *m/z* 44	Peak Channel - *m/z* 45
μ	0.06	0
σ	0.4	0.405

λ	5	5.2
Intensity Adjustment	3500	4300
Baseline	80	100

Once the EMG model was calculated (as shown in Figure 6-14) it was used for treating the data in the same way as raw data obtained from the IRMS instrument.

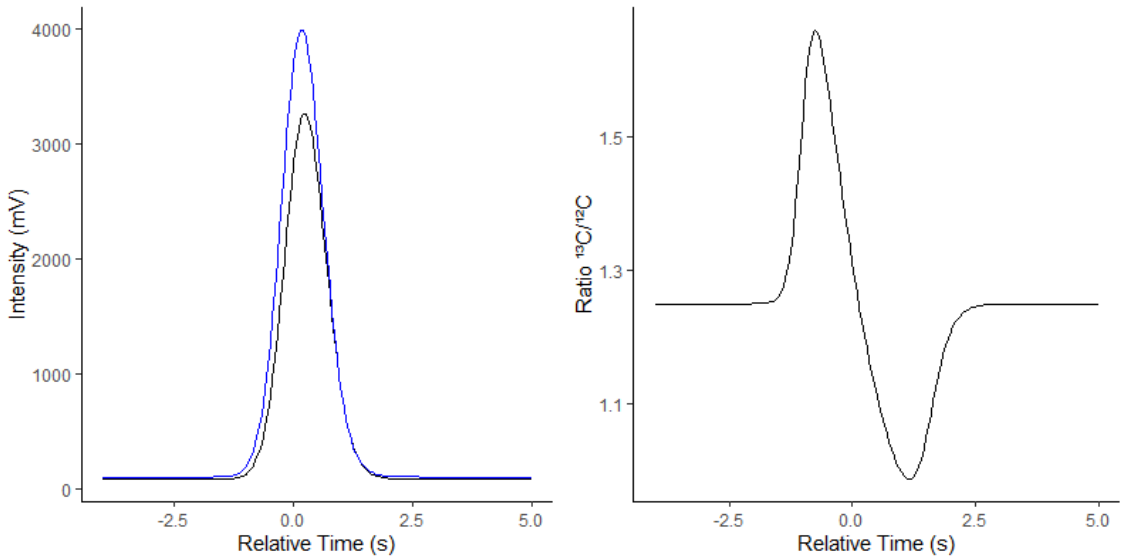

Figure 6-14: Left - EMG modelled peaks for *m/z* 44 (black) and *m/z* 45 (blue). Right - Isotope ratio calculated from EMG modelled peaks.

Due to the rapid changes of the isotope data, it was necessary to obtain derivatives from the raw signal and the isotope ratio chromatogram. The two maxima of the first and second derivatives (raw signal and isotope ratio, respectively) were used to identify the peak start and end point.

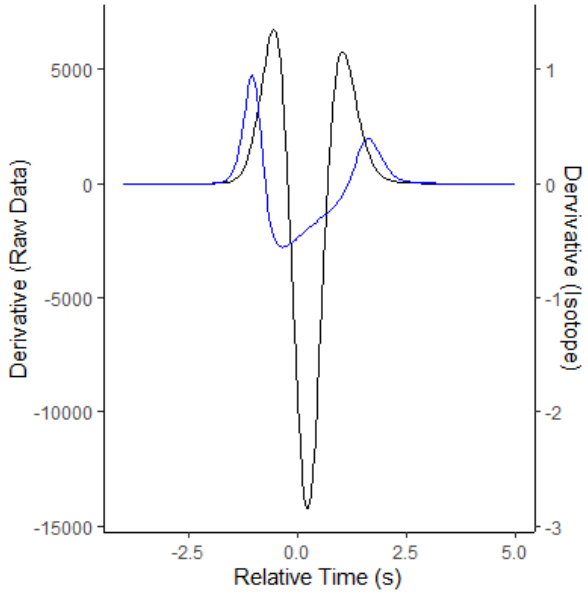

Figure 6-15: Overlayed the first derivative (blue) of the corresponding ratio of the modelled raw signal as shown on left in Figure 26 and second derivates (black) of the modelled signal *m/z* 44 as presented in Figure 26 on the right.

The second order derivative uses the two maxima to define peak start and end point as does the first derivative of the isotope signal ratio. The isotope chromatogram shows the same two points with first order derivative obtained from the isotope chromatogram. Those two points also can be taken as a start and end points of a peak. The two derivatives can be used as a more consistent method to determine the peak start and end point especially in the isotope context.

The two derivatives were compared against each other as presented in

Figure 6-15. The blue trace was the first derivative of the isotope chromatogram and the black trace shows the second derivative of the raw signal corresponding peak. Those two graphs as shown in Figure 6-15 present two maxima each. Those maxima are the identifying points of the peak. The isotope derivative is slightly wider than the raw signal. The peak widths were calculated based on the maxima of the data presented in figure 6. Width calculated for the derivative based on the raw model was 1.60 whereas the width when based on the isotope ratio was 2.65 in arbitrary time units, emulated to be in seconds. A similar effect was observed using the empirical data. The peak width was measured to be 6.7 s based on the chromatogram and 9.4 s based on the signal ratio. The difference was 2.7 s between the two ways of measurement. This indicates that if the second derivative detection was to be applied the results would end up inaccurate. Trying to account for complete isotope data the better approach would be to apply a derivative of the isotope signal. This means that basing an evaluation on the chromatogram alone may be dismissing isotopic data and may affect the accuracy of the isotopic results.

6.5 Conclusion

In this chapter it was demonstrated the importance of examining the isotope data across the peaks. The chromatographic theories and empirical data show the molecular weight and molecular cross section

vary between different isotopologues and affect the resulting chromatography. Relatively little known isotope effect on peak width was examined in more detail. It shows that peak width is a variable that needs to be considered when integrating isotope peaks. The isotope retention time was shown to be affected by GC temperature programme. Those differences affect the final result.

Based on this it is expected that the peak start and end points vary between the isotope channels. It is recommended that the future analysis considers the isotope chromatograms. This practice will help to verify the separation of the peaks in a complex chromatogram but it will also confirm the alignment between the raw signal peak and the isotope peak. Such approach can aid examining the complex chromatograms such as obtained from environmental samples and expands the opportunity to investigate complex samples. It will also assure the completeness of the isotopic data being evaluated.

There is a drift of the differences between the retention time which appears to be due to the molecule itself. The data was obtained using the GC and there is a correlation between the size of the molecule and the boiling point. Therefore, the molecules eluting later in the GC chromatogram will also tend to be larger. Since the chromatographic effect has been shown to be greater for smaller molecules it can be

indirectly correlated with the size of the molecule.

As a widely accepted approach towards the isotope chromatograms, the peak start and end point are applied in the exactly the same manner to all the isotopologue signals.[87] However, based on the observed peak shift some chromatography may require separate processing of each signal to be integrated separately. The suggested approach was to use first derivatives to the isotope signal. The observation supports the feasibility of multi compounds analysis, with some points of caution. A peak of interest should be examined for its isotope ratio signal. Therefore, the scrutiny of the peak chromatogram on the isotope level can prove useful.

This chapter highlights previously unaccounted chromatographic bias GC-C-IRMS analysis. This bias may skew the results between compounds depending on temperature and molecular size. It will have a significant impact on reporting of the isotopic values when comparing those multiple studies that did not use the same temperature setting.

With the natural distribution of the ^{13}C being 1.1 %, approx. 15.3 % of molecules containing 15 carbon atoms will contain at least one heavy isotope atom in its structure. In a molecule with 62 to 63 carbons there is a 50 % chance that the it will contain only ^{12}C or at least one ^{13}C isotope within its structure. However, as the size of the molecule grows so does

the occurrence of the multiple isotope substitutions. Therefore, the position and width of the isotope peaks depends on the molecule shape and where the isotopes are located.

7 Summary and conclusions

The work presented in this thesis considers two approaches to applications of IRMS. First, is an application of the IRMS to the measurement of analytes – phthalates as example compounds. The second aspect discussed were the isotopic effects in gas chromatography This was necessary to explain the effects of gradients and integration and impacts on final values.

Initial work identified phthalates as compounds of interest. To date, there was no information about isotopic composition of phthalates in rivers and WWTPs. Work proceeded by extracting phthalates at trace levels directly from two rivers and a waste water treatment plant. This work reported $\delta^{13}C$ values of the selected phthalates for the first time from a complex aquatic sample at trace levels. DEHP $\delta\ ^{13}C$ was measured at 28.8 ‰ and 28.4 ‰ in the WWTP and the river Trent. The same compound was measured at 27.1 ‰ in river Foss.

Furthermore, the study takes advantage of the linear response of the detector in IRMS to quantify the phthalates. The unorthodox application of GC–C–IRMS resulted in a combined technique of quantification and $\delta\ ^{13}C$ measurement. With this new technique DEHP concentrations were measured between 0.14 to 0.22 $\mu g \cdot L^{-1}$. The combined application of the

isotopic and quantitative determinations has not been reported.The findings in this chapter have been previously published and document the first time carbon isotopes were measured in the phthalates extracted directly from WWTP effluent and river.

The standard deviations obtained for this CSIA technique were in the range from 0.1‰ – 0.2‰. This precision will be the benchmark for this study. When δ13C values of the above phthalates were compared, very small differences were observed between pre- and post-purification of the samples. It should be noted, however, that a small 13C enrichment was observed in two of three samples.

The work has been cited by a review article prepared by the French Geological Survey.[218] They stated that this is an early example of CISA presented from surface waters at low concentrations. It was also stated that this was an important step towards large volume SPE for CSIA. The result of the phthalates presented in chapter 4, were also referred to by the Russian Academy of Science. They compared their results to ones obtained from this study and build on the knowledge about the stable composition of phthalates in surface waters.219 The values presented were comparable to ones presented in these studies. Despite emerging data showing that the phthalates can be of natural origin, currently the data seem to indicate that the phthalates are more of anthropogenic origin.

Non-targeted isotope was also based on a published in a peer reviewed article. This is the first time organic carbon isotopes were measured in an aquatic sample presenting such wide data from one sample and a greater granularity of isotope values.

The $\delta^{13}C$ in environmental samples is usually measured through the combined / average ratio of the sample i.e. organic compounds extracted form water would be homogenised and measured thus. This is a particular case when measuring $\delta\ ^{13}C$ of total organic compounds. During the analysis it became apparent that aside from the compounds of interest there are hundreds of unidentified compounds that could be used for additional information.

A new approach proposed in this chapter outlines a technique which allows the measurement of the complex sample with greater granularity. The method will have benefits and applications in environmental pollution studies. The approach has shown that it can be used for surface waters. The results obtained from those can be applied as a wide scale screening or targeted analysis. The benefit it provides is the combined approach of isotope ratio evaluation and quantitative analysis. This will allow detection of abnormal isotopes which in turn can be indicators of their origin. Combined quantitative aspect may prove particularly useful if the sample size is limited. Next steps suggested to this approach would be to

measure illicit drugs such as cocaine extracted directly in surface water.

Due to the nature of the IRMS, it was proposed that regardless of the molecule it is still possible to determine its $\delta^{13}C$ value. When averaged, the $\delta^{13}C$ values for all the peaks the total organic volatile carbon were 28.6, 30.8 and 29.7 ‰ in WWTP, river Trent and Foss respectively. The correlation value between the two rivers was 0.96 and it was not significant when comparing the WWTP effluent to river water.

The following chapter presents and elaborates on isotopic effects in gas chromatography. Relatively little is known about those effects despite a wide application of the technique.[36] Isotope chromatographic effect is when light isotope travels faster through a chromatographic column than its heavier counterparts. There is a second effect - a reverse isotope effect, when the elution order is opposite. Both effects are results of the differences in the cross-sections of the molecules due to affected bond energies. The heavier molecules can have slightly smaller cross-sections than the lighter counterparts. This affects the dipole moment and any interactions that result from this, between the analyte molecules and other taking part in the chromatographic separation.

Current integration practice determines start and end points of a base signal and applies them to the remaining channels. Such approach

dismisses both isotope effects. However, when measured the values can be shifted by over one unit. The peak detection happens by setting up a slope gradient for the beginning and end of the peak. The level of the gradient can affect the measured result by as much as 2 – 3 ‰.

An overlay of the signal ratio and the signal alone showed there that there is isotopic information systematically being dismissed. There is still isotope data before a start and after the end of a typical peak. This data difference can contribute to as much as 2.7 ‰ between the $\delta^{13}C$ values as obtained from a chromatographic peak and based off the ratio the signals and this highlights the importance of more thorough evaluation of peaks.

Work presented aimed to measure compound specific isotope ratio of selected phthalates. Once CISA was achieved, the collected data were further utilised to examine the unknown compounds and new tool of non-targeted isotope analysis was proposed. NTIA was supported by model studies and chromatographic effects. Chromatographic effects show that the GC temperature gradient has an effect on the isotope values as well as the integration method of peaks.

8 Future perspective

Any future, environmental studies will benefit from the non-targeted analysis and the hybrid method of quantitative compound specific isotope analysis of individual compounds. Many studies using the CSIA approach could apply these techniques from this point on. There are multiple paths the work can be continued on any compound of interest in dilute system.

The NTIA and quantitative CSIA has a great potential for range of applications. Every study involving CSIA, can use those methods. Future work can include screening of organic compounds. All the work here was demonstrated based on carbon isotope, however more information can be gained if similar studies are done with other elements in parallel. A two dimensional isotope studies allow for better distinction between study subject groups.[267] Experiment, presented in chapter 5 looking at nitrogen, hydrogen or oxygen elements would be a next stage development of this work. Nitrogen could be suggested for such work as it is quite common element in the environment but also it is quite rarely present in GC column make up. This could mean even with a gradient temperature the column interference with this element would be minimised.

In the work presented here the NTIA is performed using a GC. However,

this can be extended to HPLC / UPLC. A good screening method could be using 250 mm HPLC RP C18 column. Such approach is commonly used for wide spectrum analysis allowing to screen for a wide range of compounds. With an isocratic method many compounds still could be screened at once. Gradient method may not be suitable for isotope analysis as changes in make up can shift isotope background and that may limit the elements gradient liquid chromatography could be used for.

All of those aspects can be applied to a range of different compounds. This work focused on phthalates, however, other compounds with environmental impacts should be looked into. For example, illicit drugs are being detected in surface waters all over the world. This may involve larger scale extraction. For example, cocaine concentration in rivers is between <1 ng · L^{-1} to over 700 ng · L^{-1}.[268] With similar sensitivity of analysis, comparable levels of extraction may be required.

Thakur presented an effect of sp^2 and sp^3 isotope location.[100] Further questions remain about more complex samples. Would the extent of the effect be the same if an isotope was located at a different sp^2 and sp^3 location / position? Such knowledge could help in modelling the chromatography. This in turn would help with narrowing compounds of interest from a wide and complex chromatogram. For example, having a complex sample can be challenging in identifying the components that

research could focus on. This can require an additional testing and multiple techniques. Being able to understand different behaviours will help study pollutants in the environment by setting an expectation for the outcome. Any outliers from that can be of potential further interest.

An interesting aspect of the approaches presented in this thesis would be to measure a wide spectrum of compounds for their isotope values along the river. Understanding of such changes might allow for a back calculation to the point of origin but also environmental sinks. An approach in theory could be done from concentration changes. However, this would require knowing an initial concentration. Isotope approach might avoid such limitation. For example, with multiple WWTPs located along the same river all discharging the same compound of the same origin by knowing the rate of isotopic fractionations it could be possible to pinpoint the primary plant discharging the pollution.

Bibliography

1 K. Bunzel, M. Kattwinkel and M. Liess, Effects of organic pollutants from wastewater treatment plants on aquatic invertebrate communities, *Water Res*, 2013, **47**, 597–606.

2 B. G. de la Torre and F. Albericio, The pharmaceutical industry in 2022: an analysis of FDA drug approvals from the perspective of molecules, *Molecules*, 2023, **28**, 1038.

3 T. Deblonde, C. Cossu-Leguille and P. Hartemann, Emerging pollutants in wastewater: A review of the literature, *Int J Hyg Environ Health*, 2011, **214**, 442–448.

4 C. Di Marcantonio, A. Chiavola, S. Dossi, G. Cecchini, S. Leoni, A. Frugis, M. Spizzirri and M. R. Boni, Occurrence, seasonal variations and removal of Organic Micropollutants in 76 Wastewater Treatment Plants, *Process Safety and Environmental Protection*, 2020, **141**, 61–72.

5 S. Choi, H. Yoom, H. Son, C. Seo, K. Kim, Y. Lee and Y. M. Kim, Removal efficiency of organic micropollutants in successive wastewater treatment steps in a full-scale wastewater treatment plant: Bench-scale application of tertiary treatment processes to improve removal of organic micropollutants persisting after secondary treatment, *Chemosphere*, 2022, **288**, 132629.

6 A. Ofrydopoulou, C. Nannou, E. Evgenidou, A. Christodoulou and D.

Lambropoulou, Assessment of a wide array of organic micropollutants of emerging concern in wastewater treatment plants in Greece: Occurrence, removals, mass loading and potential risks, *Science of The Total Environment*, 2022, **802**, 149860.

7 J. A. Pemberton, C. E. M. Lloyd, C. J. Arthur, P. J. Johnes, M. Dickinson, A. J. Charlton and R. P. Evershed, Untargeted characterisation of dissolved organic matter contributions to rivers from anthropogenic point sources using direct-infusion and high-performance liquid chromatography/Orbitrap mass spectrometry, *Rapid Communications in Mass Spectrometry*, 2020, **34**, e8618.

8 R. Carson, Silent spring III, *New Yorker*.

9 N. Ranjan, P. K. Singh and N. S. Maurya, Pharmaceuticals in water as emerging pollutants for river health: A critical review under Indian conditions, *Ecotoxicol Environ Saf*, 2022, **247**, 114220.

10 S. P. Mathur, Phthalate Esters in the Environment: Pollutants or Natural Products?, *J Environ Qual*, 1974, **3**, 189–197.

11 E. Zuccato, C. Chiabrando, S. Castiglioni, D. Calamari, R. Bagnati, S. Schiarea and R. Fanelli, Cocaine in surface waters: A new evidence-based tool to monitor community drug abuse, *Environ Health*, 2005, **4**, 14.

12 B. De Felice, N. Salgueiro-González, S. Castiglioni, N. Saino and M. Parolini, Biochemical and behavioral effects induced by cocaine exposure to Daphnia magna, *Science of The Total Environment*,

2019, **689**, 141–148.

13 E. J. Mersereau, S. L. Poitra, A. Espinoza, D. A. Crossley and T. Darland, The effects of cocaine on heart rate and electrocardiogram in zebrafish (Danio rerio), *Comparative Biochemistry and Physiology Part C: Toxicology & Pharmacology*, 2015, **172–173**, 1–6.

14 M. K. Fontes, P. L. R. Dourado, B. G. de Campos, L. A. Maranho, E. A. de Almeida, D. M. de S. Abessa and C. D. S. Pereira, Environmentally realistic concentrations of cocaine in seawater disturbed neuroendrocrine parameters and energy status in the marine mussel Perna perna, *Comparative Biochemistry and Physiology Part C: Toxicology & Pharmacology*, 2022, **251**, 109198.

15 The Rivers Trust, Water pollution, https://theriverstrust.org/key-issues/water-quality#main-content, (accessed 27 May 2024).

16 Esme Stallard, Water pollution: How clean are the UK's rivers and lakes?, https://www.bbc.co.uk/news/science-environment-59898988, (accessed 27 May 2024).

17 Alex Clark, England's sewage crisis: how polluted is your local river and which regions are worst hit?, https://www.theguardian.com/environment/ng-interactive/2024/mar/27/englands-sewage-crisis-how-polluted-is-your-local-river-and-which-regions-are-worst-hit, (accessed 27 May 2024).

18 Victoria Seabrook, Shellfish industry on a 'knife edge' as sewage

dumped in designated waters for 192,000 hours last year, https://news.sky.com/story/shellfish-industry-on-a-knife-edge-as-sewage-dumped-in-designated-waters-for-192-000-hours-last-year-13126372#:~:text=Untreated%20sewage%20was%20released%20into,Democrats%2C%20shared%20with%20Sky%20News., (accessed 27 May 2024).

19 Z. Muccio and G. P. Jackson, Simultaneous Identification and δ13C Classification of Drugs Using GC with Concurrent Single Quadrupole and Isotope Ratio Mass Spectrometers, *J Forensic Sci*, 2011, **56**, S203–S209.

20 S. De Graaf, H. B. Vonhof, T. Weissbach, J. A. Wassenburg, E. J. Levy, T. Kluge and G. H. Haug, A comparison of isotope ratio mass spectrometry and cavity ring-down spectroscopy techniques for isotope analysis of fluid inclusion water, *Rapid Communications in Mass Spectrometry*, 2020, **34**, e8837.

21 B. Chidimuro, M. Holst, S. Newman, K. Keefe, M. J. Collins and M. Alexander, Grim up North? Exploring the diet of urban populations in post-medieval Greater Manchester, England, using stable isotope analysis, *Archaeol Anthropol Sci*, 2023, **15**, 174.

22 G. Sammarco, M. Rossi, M. Suman, D. Cavanna, C. Dall'Asta and P. Iacumin, in *EGU General Assembly Conference Abstracts*, 2021, pp. EGU21-4554.

23 N. Zorrozua, A. Egunez, A. Aldalur, A. Galarza, B. Diaz, J. Hidalgo, L. Jover, C. Sanpera, I. Castège and J. Arizaga, Evaluating the effect of distance to different food subsidies on the trophic ecology of an opportunistic seabird species, *J Zool*, 2020, **311**, 45–55.

24 J. Jouzel, R. B. Alley, K. M. Cuffey, W. Dansgaard, P. Grootes, G. Hoffmann, S. J. Johnsen, R. D. Koster, D. Peel and C. A. Shuman, Validity of the temperature reconstruction from water isotopes in ice cores, *J Geophys Res Oceans*, 1997, **102**, 26471–26487.

25 S. J. Johnsen, D. Dahl-Jensen, W. Dansgaard and N. Gundestrup, Greenland palaeotemperatures derived from GRIP bore hole temperature and ice core isotope profiles, *Tellus B: Chemical and Physical Meteorology*, 1995, **47**, 624–629.

26 R. H. Tykot, in *Physics methods in archaeometry*, IOS press, 2004, pp. 433–444.

27 J. A. Lee-Thorp, On isotopes and old bones, *Archaeometry*, 2008, **50**, 925–950.

28 R. Aguilera, T. E. Chapman, H. Pereira, G. C. Oliveira, R. P. Illanes, T. F. Fernandes, D. A. Azevedo and F. A. Neto, Drug testing data from the 2007 Pan American Games: δ 13C values of urinary androsterone, etiocholanolone and androstanediols determined by GC/C/IRMS, *J Steroid Biochem Mol Biol*, 2009, **115**, 107–114.

29 R. Aguilera, C. K. Hatton and D. H. Catlin, Detection of epitestosterone doping by isotope ratio mass spectrometry, *Clin*

Chem, 2002, **48**, 629–636.

30 E. K. Shibuya, J. E. Souza Sarkis, O. N. Neto, M. Z. Moreira and R. L. Victoria, Sourcing Brazilian marijuana by applying IRMS analysis to seized samples, *Forensic Sci Int*, 2006, **160**, 35–43.

31 E. K. Shibuya, J. E. S. Sarkis, O. Negrini-Neto and L. A. Martinelli, Carbon and nitrogen stable isotopes as indicative of geographical origin of marijuana samples seized in the city of São Paulo (Brazil), *Forensic Sci Int*, 2007, **167**, 8–15.

32 L. van Roij, A. Sluijs, J. J. Laks and G.-J. Reichart, Stable carbon isotope analyses of nanogram quantities of particulate organic carbon (pollen) with laser ablation nano combustion gas chromatography/isotope ratio mass spectrometry, *Rapid Communications in Mass Spectrometry*, 2017, **31**, 47–58.

33 I. J. Buerge, T. Poiger, M. D. Müller and H.-R. Buser, Caffeine, an Anthropogenic Marker for Wastewater Contamination of Surface Waters, *Environ Sci Technol*, 2003, **37**, 691–700.

34 K. Schreglmann, M. Hoeche, S. Steinbeiss, S. Reinnicke and M. Elsner, Carbon and nitrogen isotope analysis of atrazine and desethylatrazine at sub-microgram per liter concentrations in groundwater., *Anal Bioanal Chem*, 2013, **405**, 2857–2867.

35 D. C. Gooddy, M. J. Bowes, D. J. Lapworth, A. L. Lamb, P. J. Williams, R. J. Newton, C. L. Davies and B. W. J. Surridge, Evaluating the stable isotopic composition of phosphate oxygen as

a tracer of phosphorus from waste water treatment works, *Applied Geochemistry*, 2018, **95**, 139–146.

36 P. J. H. Dunn and J. F. Carter, *Publication of the second edition of the FIRMS Good Practice Guide for Isotope Ratio Mass Spectrometry*, 2018, vol. 11.

37 L.-J. Zeng, Y.-H. Huang, H. Lü, J. Geng, H.-M. Zhao, L. Xiang, H. Li, Y.-W. Li, C.-H. Mo, Q.-Y. Cai and Q. X. Li, Uptake pathways of phthalates (PAEs) into Chinese flowering cabbage grown in plastic greenhouses and lowering PAE accumulation by spraying PAE-degrading bacterial strain, *Science of The Total Environment*, 2022, **815**, 152854.

38 W. Wilcke, M. Krauss and W. Amelung, Carbon isotope signature of polycyclic aromatic hydrocarbons (PAHs): Evidence for different sources in tropical and temperate environments?, *Environ Sci Technol*, 2002, **36**, 3530–3535.

39 R. Paul Philp, in *Introduction to Environmental Forensics: Third Edition*, Academic Press, San Diego, 2014, pp. 395–455.

40 P. Pérez-Rodríguez, A.-D. Schmitt, S. Gangloff, J. Masbou and G. Imfeld, Plants affect the dissipation and leaching of anilide pesticides in soil mesocosms: Insights from compound-specific isotope analysis (CSIA), *Agric Ecosyst Environ*, 2021, **308**, 107257.

41 S. Castiglioni, R. Bagnati, M. Melis, D. Panawennage, P. Chiarelli, R. Fanelli and E. Zuccato, Identification of cocaine and its metabolites

in urban wastewater and comparison with the human excretion profile in urine, *Water Res*, 2011, **45**, 5141–5150.

42 J. Dueñas-Moreno, I. Vázquez-Tapia, A. Mora, P. Cervantes-Avilés, J. Mahlknecht, M. V Capparelli, M. Kumar and C. Wang, Occurrence, ecological and health risk assessment of phthalates in a polluted urban river used for agricultural land irrigation in central Mexico, *Environ Res*, 2024, **240**, 117454.

43 C. Torrentó, R. Bakkour, G. Glauser, A. Melsbach, V. Ponsin, T. B. Hofstetter, M. Elsner and D. Hunkeler, Solid-phase extraction method for stable isotope analysis of pesticides from large volume environmental water samples, *Analyst*, 2019, **144**, 2898–2908.

44 R. Bakkour, J. Bolotin, B. Sellergren and T. B. Hofstetter, Molecularly Imprinted Polymers for Compound-Specific Isotope Analysis of Polar Organic Micropollutants in Aquatic Environments, *Anal Chem*, 2018, **90**, 7292–7301.

45 C. Wabnitz, W. Chen, M. Elsner and R. Bakkour, Quartz Crystal Microbalance as a Holistic Detector for Quantifying Complex Organic Matrices during Liquid Chromatography: 2. Compound-Specific Isotope Analysis, *Anal Chem*, 2024, **96**, 7436–7443.

46 M. Blessing, M. A. Jochmann and T. C. Schmidt, Pitfalls in compound-specific isotope analysis of environmental samples, *Anal Bioanal Chem*, 2008, **390**, 591–603.

47 M. Elsner and G. Imfeld, Compound-specific isotope analysis (CSIA)

of micropollutants in the environment - current developments and future challenges, *Curr Opin Biotechnol*, 2016, **41**, 60–72.

48 J. C. Giddings, *Unified separation science*, Wiley New York, 1991.

49 T. Engel and P. Reid, *Physical Chemistry*, Pearson Education, Inc, 3rd edn.

50 H. Eyring, The Zero Point Energy and the Separation of Isotopes, *Proceedings of the National Academy of Sciences*, 1933, **19**, 78–81.

51 H. J. A. Dale, A. G. Leach and G. C. Lloyd-Jones, Heavy-Atom Kinetic Isotope Effects: Primary Interest or Zero Point?, *J Am Chem Soc*, 2021, **143**, 21079–21099.

52 Z. C. Kornblum and T. Ishida, Isotope effect on the zero point energy shift upon condensation. I. Formulation and application to ethylene, methane, and fluoromethanes, *J Chem Phys*, 1978, **69**, 1814–1825.

53 M. H. O'Leary, Carbon isotope fractionation in plants, *Phytochemistry*, 1981, **20**, 553–567.

54 M. Zhou, Y. Tian, W. Fei and J. Wu, Fractionation of isotopic methanes with metal–organic frameworks, *The Journal of Physical Chemistry C*, 2019, **123**, 7397–7407.

55 P. Baertschi, W. Kuhn and H. Kuhn, Fractionation of isotopes by distillation of some organic substances [3], *Nature*, 1953, **171**, 1018–1020.

56 W. J. Stahl, Compositional changes and 13C/12C fractionations

during the degradation of hydrocarbons by bacteria, *Geochim Cosmochim Acta*, 1980, **44**, 1903–1907.

57 A. T. Shepard, N. D. Danielson, R. E. Pauls, N. H. Mahle, P. J. Taylor and L. B. Rogers, *Gas-chromatographic fractionations of stable isotopes of carbon and oxygen in carbon dioxide*, Georgia Univ., Athens (USA). Dept. of Chemistry, 1975.

58 J. R. Huffman and H. C. Urey, Separation of Oxygen Isotopes by a Fractionating Column, *Ind Eng Chem*, 1937, **29**, 531–535.

59 Y. Chikaraishi, H. Naraoka and S. R. Poulson, Hydrogen and carbon isotopic fractionations of lipid biosynthesis among terrestrial (C3, C4 and CAM) and aquatic plants, *Phytochemistry*, 2004, **65**, 1369–1381.

60 H. Liu, Z. Wu, X. Huang, C. Yarnes, M. Li and L. Tong, Carbon isotopic fractionation during biodegradation of phthalate esters in anoxic condition, *Chemosphere*, 2015, **138**, 1021–1027.

61 J. Gao, Computation of kinetic isotope effects for enzymatic reactions, *Sci China Chem*, 2011, **54**, 1841–1850.

62 C. Roos, Clean Heat and Power Using Biomass Gasification for Industrial and Agricultural Projects.

63 W. Meier-Augenstein, Applied gas chromatography coupled to isotope ratio mass spectrometry, *J Chromatogr A*, 1999, **842**, 351–371.

64 P. A. de Groot, in *Handbook of Stable Isotope Analytical Techniques*,

Elsevier, Amsterdam, 2009, pp. ix–xxiii.

65 L. M. San-Emeterio, N. T. Jiménez-Morillo, L. Reina, V. Vinciguerra, P. Menéndez and J. A. González-Pérez, Pyrolysis carbon compound-specific isotope analysis (Py-CSIA) of Eucalyptus spp. bark and the extracted lignin, *J Anal Appl Pyrolysis*, 2023, **170**, 105896.

66 R. J. S. Lacombe, V. Giuliano, S. M. Colombo, M. T. Arts and R. P. Bazinet, Compound-specific isotope analysis resolves the dietary origin of docosahexaenoic acid in the mouse brain [S], *J Lipid Res*, 2017, **58**, 2071–2081.

67 J. Plewa and J. Skrzypek, Kinetics of the reduction of copper oxide with carbon monoxide, *Chem Eng Sci*, 1989, **44**, 2817–2824.

68 J. Sikora, B. Kania and J. Mroczka, Thermionic Electron Beam Current and Accelerating Voltage Controller for Gas Ion Sources, *Sensors*, 2021, **21**, 2878.

69 J. H. Gross, in *Mass Spectrometry: A Textbook*, ed. J. H. Gross, Springer International Publishing, Cham, 2017, pp. 29–84.

70 S. Meyerson and R. W. Vander Haar, Multiply Charged Organic Ions in Mass Spectra, *J Chem Phys*, 1962, **37**, 2458–2462.

71 T. D. Mark, Fundamental aspects of electron impact ionization, *International Journal of Mass Spectrometry and Ion Physics*, 1982, **45**, 125–145.

72 E. De Hoffmann and V. Stroobant, *Mass spectrometry: principles and applications*, John Wiley & Sons, 2007.

73 V. S. Sevastyanov, *Isotope Ratio Mass Spectrometry of Light Gas-Forming Elements*, CRC Press, 2016.

74 T. B. Coplen, Guidelines and recommended terms for expression of stable-isotope-ratio and gas-ratio measurement results, *Rapid Communications in Mass Spectrometry*, 2011, **25**, 2538–2560.

75 H. D. Smyth and E. C. G. Stueckelberg, The Ionization of Carbon Dioxide by Electron Impact, *Physical Review*, 1930, **36**, 472–477.

76 J. H. Gross, in *Mass Spectrometry: A Textbook*, ed. J. H. Gross, Springer International Publishing, Cham, 2017, pp. 151–292.

77 X. Tian, H. Jiang, L. Hu, M. Wang, W. Cui, J. Shi, G. Liu, Y. Yin, Y. Cai and G. Jiang, Simultaneous multi-element and multi-isotope detection in single-particle ICP-MS analysis: Principles and applications, *TrAC Trends in Analytical Chemistry*, 2022, **157**, 116746.

78 K. L. Brown and G. W. Tautfest, Faraday-Cup Monitors for High-Energy Electron Beams, *Review of Scientific Instruments*, 1956, **27**, 696–702.

79 J. M. Eiler, M. Clog, P. Magyar, A. Piasecki, A. Sessions, D. Stolper, M. Deerberg, H. J. Schlueter and J. Schwieters, A high-resolution gas-source isotope ratio mass spectrometer, *Int J Mass Spectrom*, 2013, **335**, 45–56.

80 Thermo Fisher Scientific, *Delta V Advantage Operating Manual*, 2011.

81 J. Santrock, S. A. Studley and J. M. Hayes, Isotopic Analyses Based on the Mass Spectra of Carbon Dioxide, *Anal Chem*, 1985, **57**, 1444–1448.

82 W. A. Brand, S. S. Assonov and T. B. Coplen, Correction for the 17O interference in δ(13C) measurements when analyzing CO2 with stable isotope mass spectrometry (IUPAC Technical Report), *Pure and Applied Chemistry*, 2010, **82**, 1719–1733.

83 S. S. Assonov and C. A. M. Brenninkmeijer, On the 17O correction for CO2 mass spectrometric isotopic analysis, *Rapid Communications in Mass Spectrometry*, 2003, **17**, 1007–1016.

84 H. Craig, Isotopic standards for carbon and oxygen and correction factors for mass-spectrometric analysis of carbon dioxide, *Geochim Cosmochim Acta*, 1957, **12**, 133–149.

85 J. F. Carter and B. Fry, Ensuring the reliability of stable isotope ratio data—beyond the principle of identical treatment, *Anal Bioanal Chem*, 2013, **405**, 2799–2814.

86 D. Paul, G. Skrzypek and I. Fórizs, Normalization of measured stable isotopic compositions to isotope reference scales - A review, *Rapid Communications in Mass Spectrometry*, 2007, **21**, 3006–3014.

87 Y. Zhang, H. J. Tobias, G. L. Sacks and J. Thomas Brenna, Calibration and data processing in gas chromatography combustion isotope ratio mass spectrometry, *Drug Test Anal*, 2012, **4**, 912–922.

88 P. Szpak, J. Z. Metcalfe and R. A. Macdonald, Best practices for calibrating and reporting stable isotope measurements in archaeology, *J Archaeol Sci Rep*, 2017, **13**, 609–616.

89 K. A. van Leeuwen, P. D. Prenzler, D. Ryan and F. Camin, Gas chromatography-combustion-isotope ratio mass spectrometry for traceability and authenticity in foods and beverages, *Compr Rev Food Sci Food Saf*, 2014, **13**, 814–837.

90 G. Skrzypek and P. J. H. Dunn, Absolute isotope ratios defining isotope scales used in isotope ratio mass spectrometers and optical isotope instruments, *Rapid Communications in Mass Spectrometry*, 2020, **34**, e8890.

91 T. B. Coplen, Reporting of stable hydrogen, carbon, and oxygen isotopic abundances (Technical Report), 1994, **66**, 273–276.

92 R. A. Werner and W. A. Brand, Referencing strategies and techniques in stable isotope ratio analysis, *Rapid Communications in Mass Spectrometry*, 2001, **15**, 501–519.

93 G. Junk and H. J. Svec, The absolute abundance of the nitrogen isotopes in the atmosphere and compressed gas from various sources, *Geochim Cosmochim Acta*, 1958, **14**, 234–243.

94 J. Kaiser, Reformulated 17O correction of mass spectrometric stable isotope measurements in carbon dioxide and a critical appraisal of historic 'absolute' carbon and oxygen isotope ratios, *Geochim Cosmochim Acta*, 2008, **72**, 1312–1334.

95 M. Matucha, W. Jockisch, P. Verner and G. Anders, Isotope effect in gas—liquid chromatography of labelled compounds, *J Chromatogr A*, 1991, **588**, 251–258.

96 M. Matucha, The isotope effect in the chromatography of organic compounds and its interpretation.

97 K. E. Wilzbach and P. Riesz, Isotope Effects in Gas-Liquid Chromatography, *Science (1979)*, 1957, **126**, 748–749.

98 D. Wade, Deuterium isotope effects on noncovalent interactions between molecules, *Chem Biol Interact*, 1999, **117**, 191–217.

99 Gianpaolo. Cartoni, Arnaldo. Liberti and Alberto. Pela, Gas chromatographic separation of polar isotopic molecules, *Anal Chem*, 1967, **39**, 1618–1622.

100 N. Thakur, S. Aslani and D. W. Armstrong, Evaluation of gas chromatography for the separation of a broad range of isotopic compounds, *Anal Chim Acta*, 2021, **1165**, 338490.

101 S. Aslani and D. W. Armstrong, Effect of position of deuterium atoms on gas chromatographic isotope effects, *Talanta*, 2023, **265**, 124857.

102 D. P. Downes, T. Kasumov, N. A. Daurio, N. B. Wood, M. J. Previs, P. R. Sheth, D. G. McLaren and S. F. Previs, Isotope fractionation during gas chromatography can enhance mass spectrometry-based measures of 2H-labeling of small molecules, *Metabolites*, 2020, **10**, 474.

103 R. Zhang, C. S. Sioma, R. A. Thompson, L. Xiong and F. E. Regnier, Controlling deuterium isotope effects in comparative proteomics, *Anal Chem*, 2002, **74**, 3662–3669.

104 A. Valleix, S. Carrat, C. Caussignac, E. Léonce and A. Tchapla, Secondary isotope effects in liquid chromatography behaviour of 2H and 3H labelled solutes and solvents, *J Chromatogr A*, 2006, **1116**, 109–126.

105 L. Bijlsma, A. M. Botero-Coy, R. J. Rincón, G. A. Peñuela and F. Hernández, Estimation of illicit drug use in the main cities of Colombia by means of urban wastewater analysis, *Science of the Total Environment*, 2016, **565**, 984–993.

106 P. Du, K. Li, J. Li, Z. Xu, X. Fu, J. Yang, H. Zhang and X. Li, Methamphetamine and ketamine use in major Chinese cities, a nationwide reconnaissance through sewage-based epidemiology, *Water Res*, 2015, **84**, 76–84.

107 L. You, V. T. Nguyen, A. Pal, H. Chen, Y. He, M. Reinhard and K. Y. H. Gin, Investigation of pharmaceuticals, personal care products and endocrine disrupting chemicals in a tropical urban catchment and the influence of environmental factors, *Science of the Total Environment*, 2015, **536**, 955–963.

108 B. D. Blair, J. P. Crago, C. J. Hedman and R. D. Klaper, Pharmaceuticals and personal care products found in the Great Lakes above concentrations of environmental concern,

Chemosphere, 2013, **93**, 2116–2123.

109 M. Claessens, L. Vanhaecke, K. Wille and C. R. Janssen, Emerging contaminants in Belgian marine waters: Single toxicant and mixture risks of pharmaceuticals, *Mar Pollut Bull*, 2013, **71**, 41–50.

110 C. D. S. Pereira, L. A. Maranho, F. S. Cortez, F. H. Pusceddu, A. R. Santos, D. A. Ribeiro, A. Cesar and L. L. Guimarães, Occurrence of pharmaceuticals and cocaine in a Brazilian coastal zone, *Science of the Total Environment*, 2016, **548–549**, 148–154.

111 M. Kim, M. C. Kennicutt and Y. Qian, Source characterization using compound composition and stable carbon isotope ratio of PAHs in sediments from lakes, harbor, and shipping waterway, *Science of the Total Environment*, 2008, **389**, 367–377.

112 S. J. Granger, T. H. E. Heaton, V. Pfahler, M. S. A. Blackwell, H. Yuan and A. L. Collins, The oxygen isotopic composition of phosphate in river water and its potential sources in the Upper River Taw catchment, UK, *Science of the Total Environment*, 2017, **574**, 680–690.

113 R. Popescu, T. Mimmo, O. R. Dinca, C. Capici, D. Costinel, C. Sandru, R. E. Ionete, I. Stefanescu and D. Axente, Using stable isotopes in tracing contaminant sources in an industrial area: A case study on the hydrological basin of the Olt River, Romania, *Science of the Total Environment*, 2015, **533**, 17–23.

114 C. Dargnat, M. J. Teil, M. Chevreuil and M. Blanchard, Phthalate

removal throughout wastewater treatment plant. Case study of Marne Aval station (France), *Science of the Total Environment*, 2009, **407**, 1235–1244.

115 V. Papakosta, R. H. Smittenberg, K. Gibbs, P. Jordan and S. Isaksson, Extraction and derivatization of absorbed lipid residues from very small and very old samples of ceramic potsherds for molecular analysis by gas chromatography-mass spectrometry (GC-MS) and single compound stable carbon isotope analysis by gas chromatogra, *Microchemical Journal*, 2015, **123**, 196–200.

116 Y. Chung, D. Jang, H. Kim, G. Oh, H. Tak, C. Son, M. J. Jeon, S.-H. Chae, Y. Hong, M. S. Wong and S. Kang, Occurrence and Treatment of DEHP in Water Treatment Plants: Case study in South Korea, *ACS ES&T Engineering*, DOI:10.1021/acsestengg.3c00396.

117 R. Wang, M. Ji, H. Zhai and Y. Liu, Occurrence of phthalate esters and microplastics in urban secondary effluents, receiving water bodies and reclaimed water treatment processes, *Science of The Total Environment*, 2020, **737**, 140219.

118 U. Kotowska, J. Kapelewska and R. Sawczuk, Occurrence, removal, and environmental risk of phthalates in wastewaters, landfill leachates, and groundwater in Poland, *Environmental Pollution*, 2020, **267**, 115643.

119 C. L. Perrin, in *Encyclopedia of Physical Science and Technology (Third Edition)*, ed. R. A. Meyers, Academic Press, New York, 2003,

pp. 211–243.

120 J. D. Marshall, J. Renée Brooks and K. Lajtha, in *Stable Isotopes in Ecology and Environmental Science: Second Edition*, Blackwell Publishing Ltd, 2008, pp. 22–60.

121 M. Fiedziukiewicz and Q. Hanley, Compound specific isotope analysis (CSIA) of phthalates and non-targeted isotope analysis (NTIA) of SPE-extractable organic carbon in dilute aquatic environments, *Environmental Advances*, 2021, **4**, 100050.

122 Environment Agency, Daily River Flow, https://environment.data.gov.uk/hydrology/explore.

123 X. Peng, X. Li and L. Feng, Behavior of stable carbon isotope of phthalate acid esters during photolysis under ultraviolet irradiation, *Chemosphere*, 2013, **92**, 1557–1562.

124 A. M. Ali, H. T. Rønning, W. M. Al Arif, R. Kallenborn and R. Kallenborn, Occurrence of pharmaceuticals and personal care products in effluent-dominated Saudi Arabian coastal waters of the Red Sea, *Chemosphere*, 2017, **175**, 505–513.

125 W. G. Mallard and J. Reed, Automated Mass Spectral Deconvolution & Identification System, *US Department of Commerce, Technology Administration, National Institute of Standards and Technology, Gaithersburg, MD*.

126 H. Fang, J. Wang and R. A. Lynch, Migration of di(2-ethylhexyl)phthalate (DEHP) and di-n-butylphthalate (DBP) from

polypropylene food containers, *Food Control*, 2017, **73**, 1298–1302.

127 X. L. Cao, Phthalate Esters in Foods: Sources, Occurrence, and Analytical Methods, *Compr Rev Food Sci Food Saf*, 2010, **9**, 21–43.

128 N. Van den Eede, G. Tomy, F. Tao, T. Halldorson, S. Harrad, H. Neels and A. Covaci, Kinetics of tris (1-chloro-2-propyl) phosphate (TCIPP) metabolism in human liver microsomes and serum, *Chemosphere*, 2016, **144**, 1299–1305.

129 D. Richter, G. Massmann and U. Dünnbier, Identification and significance of sulphonamides (p-TSA, o-TSA, BSA) in an urban water cycle (Berlin, Germany), *Water Res*, 2008, **42**, 1369–1378.

130 R. de A. Cordeiro, G. C. Nogueira, R. S. N. Brilhante, C. E. C. Teixeira, C. I. Mourão, D. de S. C. M. Castelo-Branco, M. de A. N. Paiva, J. F. Ribeiro, A. J. Monteiro, J. J. C. Sidrim and M. F. G. Rocha, Farnesol inhibits in vitro growth of the Cryptococcus neoformans species complex with no significant changes in virulence-related exoenzymes, *Vet Microbiol*, 2012, **159**, 375–380.

131 A. Lapczynski, S. P. Bhatia, C. S. Letizia and A. M. Api, Fragrance material review on farnesol, *Food and Chemical Toxicology*, 2008, **46**, S149–S156.

132 P. J. Watkins, G. Rose, R. D. Warner, F. R. Dunshea and D. W. Pethick, A comparison of solid-phase microextraction (SPME) with simultaneous distillation-extraction (SDE) for the analysis of volatile compounds in heated beef and sheep fats, *Meat Sci*, 2012, **91**, 99–

107.

133 L. Badoil and D. Benanou, Characterization of volatile and semivolatile compounds in waste landfill leachates using stir bar sorptive extraction-GC/MS, *Anal Bioanal Chem*, 2009, **393**, 1043–1054.

134 H. Fromme, in *Encyclopedia of Environmental Health*, Elsevier, 2019, pp. 174–188.

135 H. T. Tran, C. Lin, X.-T. Bui, M. K. Nguyen, N. D. T. Cao, H. Mukhtar, H. G. Hoang, S. Varjani, H. H. Ngo and L. D. Nghiem, Phthalates in the environment: characteristics, fate and transport, and advanced wastewater treatment technologies, *Bioresour Technol*, 2022, **344**, 126249.

136 T. Salaudeen, O. Okoh, F. Agunbiade and A. Okoh, Phthalates removal efficiency in different wastewater treatment technology in the Eastern Cape, South Africa, *Environ Monit Assess*, DOI:10.1007/s10661-018-6665-8.

137 M. Clara, G. Windhofer, W. Hartl, K. Braun, M. Simon, O. Gans, C. Scheffknecht and A. Chovanec, Occurrence of phthalates in surface runoff, untreated and treated wastewater and fate during wastewater treatment, *Chemosphere*, 2010, **78**, 1078–1084.

138 B. Subedi, K. D. Sullivan and B. Dhungana, Phthalate and non-phthalate plasticizers in indoor dust from childcare facilities, salons, and homes across the USA, *Environmental Pollution*, 2017, **230**,

701–708.

139 M. Samara, A. Nasser and U. Mingelgrin, Mechanochemical removal of carbamazepine, *Chemosphere*, 2016, **160**, 266–272.

140 W. Lilienblum, Opinion of the Scientific Committee on Consumer Safety (SCCS) – Final version of the opinion on Phenoxyethanol in cosmetic products, *Regulatory Toxicology and Pharmacology*, 2016, **82**, 156.

141 H.-J. Park, M.-J. Kim, M. Shin, J.-D. Lee, J.-Y. Kim, H.-M. Gwak, J.-H. Hyeon, Y.-M. Um, J.-Y. Son, K. Kim, R. Sachan, U. De, Y. Kang and B.-M. Lee, Human health risk assessment of phenoxyethanol in cosmetics, *Toxicol Lett*, 2014, **229**, S133.

142 Cotterill 1972, preprint.

143 R. W. Lewis, Squalene distribution in fish with normal and pathologically fatty livers, *International Journal of Biochemistry*, 1971, **2**, 609–614.

144 G. Matsumoto and T. Hanya, Presence of squalane in urban aquatic environments, *J Chromatogr A*, 1980, **194**, 199–204.

145 L. Boulard, G. Dierkes, M. P. Schlüsener, A. Wick, J. Koschorreck and T. A. Ternes, Spatial distribution and temporal trends of pharmaceuticals sorbed to suspended particulate matter of German rivers, *Water Res*, 2020, **171**, 115366.

146 M. J. Gómez, M. J. Martínez Bueno, S. Lacorte, A. R. Fernández-Alba and A. Agüera, Pilot survey monitoring pharmaceuticals and related

compounds in a sewage treatment plant located on the Mediterranean coast, *Chemosphere*, 2007, **66**, 993–1002.

147 P. Hu, C. Guo, Y. Zhang, J. Lv, Y. Zhang and J. Xu, Occurrence, distribution and risk assessment of abused drugs and their metabolites in a typical urban river in north China, *Front Environ Sci Eng*, 2019, **13**, 56.

148 R. Loos, B. M. Gawlik, G. Locoro, E. Rimaviciute, S. Contini and G. Bidoglio, EU-wide survey of polar organic persistent pollutants in European river waters, *Environmental Pollution*, 2009, **157**, 561–568.

149 S. M. Duty, R. M. Ackerman, A. M. Calafat and R. Hauser, Personal care product use predicts urinary concentrations of some phthalate monoesters, *Environ Health Perspect*, 2005, **113**, 1530–1535.

150 C. J. Hsieh, Y. H. Chang, A. Hu, M. L. Chen, C. W. Sun, R. F. Situmorang, M. T. Wu and S. L. Wang, Personal care products use and phthalate exposure levels among pregnant women, *Science of the Total Environment*, 2019, **648**, 135–143.

151 M. Zolfaghari, P. Drogui, B. Seyhi, S. K. Brar, G. Buelna and R. Dubé, Occurrence, fate and effects of di (2-ethylhexyl) phthalate in wastewater treatment plants: A review, *Environmental Pollution*, 2014, **194**, 281–293.

152 L. J. Fono, E. P. Kolodziej and D. L. Sedlak, Attenuation of wastewater-derived contaminants in an effluent-dominated river,

Environ Sci Technol, 2006, **40**, 7257–7262.

153 P. R. Graham, Phthalate ester plasticizers--why and how they are used., *Environ Health Perspect*, 1973, **3**, 3–12.

154 A. Pace, A. Vaglica, A. Maccotta and D. Savoca, The Origin of Phthalates in Algae: Biosynthesis and Environmental Bioaccumulation, *Environments*, 2024, **11**, 78.

155 C. Y. Chen, Biosynthesis of di-(2-ethylhexyl) phthalate (DEHP) and di-n-butyl phthalate (DBP) from red alga - Bangia atropurpurea, *Water Res*, 2004, **38**, 1014–1018.

156 L. Huang, X. Zhu, S. Zhou, Z. Cheng, K. Shi, C. Zhang and H. Shao, Phthalic acid esters: Natural sources and biological activities, *Toxins (Basel)*, 2021, **13**, 495.

157 C. Tian, J. Ni, F. Chang, S. Liu, N. Xu, W. Sun, Y. Xie, Y. Guo, Y. Ma, Z. Yang, C. Dang, Y. Huang, Z. Tian and Y. Wang, Bio-Source of di-n-butyl phthalate production by filamentous fungi, *Sci Rep*, 2016, **6**, 19791.

158 K.-P. Chao, C.-S. Huang and C.-Y. Wei, Health risk assessments of DEHP released from chemical protective gloves, *J Hazard Mater*, 2015, **283**, 53–59.

159 R. Jaimes, A. Swiercz, M. Sherman, N. Muselimyan, P. J. Marvar and N. G. Posnack, Plastics and cardiovascular health: Phthalates may disrupt heart rate variability and cardiovascular reactivity, *Am J Physiol Heart Circ Physiol*, 2017, **313**, H1044–H1053.

160 Y. Yu and L. Wu, Analysis of endocrine disrupting compounds, pharmaceuticals and personal care products in sewage sludge by gas chromatography-mass spectrometry, *Talanta*, 2012, **89**, 258–263.

161 Y. Wang and H. Qian, in *Healthcare*, Multidisciplinary Digital Publishing Institute, 2021, vol. 9, p. 603.

162 S. Benjamin, E. Masai, N. Kamimura, K. Takahashi, R. C. Anderson and P. A. Faisal, Phthalates impact human health: Epidemiological evidences and plausible mechanism of action, *J Hazard Mater*, 2017, **340**, 360–383.

163 R. Hauser and A. M. Calafat, Phthalates and human health, *Occup Environ Med*, 2005, **62**, 806–818.

164 O. O. Olujimi, O. A. Aroyeun, T. F. Akinhanmi and T. A. Arowolo, Occurrence, removal and health risk assessment of phthalate esters in the process streams of two different wastewater treatment plants in Lagos and Ogun States, Nigeria, *Environ Monit Assess*, 2017, **189**, 345.

165 C. G. Bornehag, J. Sundell, C. J. Weschler, T. Sigsgaard, B. Lundgren, M. Hasselgren and L. Hägerhed-Engman, The association between asthma and allergic symptoms in children and phthalates in house dust: A nested case-control study, *Environ Health Perspect*, 2004, **112**, 1393–1397.

166 R. Biemann, M. Blüher and B. Isermann, Exposure to endocrine-

disrupting compounds such as phthalates and bisphenol A is associated with an increased risk for obesity, *Best Pract Res Clin Endocrinol Metab*, 2021, **35**, 101546.

167 Y. Liu, N.-N. Wu, R. Xu, Z.-H. Li, X.-R. Xu and S. Liu, Phthalates released from microplastics can't be ignored: Sources, fate, ecological risks, and human exposure risks, *TrAC Trends in Analytical Chemistry*, 2024, **179**, 117870.

168 Y. Cao, H. Lin, K. Zhang, S. Xu, M. Yan, K. M. Y. Leung and P. K. S. Lam, Microplastics: A major source of phthalate esters in aquatic environments, *J Hazard Mater*, 2022, **432**, 128731.

169 J. H. Petersen and L. K. Jensen, Phthalates and food-contact materials: enforcing the 2008 European Union plastics legislation, *Food Addit Contam*, 2010, **27**, 1608–1616.

170 A. C. Alp and P. Yerlikaya, Phthalate ester migration into food: Effect of packaging material and time, *European Food Research and Technology*, 2020, **246**, 425–435.

171 Food & Drug Administration, Phthalates in Cosmetics, https://www.fda.gov/Cosmetics/ProductsIngredients/Ingredients/ucm128250.htm, (accessed 26 May 2024).

172 The European Parliament and the Council, Regulation (EC) No 1907/2006 of the European Parlimetn and of the Council of 18 December 2006 concerning the Registration, Evaluation, Authorisation and Restriction of Chemicals (REACH), establishing a

European Chemicals Agency, amending Directive 1999/45/EC and repealing Council Regulation (EEC) No 793/93 and Commission Regulation (EC) No 1488/94 as well as Council Directive 76/769/EEC and Commission Directives 91/155/EEC, 93/67/EEC, 93/105/EC and 2000/21/EC.

173 The European Parliment and The Council of the European Union, Regulation (EC) No 1223/2009 of the European Parliament and of the Council of 30 November 2009 on cosmetic products, https://health.ec.europa.eu/document/download/47f167ec-b5db-4ec9-9d12-3d807bf3e526_en, (accessed 26 May 2024).

174 Medicines & Healthcare products Regulatory Agency, DEHP phthalates in medical devices, https://www.gov.uk/government/publications/dehp-phthalates-in-medical-devices/dehp-phthalates-in-medical-devices, (accessed 27 May 2024).

175 F. Zeng, Y. Lin, K. Cui, J. Wen, Y. Ma, H. Chen, F. Zhu, Z. Ma and Z. Zeng, Atmospheric deposition of phthalate esters in a subtropical city, *Atmos Environ*, 2010, **44**, 834–840.

176 M. Szewczyńska, M. Pośniak and E. Dobrzyńska, Determination of phthalates in particulate matter and gaseous phase emitted into the air of the working environment, *International journal of environmental science and technology*, 2020, **17**, 175–186.

177 L. Huang, Y. Qiao, S. Deng, M. Zhou, W. Zhao and Y. Yue, Airborne

phthalates in indoor environment: Partition state and influential built environmental conditions, *Chemosphere*, 2020, **254**, 126782.

178 M. J. Teil, M. Blanchard, C. Dargnat, K. Larcher-Tiphagne and M. Chevreuil, Occurence of phthalate diesters in rivers of the Paris district (France), *Hydrol Process*, 2007, **21**, 2515–2525.

179 D. W. Gao and Z. D. Wen, Phthalate esters in the environment: A critical review of their occurrence, biodegradation, and removal during wastewater treatment processes, *Science of the Total Environment*, 2016, **541**, 986–1001.

180 B. Nas, H. Ateş, T. Dolu, E. Yel, M. E. Argun, S. Koyuncu, M. Kara and S. Dinç, Evaluation of occurrence, fate and removal of priority phthalate esters (PAEs) in wastewater and sewage sludge by advanced biological treatment, waste stabilization pond and constructed wetland, *Chemosphere*, 2022, **295**, 133864.

181 D. Gao, Z. Li, Z. Wen and N. Ren, Occurrence and fate of phthalate esters in full-scale domestic wastewater treatment plants and their impact on receiving waters along the Songhua River in China, *Chemosphere*, 2014, **95**, 24–32.

182 W. J. G. M. Peijnenburg and J. Struijs, Occurrence of phthalate esters in the environment of the Netherlands, *Ecotoxicol Environ Saf*, 2006, **63**, 204–215.

183 B. Babu and J. T. Wu, Production of phthalate esters by nuisance freshwater algae and cyanobacteria, *Science of the Total*

Environment, 2010, **408**, 4969–4975.

184 J. Gasperi, S. Garnaud, V. Rocher and R. Moilleron, Priority pollutants in wastewater and combined sewer overflow, *Science of the Total Environment*, 2008, **407**, 263–272.

185 G. Schwedler, E. Rucic, R. Lange, A. Conrad, H. M. Koch, C. Pälmke, T. Brüning, C. Schulz, M. I. H. Schmied-Tobies, A. Daniels and M. Kolossa-Gehring, Phthalate metabolites in urine of children and adolescents in Germany. Human biomonitoring results of the German Environmental Survey GerES V, 2014–2017, *Int J Hyg Environ Health*, 2020, **225**, 113444.

186 H. M. Koch, M. Rüther, A. Schütze, A. Conrad, C. Pälmke, P. Apel, T. Brüning and M. Kolossa-Gehring, Phthalate metabolites in 24-h urine samples of the German Environmental Specimen Bank (ESB) from 1988 to 2015 and a comparison with US NHANES data from 1999 to 2012, *Int J Hyg Environ Health*, 2017, **220**, 130–141.

187 H. M. Koch, R. Preuss, J. Angerer, P. Foster, R. Sharpe and J. Toppari, Di(2-ethylhexyl)phthalate (DEHP): Human metabolism and internal exposure - An update and latest results, *Int J Androl*, 2006, **29**, 155–165.

188 W. Kessler, W. Numtip, W. Völkel, E. Seckin, G. A. Csanády, C. Pütz, D. Klein, H. Fromme and J. G. Filser, Kinetics of di(2-ethylhexyl) phthalate (DEHP) and mono(2-ethylhexyl) phthalate in blood and of DEHP metabolites in urine of male volunteers after single ingestion

of ring-deuterated DEHP, *Toxicol Appl Pharmacol*, 2012, **264**, 284–291.

189 X. Zhang, S. Tang, T. Qiu, X. Hu, Y. Lu, P. Du, L. Xie, Y. Yang, F. Zhao, Y. Zhu and J. P. Giesy, Investigation of phthalate metabolites in urine and daily phthalate intakes among three age groups in Beijing, China, *Environmental Pollution*, 2020, **260**, 114005.

190 J. Zhang, C. Zhang, Y. Zhu, J. Li and X. Li, Biodegradation of seven phthalate esters by Bacillus mojavensis B1811, *Int Biodeterior Biodegradation*, 2018, **132**, 200–207.

191 R. Sennaj, K. Dari, M. Timinouni, T. Benali, A. Fassouane, K. Harboul and H. Aassila, Evaluation of Bioremediation Potentiality of Bacillus mojavensis Isolated from Wastewater for the Elimination of Reactive Yellow 145 and Methyl Orange, *Curr Microbiol*, 2023, **80**, 326.

192 F. Al Ajeel, M. Kishk and E. Ibrahim, Identification of microbial groups in the aeration tanks of secondary wastewater treatment stage, *Kuwait Journal of Science*, 2024, **51**, 100279.

193 P. Fauser, J. Vikelsøe, P. B. Sørensen and L. Carlsen, Phthalates, nonylphenols and LAS in an alternately operated wastewater treatment plant - Fate modelling based on measured concentrations in wastewater and sludge, *Water Res*, 2003, **37**, 1288–1295.

194 V. A. Vavilin, Corrected first-order model of DEHP degradation, *Chemosphere*, 2007, **68**, 1992–1995.

195 M. S. Fountoulakis, K. Stamatelatou, D. J. Batstone and G.

Lyberatos, Simulation of DEHP biodegradation and sorption during the anaerobic digestion of secondary sludge, *Water Science and Technology*, 2006, **54**, 119–128.

196 C. Li and K. H. D. Tang, Effects of pH and temperature on the leaching of di (2-ethylhexyl) phthalate and di-n-butyl phthalate from microplastics in simulated marine environment, *Biointerface Res Appl Chem*.

197 Y. Han, J. Cheng, Z. Tang, Y. He and Y. Lyu, Widespread occurrence of phthalates in popular take-out food containers from China and the implications for human exposure, *J Clean Prod*, 2021, **290**, 125851.

198 D. Zhang, L. Wu, J. Yao, H. Herrmann and H. H. Richnow, Carbon and hydrogen isotope fractionation of phthalate esters during degradation by sulfate and hydroxyl radicals, *Chemical Engineering Journal*, 2018, **347**, 111–118.

199 M. Elsner and G. Imfeld, Compound-specific isotope analysis (CSIA) of micropollutants in the environment - current developments and future challenges, *Curr Opin Biotechnol*, 2016, **41**, 60–72.

200 X. Peng, L. Feng and X. Li, Pathway of diethyl phthalate photolysis in sea-water determined by gas chromatography-mass spectrometry and compound-specific isotope analysis, *Chemosphere*, 2013, **90**, 220–226.

201 E. Lichtfouse, Compound-specific isotope analysis. Application to

archaelogy, biomedical sciences, biosynthesis, environment, extraterrestrial chemistry, food science, forensic science, humic substances, microbiology, organic geochemistry, soil science and sport, *Rapid Communications in Mass Spectrometry*, 2000, **14**, 1337–1344.

202 S. Pizzarello and W. Holmes, Nitrogen-containing compounds in two CR2 meteorites: 15N composition, molecular distribution and precursor molecules, *Geochim Cosmochim Acta*, 2009, **73**, 2150–2162.

203 C. Yan, Z. Li, S. Li, Z. Wang, L. Xing, Y. Liu, W. Mou and K. Wang, Determination of δ 13C of Trace Hydrocarbons in Natural Gas Using Syringe Solid Phase Extraction (SSPE) Coupled with Gas Chromatography/Isotope Ratio Mass Spectrometry (GC/IRMS), *Geofluids*, 2019, **2019**, 6352378.

204 V. S. Sevastyanov, Isotope Ratio Mass Spectrometry of Light Gas-Forming Elements, 2016, preprint, DOI: 10.1201/b17227.

205 X. Peng and X. Li, Compound-specific isotope analysis for aerobic biodegradation of phthalate acid esters, *Talanta*, 2012, **97**, 445–449.

206 S. Spahr, J. Bolotin, J. Schleucher, I. Ehlers, U. Von Gunten and T. B. Hofstetter, Compound-specific carbon, nitrogen, and hydrogen isotope analysis of n -nitrosodimethylamine in aqueous solutions, *Anal Chem*, 2015, **87**, 2916–2924.

207 M. P. Maier, C. Prasse, S. G. Pati, S. Nitsche, Z. Li, M. Radke, A. Meyer, T. B. Hofstetter, T. A. Ternes and M. Elsner, Exploring Trends of C and N Isotope Fractionation to Trace Transformation Reactions of Diclofenac in Natural and Engineered Systems, *Environ Sci Technol*, 2016, **50**, 10933–10942.

208 S. J. Taipale, E. Peltomaa, J. V. K. Kukkonen, M. J. Kainz, P. Kautonen and M. Tiirola, Tracing the fate of microplastic carbon in the aquatic food web by compound-specific isotope analysis, *Sci Rep*, 2019, **9**, 19894.

209 H. W. Yeh and W. M. Wang, Factors affecting the isotopic composition of organic matter. (1) Carbon isotopic composition of terrestrial plant materials., *Proc Natl Sci Counc Repub China B*, 2001, **25**, 137–147.

210 M. P. Maier, S. De Corte, S. Nitsche, T. Spaett, N. Boon and M. Elsner, C & N isotope analysis of diclofenac to distinguish oxidative and reductive transformation and to track commercial products, *Environ Sci Technol*, 2014, **48**, 2312–2320.

211 J. W. Washington, C. G. Rosal, E. M. Ulrich and T. M. Jenkins, Use of carbon isotopic ratios in nontargeted analysis to screen for anthropogenic compounds in complex environmental matrices, *J Chromatogr A*, 2019, **1583**, 73–79.

212 Y. Wu, D. Luo, H. Dong, J. Wan, H. Luo, Y. Xian, X. Guo, F. Qin, W. Han, L. Wang and B. Wang, Geographical origin of cereal grains

based on element analyser-stable isotope ratio mass spectrometry (EA-SIRMS), *Food Chem*, 2015, **174**, 553–557.

213 B. Thornton, Z. Zhang, R. W. Mayes, M. N. Högberg and A. J. Midwood, Can gas chromatography combustion isotope ratio mass spectrometry be used to quantify organic compound abundance?, *Rapid Commun Mass Spectrom*, 2011, **25**, 2433–2438.

214 J. Granger, D. S. Boshers, J. K. Böhlke, D. Yu, N. Chen and C. R. Tobias, The influence of sample matrix on the accuracy of nitrite N and O isotope ratio analyses with the azide method, *Rapid Communications in Mass Spectrometry*, 2020, **34**, e8569.

215 H. Liu, Y. X. Li, X. He, Z. Sissou, L. Tong, C. Yarnes and X. Huang, Compound-specific carbon isotopic fractionation during transport of phthalate esters in sandy aquifer, *Chemosphere*, 2016, **144**, 1831–1836.

216 M. A. Jochmann, M. Blessing, S. B. Haderlein and T. C. Schmidt, A new approach to determine method detection limits for compound-specific isotope analysis of volatile organic compounds, *Rapid Communications in Mass Spectrometry*, 2006, **20**, 3639–3648.

217 T. C. Schmidt, Analysis of methyl tert-butyl ether (MTBE) and tert-butyl alcohol (TBA) in ground and surface water, *TrAC - Trends in Analytical Chemistry*, 2003, **22**, 776–784.

218 M. Blessing and N. Baran, A review on environmental isotope analysis of aquatic micropollutants: Recent advances, pitfalls and

perspectives, *TrAC Trends in Analytical Chemistry*, 2022, **157**, 116730.

219 A. Kuzmin, T. Grigoryeva and A. Gorshkov, Assessment of stable carbon isotope 13C/12C ratio in phthalates from surface waters using HPLC-HRMS-TOF approach, *Environmental Science and Pollution Research*, 2023, **30**, 87734–87742.

220 X. Han, X. Cheng, S. Li, J. Yuan and Q. Zhang, Carbon concentrations and their stable isotopic signatures in the upper Han River, China, *Environmental Science and Pollution Research*, 2019, **26**, 14116–14127.

221 Y. Liu, X. Wang, Q. Wen and N. Zhu, Identifying sources and variations of organic matter in an urban river in Beijing, China using stable isotope analysis, *Ecol Indic*, 2019, **102**, 783–790.

222 B. Peterson, B. Fry, M. Hullar, S. Saupe and R. Wright, The distribution and stable carbon isotopic composition of dissolved organic carbon in estuaries, *Estuaries*, 1994, **17**, 111–121.

223 *Harris 2010 - Quantitative_Chemical_Analysis*, .

224 Y. Zhang, H. J. Tobias, G. L. Sacks and J. Thomas Brenna, Calibration and data processing in gas chromatography combustion isotope ratio mass spectrometry, *Drug Test Anal*, 2012, **4**, 912–922.

225 J. F. Hélie and C. Hillaire-Marcel, Sources of particulate and dissolved organic carbon in the St Lawrence River: Isotopic

approach, *Hydrol Process*, 2006, **20**, 1945–1959.

226 S. L. Connin, R. A. Virginia and C. P. Chamberlain, Carbon isotopes reveal soil organic matter dynamics following arid land shrub expansion, *Oecologia*, 1997, **110**, 374–386.

227 C. Lee, J. A. McKenzie and Z. M. Sturm, Carbon isotope fractionation and changes in the flux and composition of particulate matter resulting from biological activity during a sediment trap experiment in Lake Greifen, Switzerland, *Limnol Oceanogr*, 1987, **32**, 83–96.

228 D. Goevert and R. Conrad, Carbon isotope fractionation by sulfate-reducing bacteria using different pathways for the oxidation of acetate, *Environ Sci Technol*, 2008, **42**, 7813–7817.

229 N. Min, J. Yao, H. Li, J. Zhu, S. Kümmel, T. Schaefer, H. Herrmann and H. H. Richnow, Carbon isotope fractionation of di-(2-ethylhexyl)-phthalate during photosensitized degradation by •OH and SO4·- for characterization of reaction mechanisms, *Chemical Engineering Journal*, 2023, **475**, 145950.

230 J. C. Finlay, Patterns and controls of lotic algal stable carbon isotope ratios, *Limnol Oceanogr*, 2004, **49**, 850–861.

231 D. Goevert and R. Conrad, Carbon isotope fractionation by sulfate-reducing bacteria using different pathways for the oxidation of acetate, *Environ Sci Technol*, 2008, **42**, 7813–7817.

232 E. Davoli, E. Zuccato and S. Castiglioni, Illicit drugs in drinking water, *Curr Opin Environ Sci Health*, 2019, **7**, 92–97.

233 J. R. Ehleringer, D. A. Cooper, M. J. Lott and C. S. Cook, Geo-location of heroin and cocaine by stable isotope ratios, *Forensic Sci Int*, 1999, **106**, 27–35.

234 J. Meikle, S. L. Cresswell, S. E. Boyd, J. F. Carter and S. P. Collett, A stable isotope ratio approach to investigate the origins of illicit methylamphetamine in Queensland, Australia, *Forensic Chemistry*, 2019, **16**, 100174.

235 S. Mercan, M. Kuloglu, T. Tekin, Z. Turkmen, A. O. Dogru, A. N. Safran, M. Acikkol and F. Asicioglu, Wastewater-based monitoring of illicit drug consumption in Istanbul: Preliminary results from two districts, *Science of the Total Environment*, 2019, **656**, 231–238.

236 E. Zuccato, C. Chiabrando, S. Castiglioni, D. Calamari, R. Bagnati, S. Schiarea and R. Fanelli, Cocaine in surface waters: A new evidence-based tool to monitor community drug abuse, *Environ Health*, 2005, **4**, 1–7.

237 W. Meier-Augenstein, Applied gas chromatography coupled to isotope ratio mass spectrometry, *J Chromatogr A*, 1999, **842**, 351–371.

238 L. Huang, J. R. Brook, W. Zhang, S. M. Li, L. Graham, D. Ernst, A. Chivulescu and G. Lu, Stable isotope measurements of carbon fractions (OC/EC) in airborne particulate: A new dimension for source characterization and apportionment, *Atmos Environ*, 2006, **40**, 2690–2705.

239 J. M. Hayes, K. H. Freeman, B. N. Popp and C. H. Hoham, Compound-specific isotopic analyses: A novel tool for reconstruction of ancient biogeochemical processes, *Org Geochem*, 1990, **16**, 1115–1128.

240 N. F. Ishikawa, N. O. Ogawa, Y. Sun, Y. Chikaraishi, Y. Takano and N. Ohkouchi, Integrative assessment of amino acid nitrogen isotopic composition in biological tissue samples determined by GC/C/IRMS, LC × EA/IRMS, and LC × GC/C/IRMS, *Limnol Oceanogr Methods*, 2022, **20**, 531–542.

241 K. Kuntze, H. Eisenmann, H.-H. Richnow and A. Fischer, Compound-specific stable isotope analysis (CSIA) for evaluating degradation of organic pollutants: An overview of field case studies, *Anaerobic Utilization of Hydrocarbons, Oils, and Lipids*, 2020, 323–360.

242 W. Meier-Augenstein, P. W. Watt and C. D. Langhans, Influence of gas chromatographic parameters on measurement of 13C/12C isotope by gas-liquid chromatography-combustion isotope ratio mass spectrometry. I, *J Chromatogr A*, 1996, **752**, 233–241.

243 A. L. Sessions, Isotope-ratio detection for gas chromatography, *J Sep Sci*, 2006, **29**, 1946–1961.

244 N. M. Razali and Y. B. Wah, Power comparisons of shapiro-wilk, kolmogorov-smirnov, lilliefors and anderson-darling tests, *Journal of statistical modeling and analytics*, 2011, **2**, 21–33.

245 E. Hirota, K. Matsumura, M. Imachi, M. Fujio, Y. Tsuno and C.

Matsumura, Microwave spectra of 13CH3 12CD3 and 12CH3 13CD3 and the C–C bond length of ethane, *J Chem Phys*, 1977, **66**, 2660–2663.

246 P. W. Carr, Fundamental, predictive approach to dipole-dipole interactions based on the dipole moment of the solute and the dielectric constant of the solvent, *J Chromatogr A*, 1980, **194**, 105–119.

247 W. A. Brand, T. B. Coplen, A. T. Aerts-Bijma, J. K. Böhlke, M. Gehre, H. Geilmann, M. Gröning, H. G. Jansen, H. A. J. Meijer, S. J. Mroczkowski, H. Qi, K. Soergel, H. Stuart-Williams, S. M. Weise and R. A. Werner, Comprehensive inter-laboratory calibration of reference materials for δ18O versus VSMOW using various on-line high-temperature conversion techniques, *Rapid Communications in Mass Spectrometry*, 2009, **23**, 999–1019.

248 R. D. Wigglesworth, W. T. Raynes, S. Kirpekar, J. Oddershede and S. P. A. Sauer, Nuclear magnetic shielding in the acetylene isotopomers calculated from correlated shielding surfaces, *J Chem Phys*, 2000, **112**, 736–746.

249 L. Moravský, B. Michalczuk, A. Fateh Borkhari, P. Papp, A. A. Sysoev and Š. Matejčík, Study of atmospheric pressure chemical ionization of phthalates in air by ion mobility spectrometry/mass spectrometry, *Rapid Communications in Mass Spectrometry*, 2021, **35**, e9145.

250 M. J. E. Golay, Gas Chromatography 1958, *Edited by DH Desty*.

251 J. C. Giddings, *Dynamics of chromatography: principles and theory*, CRC Press, 2002.

252 W. F. Libby, Isotope Size Effect in Van der Waals Radii and the Barrier to Rotation around the Carbon-Carbon Single Bond, *J Chem Phys*, 1961, **35**, 1527.

253 J. B. Wooten, G. B. Savitsky, A. L. Beyerlein and J. Jacobus, Isotope effects on the carbon-hydrogen bond orientation of methyl iodide in nematic phase, *Journal of Magnetic Resonance (1969)*, 1978, **29**, 35–37.

254 E. N. Fuller, P. D. Schettler and J. Calvin. Giddings, NEW METHOD FOR PREDICTION OF BINARY GAS-PHASE DIFFUSION COEFFICIENTS, *Ind Eng Chem*, 1966, **58**, 18–27.

255 J. T. Edward, Molecular volumes and the Stokes-Einstein equation, *J Chem Educ*, 1970, **47**, 261.

256 A. A. Shvartsburg, D. E. Clemmer and R. D. Smith, Isotopic Effect on Ion Mobility and Separation of Isotopomers by High-Field Ion Mobility Spectrometry, *Anal Chem*, 2010, **82**, 8047–8051.

257 A. T. Kirk, C.-R. Raddatz and S. Zimmermann, Separation of Isotopologues in Ultra-High-Resolution Ion Mobility Spectrometry, *Anal Chem*, 2017, **89**, 1509–1515.

258 D. S. Stratiev, R. K. Dinkov, I. K. Shishkova, A. D. Nedelchev, T. Tasaneva, E. Nikolaychuk, I. M. Sharafutdinov, N. Rudney, S.

Nenov, M. Mitkova, M. Skunov and D. Yordanov, An Investigation on the Feasibility of Simulating the Distribution of the Boiling Point and Molecular Weight of Heavy Oils, *Pet Sci Technol*, 2015, **33**, 527–541.

259 A. R. Katritzky, L. Mu, V. S. Lobanov and M. Karelson, Correlation of Boiling Points with Molecular Structure. 1. A Training Set of 298 Diverse Organics and a Test Set of 9 Simple Inorganics, *J Phys Chem*, 1996, **100**, 10400–10407.

260 J. Lu, M. J. Trnka, S.-H. Roh, P. J. J. Robinson, C. Shiau, D. G. Fujimori, W. Chiu, A. L. Burlingame and S. Guan, Improved Peak Detection and Deconvolution of Native Electrospray Mass Spectra from Large Protein Complexes, *J Am Soc Mass Spectrom*, 2015, **26**, 2141–2151.

261 S. Peters, G. Vivó-Truyols, P. J. Marriott and P. J. Schoenmakers, Development of an algorithm for peak detection in comprehensive two-dimensional chromatography, *J Chromatogr A*, 2007, **1156**, 14–24.

262 L. E. Niezen, P. J. Schoenmakers and B. W. J. Pirok, Critical comparison of background correction algorithms used in chromatography, *Anal Chim Acta*, 2022, **1201**, 339605.

263 J. A. Roberts and G. Carta, Protein adsorption and separation with monomodal and multimodal anion exchange chromatography resins. Part II. Mechanisms of protein aggregation on the

chromatographic surface, *Journal of Chemical Technology & Biotechnology*, 2023, **98**, 357–368.

264 S. Iftekhar, S. Poddar, M. Rauhauser, D. D. Snow and D. S. Hage, Preparation of entrapment-based microcolumns for analysis of drug-humic acid interactions by high-performance affinity chromatography, *Anal Chim Acta*, 2023, **1239**, 340629.

265 M. L. Phillips and R. L. White, Dependence of Chromatogram Peak Areas Obtained by Curve-Fitting on the Choice of Peak Shape Function, *J Chromatogr Sci*, 1997, **35**, 75–81.

266 Y. Kalambet, Y. Kozmin, K. Mikhailova, I. Nagaev and P. Tikhonov, Reconstruction of chromatographic peaks using the exponentially modified Gaussian function, *J Chemom*, 2011, **25**, 352–356.

267 C. Wiegert, C. Aeppli, T. Knowles, H. Holmstrand, R. Evershed, R. D. Pancost, J. Macháčková and Ö. Gustafsson, Dual Carbon–Chlorine Stable Isotope Investigation of Sources and Fate of Chlorinated Ethenes in Contaminated Groundwater, *Environ Sci Technol*, 2012, **46**, 10918–10925.

268 I. Y. López-Pacheco, A. Silva-Núñez, C. Salinas-Salazar, A. Arévalo-Gallegos, L. A. Lizarazo-Holguin, D. Barceló, H. M. N. Iqbal and R. Parra-Saldívar, Anthropogenic contaminants of high concern: Existence in water resources and their adverse effects, *Science of The Total Environment*, 2019, **690**, 1068–1088.

Appendix A: Santrock – Studley – Hayes (RStudio script)

```
###### SSH calculation ######

#Santrock, J., Studley, S.A., Hayes, J.M., 1985. Isotopic analyses based
#on the mass spectra of carbon dioxide. Anal. Chem. 57, 1444-1448.
#10.1021/ac00284a060

#Brand, W.A., Assonov, S.S., Coplen, T.B., 2010. Correction for the 17O
#interference in δ(13C) measurements when analyzing CO2 with stable
#isotope mass spectrometry (IUPAC Technical Report). Pure Appl. Chem.
#82, 1719–1733.

#Input ratios (example)
R45 <- 0.0119756
R46 <- 0.0040168

#Constants
Lambda <- 0.51600000
K <- 0.00992350

#Defines number of cycles for calculation
cycles <- 4
```

```
#Initial R18 calculation
R18 <- R46 / 2

#R18 cycled calculation
for (i in 1:cycles){
 fR18 <- (-3*K^2*R18^(2*Lambda)) + (2*K*R45*(R18^Lambda)) +
((2*R18)-R46)
 ffR18 <- -6*K^2*Lambda*R18^(2*Lambda-1) +
2*K*R45*Lambda*R18^(Lambda-1) +2
 R18 <- R18-fR18/ffR18

 i <- i+1
}

#Final R18, and R13 calculation
R18_Final <- R18-(fR18/ffR18)
R17 <- K*(R18_Final^Lambda)
R13 <- R45-2*K*(R18_Final^Lambda)

#Print output - R13 to 59 decimal places
print(sprintf("%.59f", R13)
```

Appendix B: Statistical bootstrapping (RStudio script)

```
#Table for bootstrapping with B number of columns.
#nrow should be = n[x]

bootdata<- matrix(0, ncol = B, nrow = 19)

#Populates the table 'bootdatax B number of times
#Uses 'sample()' function to rantomly select a value from x
#and puts that number to populate a column.
#The 'for()' function repeats the operation B number of times.
for(b in 1:B){
        bootdata[, b]<- sample(data$x, dim(data)[1], replace =TRUE)
}

#Creates a mean value for each column from 'bootdata' table.
meansx <- apply(bootdata,2, mean)
```

Appendix C: Binomial calculation of distribution of ^{13}C in a molecule (RStudio script)

```
#probability of 13C
n <- 0.009626

#how many carbon atoms in a molecule
b <- 12

#how many 13C in a molecule
m <- 0

#binomial
x <- dbinom(m, b, n)
x
#convert a factor to percentage
x <- x*100
x

#how many 13C in a molecule
k <- 1

#binomial
y <- dbinom(k, b, n)

#convert a factor to percentage
y <- y*100

#Percentage chance of two or more 13C
100 - (x+y)
```

Appendix D: Compound screen list

The table below present the list of possible compounds based on the NIST database identification.

Compound Name	Count
Cholesterol	5
Ethanol, 2-phenoxy-	5
Nonanoic acid	5
Octanoic Acid	5
Pentadecanoic acid	5
Pentanoic acid	5
Squalene	5
Tris(1,3-dichloroisopropyl)phosphate	5
1,2-Benzenedicarboxylic acid, mono(2-ethylhexyl) ester	4
1H-Pyrrole-2,5-dione, 3-ethyl-4-methyl-	4
2,6,6-Trimethyl-2-cyclohexene-1,4-dione	4
Benzoic acid	4
Carbamazepine	4
Cholestan-3-ol, (3á,5á)-	4
Ethyl citrate	4
Heptadecanoic acid	4
Nonanal	4
Phenol, 2,4-bis(1,1-dimethylethyl)-	4
Ribitol, 1,3:2,4-di-O-benzylidene-	4
Triphenyl phosphate	4
Vitamin E	4
1(3H)-Isobenzofuranone	3
13-Docosenamide, (Z)- (Erucylamide)	3
1H-Pyrrole-2,5-dione, 3-ethenyl-4-methyl-	3
1-Penten-3-one, 1-(2,6,6-trimethyl-2-cyclohexen-1-yl)-	3
2,4-Dimethylcyclohex-1-ene-5-carboxylic acid (trans)	3
2H-Indol-2-one, 1-(2,6-dichlorophenyl)-1,3-dihydro-	3
2-Propenenitrile, 3,3-diphenyl-	3

3,5-di-tert-Butyl-4-hydroxyphenylpropionic acid	3
7-Acetyl-6-ethyl-1,1,4,4-tetramethyltetralin	3
Acetamide, 2,2,2-trifluoro-	3
Benzeneacetic acid, 3-methoxy-à,4-bis[(trimethylsilyl)oxy]-,trimethylsilyl ester	3
Benzenecarbothioic acid, 2,4,6-triethyl-, S-(2-phenylethyl) ester	3
Benzenesulfonamide, 2-methyl-	3
Benzenesulfonamide, N-butyl-	3
Benzoic acid, 4-(4-propylcyclohexyl)-, 4'-cyano[1,1'-biphenyl]-4-yl ester	3
Bumetrizole	3
Butyl citrate	3
Diphenyl sulfone	3
Ethanol, 2-butoxy-, phosphate (3:1)	3
Ethanone, 2,2'-(octahydro-2,3-quinoxalinediylidene)bis[1-phenyl-	3
Hexacosane	3
Hexanoic acid	3
Iminostilbene (dibenzazepine)	3
Methyl tetradecanoate	3
n-Decanoic acid	3
n-Hexadecanoic acid	3
n-Hexyl salicylate	3
Nonanamide	3
Phlorobutyrophenone	3
p-Octylacetophenone	3
Silane, trimethyl(3-methylphenoxy)-	3
Tetracosane	3
Tetradecanamide	3
Tri(2-chloroethyl) phosphate	3
Tributyl phosphate	3
1-(Prop-2-ynyloxy)-3,4-methylenedioxybenzene	2
1,2,4,5-Tetrazine	2
1,2-Bis(4-methoxyphenyl)-N,N,N',N'-tetramethylethane-1,2-diamine	2
1,2-Dimethyl-4-tertbutyl-6-cyclopentylbenzene	2
1,3-Dioxolane, 2-methyl-2-(5-phenyl-3-pentenyl)-	2

1,4-Naphthoquinone, 6-acetyl-2,5-dihydroxy-	2
1,8-Naphthalic anhydride	2
11,12-Dihydroxyseychellane	2
17,21-Dimethylheptatriacontane	2
1-Dodecanamine, N,N-dimethyl-	2
1-Ethyl-1-nonyloxy-1-silacylopentane	2
1H-Indole, 5,7-dibromo-	2
1-Penten-3-one, 1-(2,6,6-trimethyl-1-cyclohexen-1-yl)-	2
1-Phenyl-1-decanol	2
2,3-Diphenyl-6,7-dimethylquinoxaline	2
2,5-di-tert-Butyl-1,4-benzoquinone	2
2,5-Furandione, 3,4-dimethyl-	2
2,6,10-Dodecatrien-1-ol, 3,7,11-trimethyl-, acetate, (E,E)-(Farnesyl acetate)	2
2,6-Bis(1,1-dimethylethyl)-4-phenylmethylenecyclohexa-2,5-dien-1-one	2
2-Acetyl-5-methylfuran	2
2-Cyclohexen-1-one, 3,5-dimethyl-	2
2-Ethylhexanoic acid, dimethyl(tert-butyl)silyl ester	2
2-Ethylhexyl trans-4-methoxycinnamate	2
2-Furancarboxaldehyde, 5-methyl-	2
2H-1-Benzopyran-2-one, 7-amino-4-(trifluoromethyl)-	2
2H-Azepin-2-one, hexahydro-7-methyl-	2
2-Methyl-3-(2-chloro-5-hydroxyphenyl)-4(3H)-quinazolinone	2
2-Propenoic acid	2
3(2H)-Benzofuranone, 6-methoxy-2-[(3-methylphenyl)methylene]-, (E)-	2
3,4-Dichlorophenylacetic acid	2
4-(2-Hydroxy-1-naphthylmethylidene)-2-phenyl-2-oxazolin-5-one	2
4-Acetoxy-3-methoxystyrene	2
4-Ethylbenzoic acid	2
4-Methylurazole	2
5-Cyano-2-methyl-4-methylthio-6-phenylpyrimidine	2
6-Thiopyrazolo[3,4-d]pyrimidin-4,6(5H,7H)-dione-3-carboxamide	2
7-Methyl-5-phenyl-5H-pyrazolo[3,4-e]-1,2,4-triazine-3-	2

thiol	
8-Phenyl-6-thio-theophylline	2
Acetic acid, (3,4-dimethoxyphenyl)(trimethylsiloxy)-, methyl ester	2
Acridine, 9-butyl-9,10-dihydro-	2
Acridine-9-carbaldehyde	2
à-Damascone	2
á-D-Fructopyranose, 2,3:4,5-bis-O-(1-methylethylidene)-(Topiramate derivative)	2
Bayer 28,589	2
Benzaldehyde	2
Benzenamine, 4,4'-[(1-methylethylidene)bis(4,1-phenyleneoxy)]bis-	2
Benzenamine, N-(1,1-dimethyl-2-propenyl)-4-(1-methylethyl)-	2
Benzenepropanoic acid	2
Benzenesulfonamide, 4-methyl-	2
Benzenesulfonamide, 4-methyl-N-propyl-	2
Benzenesulfonamide, N-ethyl-4-methyl-	2
Benzenesulfonanilide	2
Benzoic acid, 2,4,6-trimethyl-	2
Benzoic acid, 2-phenoxy-	2
Benzoic acid, 3,5-bis(1,1-dimethylethyl)-4-hydroxy-	2
Benzoic acid, 4-[(2,4-dimethoxy-6-pentylbenzoyl)oxy]-2-methoxy-6-pentyl-, methyl ester	2
Benzoic acid, octyl ester	2
Benzophenone	2
Benzophenone, 2',5-dichloro-2-[methyl[(4-methylphenyl)sulfonyl]amino]-	2
Bicyclo[3.1.0]hexan-2-one, 1,5-bis(1,1-dimethylethyl)-3,3-dimethyl-	2
Bicyclo[3.1.0]hexan-3-one (Chrysanthone)	2
Bis(1-chloro-2-propyl)(3-chloro-1-propyl)phosphate	2
Butanedioic acid, monomethyl ester	2
Butanoic acid, 2,2-dimethyl-	2
Butanoic acid, 3-methyl-	2
Cholest-3-ene, (5à)-	2
Cholestanol	2

Codeine	2
ç-Tocopherol	2
Cyclobutaneacetonitrile, 1-methyl-2-(1-methylethenyl)-	2
Cyclohexanol, 2-[(dimethylamino)methyl]-1-(3-methoxyphenyl)-,trans-(ñ)-	2
Cyclopenta[g]-2-benzopyran, 1,3,4,6,7,8-hexahydro-4,6,6,7,8,8-hexamethyl-	2
Cyclopentanone, 2-acetyl-3,3-dimethyl-2-(3-oxo-1-butenyl)-, (E)-	2
Dextromethorphan	2
Diethyl Phthalate	2
Dimethoxymethyl-hydroxy-triphenyl phosphide	2
Dimethyl trisulfide	2
Disiloxane, hexamethyl-	2
Docosanoic acid	2
Dodecane, 1,1-dimethoxy-	2
Dodecanoic acid	2
Dodecanoic acid (Lauric acid)	2
Ethanamine, 2,2'-oxybis[N,N-dimethyl-	2
Ethanone, 1-(2-hydroxy-5-methylphenyl)-	2
Ethyl [5-hydroxy-1-(6-methoxy-4-methyl-3-quinolinyl)-3-methyl-1Hpyrazol- 4-yl]acetate	2
Furan, 2-methoxy-	2
Furo[2,3-b]pyridine, 2-methyl-	2
Galaxolide 1	2
Guaifenesin	2
Heptanoic acid	2
Hexadecanoic acid, 2-hydroxy-1-(hydroxymethyl)ethyl ester (2 - Monopalmitin)	2
Hexadecenoic acid, Z-11-	2
Hexanedioic acid, monomethyl ester	2
Hexanoic acid, 2-ethyl-	2
Hydrogen chloride	2
Indano[2,1-d]1,3-dioxane,	2
Isopropyl Palmitate	2
Methane, diethoxy-	2
N-(But-1-enyl)-pyrrolidin-2-one	2
Nonanal dimethyl acetal	2

Octadecanoic acid	2
Octanal, 2-(phenylmethylene)-	2
Octicizer	2
Oleanitrile	2
Oxime-, methoxy-phenyl-	2
Oxybenzone	2
Phenol	2
Phenol, 2,4-bis(1,1-dimethylpropyl)-	2
Phenol, 2,4-di-t-butyl-6-nitro-	2
Phenol, 2,6-bis(1,1-dimethylethyl)-4-isocyano-	2
Phenol, 4,4'-(1-methylethylidene)bis-	2
Phenol, 4-ethyl-	2
Phenol, p-tert-butyl-	2
Phentermine, N-4-carbethoxyhexafluorobutyryl deriv.	2
Phentermine, n-heptafluorobutyryl deriv	2
Phosphoric acid, (1-methylethyl)phenyl diphenyl ester	2
Phthalic acid, 3,5-dimethylphenyl 4-methoxyphenyl ester	2
Propanamide	2
Propanoic acid	2
Propanoic acid, 2-methyl-, 1-(1,1-dimethylethyl)-2-methyl-1,3-propanediyl ester	2
Propanoic acid, 2-methyl-3-[4-t-butyl]phenyl-	2
Pyrazine, 2,3-dimethyl-	2
Pyrazine, trimethyl-	2
Pyridine	2
Pyrimidine, 4-(2-hydroxy-5-methoxyphenyl)-	2
Quinoline-7-carboxylic acid, 2-phenyl-, methyl ester	2
Salicylic acid	2
Silane, (1,1-dimethylethyl)dimethyl(phenylmethoxy)-	2
Silane, (3-iodopropyl)trimethyl-	2
Silane, decyldiethylmethyl-	2
Silanol, (1,1-dimethylethyl)dimethyl-, benzoate	2
Tetradecanoic acid	2
Tetradecanoic acid (Myristic acid)	2
Tetradecanoic acid, 10,13-dimethyl-, methyl ester	2
Triacetin	2
Triclosan	2
Tridecanoic acid	2

Triisopropylphosphate	2
Trimethyl(2,6 ditert.-butylphenoxy)silane	2
Tris(3-chloropropyl) phosphate	2
Undecanoic acid	2
Venlafaxine	2
(+-)-3-Methyl-1-penten-3-ol	1
(1aR,3S,3aS,7R,7aR,7bS)-(-)-1a,2,3,3a,4,5,6,7,7a,7b-Decahydro-1,1,7,7a-tetramethyl-1H-cyclopropa[a]naphthalen-3-ol	1
(2R,4S)-2,4-Dimethyladipic acid dimethyl ester	1
(4-[(E)-2-(4-Bromophenyl)ethenyl]phenoxy)acetic acid	1
(4'-Methoxycarbonylmethoxy-biphenyl-4-yloxy)-acetic acid, methyl ester	1
(7-Methylbenzo(b)thien-3-yl)acetic acid	1
(9S,10R)-9,10-Epoxy-3Z,6Z-heneicosadiene	1
(E)-2-Hydroxy-4'-dimethylamino-stilbene	1
(E)-4-Hydroxy-2-methyl-pent-2-enoic acid	1
(N-Methylcarbamoyloxymethyl)trivinylsilane	1
(Z)-tert-Amylsulfinyl-2-phenylethene	1
[1,1'-Biphenyl]-2-acetic acid	1
[1,1'-Biphenyl]-4-carboxylic acid, 2',4'-dimethyl-, ethyl ester	1
[1,2,4]Oxadiazole, 5-phenoxymethyl-3-(thiophen-2-yl)-	1
[1,2,4]Triazolo[4,3-b][1,2,4]triazole, 7-amino-3-(2-butylsulfanylethylsulfanyl)-	1
[1,2'-Binaphthalene]-5,5',8,8'-tetrone, 1',4-dihydroxy-2,3'-dimethyl-, (-)-	1
1-(1-Adamantyl)-2-tripropylsilyloxyethane	1
1-(2-Chloroethyl)-4-dimethylamino-6-(N-methoxy-N-methylamino)-1,3,5-triazin-2(1H)-one	1
1(3H)-Isobenzofuranone, 6-nitro-	1
1-(4-Nitrophenyl)piperazine	1
1-(Anilinomethylene)-2-indanone	1
1-(Trihexylsilyloxy)heptane	1
1-(Trihexylsilyloxy)octane	1
1,1-Cyclobutanedicarboxamide, N,N'-dimethyl-	1
1,1-Cyclopropanedicarboxylic acid, 2,6-bis(1,1-dimethylethyl)-4-methylphenyl methyl ester	1

1,1-Dimethoxy-2-phenylpropane	1
1,1-Dimethyl-2,2-di(pentafluorobenzoyl)-hydrazine	1
1,1-Ethanediol, diacetate	1
1,2,3,3a,4,5,7,8,9,10,11,12,12a-Tetradecahydrobenzo[a]pyrene	1
1,2,3-Propanetriol, diacetate	1
1,2,3-Propanetriol, monoacetate	1
1,2,4-Thiadiazole, 5-amino-	1
1,2,4-Thiadiazole, 5-hydrazino-3-methyl-	1
1,2,4-Triazine-5-thiol, 3-amino-6-methyl-	1
1,2:3,4-Di-O-isopropylidene-6-O-(5-dimethylamino-1-naphthalenesulfonyl)-à-d-galactopyranose	1
1,2-Benzenedicarboperoxoic acid, bis(1,1-dimethylethyl) ester	1
1,2-Benzenedicarboxylic acid	1
1,2-Benzenedicarboxylic acid (Phthalic acid)	1
1,2-Benzenedicarboxylic acid, dicyclohexyl ester	1
1,2-Benzenedicarboxylic acid, monobutyl ester	1
1,2-Benzenediol	1
1,2-Bis(3,5,5-trimethyl-2-cyclohexenylidene)hydrazine	1
1,2-Cyclopropanedicarbonitrile, 3-(2-pyridinyl)-	1
1,2-Dibenzoyl-3-methyldiaziridine	1
1,2-Ethanediamine, N,N,N',N'-tetramethyl-	1
1,2-Ethanediol, monobenzoate	1
1,2-Hydrazinedicarboxamide	1
1,2-Hydrazinedicarboxylic acid, diethyl ester	1
1,2-Propanediol, 2-methyl-, 1-methanesulfonate	1
1,3,5-Triazine-2,4,6(1H,3H,5H)-trione	1
1,3,5-Triazine-2,4,6(1H,3H,5H)-trione, 1,3,5-tri-2-propenyl-	1
1,3,5-Triazine-2,4-diamine, N,N'-bis(3-aminophenyl)-	1
1,3,6-Trioxocane	1
1,3-Benzenediol, 2-[5-methyl-2-(1-methylethyl)cyclohexyl]-5-pentyl-	1
1,3-Cyclohexadiene, 1,2,3,4,5,5,6,6-octafluoro-	1
1,3-Diamino-5,6-dihydro-8-methoxybenzo[f]quinazoline	1
1,3-Dimethyl-5,7-di-n-propyladamantane	1
1,3-Dioxa-2,4,6-trisilacyclohexane, 2,2,4,4,6,6-	1

hexamethyl-	
1,3-Dioxan-4-one, 2-(1,1-dimethylethyl)-5-methyl-, (2s-cis)-	1
1,3-Dioxepane, 2-pentadecyl-	1
1,3-Dioxolane, 2-(1-phenylethyl)-	1
1,3-Dioxolane, 2-(2-phenyl-2-propyl)-	1
1,3-Dioxolane, 2,2-dimethyl-	1
1,3-Dioxolane-2-heptanenitrile, à-methyl-ë-oxo-2-phenyl-	1
1,3-Dioxolane-2-propanoic acid, 2,4-dimethyl-, ethyl ester	1
1,3-Dioxolane-2-propanoic acid, 2-methyl-, methyl ester	1
1,3-Dioxolane-4-methanol, 2-ethyl-	1
1,3-Dithiol-1-ium, 2-(4-chlorophenyl)-4-hydroxy-, hydroxide, inner salt	1
1,3-Oxazetidin-2-one, 3-phenyl-	1
1,3-Propanediol, 2-(hydroxymethyl)-2-methyl-, monobenzoate	1
1,4-Benzenedicarboxylic acid, bis(2-hydroxyethyl) ester	1
1,4-Dioxacyclohexadecane-5,16-dione	1
1,4-Methanobenzocyclodecene, 1,2,3,4,4a,5,8,9,12,12a-decahydro-	1
1,4-Naphthalenedione, 2,3-dimethyl-	1
1,4-Naphthalenedione, 2-methyl-3-(3-methyl-2-butenyl)-	1
1,4-Oxathian-2-one, 6-methyl-	1
1,5-Benzoxazepin-4(5H)-one, 2,3-dihydro-3-phenyl-	1
1,5-Diphenyl-2H-1,2,4-triazoline-3-thione	1
1,8:2,7-Dimethanodibenzo[a,e]cyclobuta[c]cycloocten-13-one, 1,2,2a,7,8,12b-hexahydro-1-methoxy-	1
1,8-cis-Undecadien-5-yne 3,7-bis-trimethylsilyl ether	1
1,8-Diazacyclotetradecane-2,7-dione	1
1,8-Dihydroxy-3-methylanthraquinone	1
1,8-Naphthalenediol, 2,7-diacetyl-3,6-dimethyl-	1
1,N-Dimethyl-2-phenylethylamine, pentafluorobenzoyl-	1
1-[(2-Hydroxyphenyl)thioxomethyl]piperidine	1
1-[2-Methoxy-5-nitrophenyl]-3-amidineurea	1
10H-Phenoxaphosphine, 2,8-diethyl-10-hydroxy-, 10-oxide	1
10-Pentadecen-5-yn-1-ol, (E)-	1
13,14-Benzo-1,4,8,11-tetrathiacyclopentadecane	1
17-(1,5-Dimethylhexyl)-1,10,13-	1

trimethylhexadecahydrocyclopenta[a]phenanthren-3-one	
17à-Methyl-17á-hydroxy-1,4,6-androstatrien-3-one, mono-TMS	1
1-Amino-2-methylnaphthalene	1
1-Butanamine, N-butyl-	1
1-Butanamine, N-ethyl-	1
1-Butanol, 3-methoxy-	1
1-Butanone, 4-chloro-1-(4-hydroxyphenyl)-	1
1-Butene, 4-isothiocyanato-	1
1-Chloromethyl-3,5-dimethylbenzene	1
1-Ethyl-1-(2-ethylhexyloxy)-1-silacyclopentane	1
1-Ethyl-2-pyrrolidinone	1
1-Ethyl-3-propyladamantane	1
1-Formyl-2,2-dimethyl-3-trans-(3-methyl-but-2-enyl)-6-methylidenecyclohexane	1
1-Formyl-2-hydroxy-9-methyl-anthracene	1
1H-1,4-Diazepine-5,7(2H,6H)-dione, 3-(dimethylamino)-6,6-diethyl-2,2-dimethyl-	1
1H-1-Benzazepine-3,4-dicarboxylic acid, 1-methyl-, dimethyl ester	1
1H-Azepine, 1-(phenylsulfonyl)-	1
1H-Benz[de]isoquinoline-1,3(2H)-dione	1
1H-Benzoimidazole, 2-(3-nitrophenyl)-	1
1H-Imidazole-4-carboxamide, 5-amino-	1
1H-Indene, 2,3-dihydro-1,1,3-trimethyl-3-phenyl-	1
1H-Indole, 1-benzoyl-	1
1H-Indole-2-carboxylic acid, 6-(4-ethoxyphenyl)-3-methyl-4-oxo-4,5,6,7-tetrahydro-, isobutyl ester	1
1H-Isoindole-1,3(2H)-dione, 2-hydroxy-	1
1H-Purine-6-carbonitrile	1
1H-Pyrazole, 5-methoxy-1,3-dimethyl-	1
1H-Pyrrole, 1-(2,3,4,6-tetrachloro-5-methylphenyl)-	1
1H-Pyrrole, 1-(2-furanylmethyl)-	1
1H-Pyrrole, 2,4-diphenyl-	1
1H-Pyrrole, 2-ethyl-	1
1H-Pyrrole, 2-methyl-	1
1H-Pyrrole, 3-ethyl-2,4,5-trimethyl-	1
1H-Pyrrolo[2,3-b]pyridine, 3-amino-2-phenyl-	1

1-Hydroxycyclohexanecarboxylic acid	1
1-Imidazolidinecarboxamide-4-oxo,N1-(1-methylethyl)-2-(1,1-dimethylethyl)-3-methyl	1
1-Methyl-2-(quinoxolin-3-yl)benzimidazole	1
1-Methyl-bis(1,2,4)-triazole-5,1	1
1-Phenanthrenecarboxylic acid, 1,2,3,4,4a,9,10,10a-octahydro-1,4adimethyl-7-(1-methylethyl)-, [1R-(1à,4aá,10aà)]-	1
1-Proline, N-(2-thienylcarbonyl)-, methyl ester	1
1-Propanol, 2-(2-hydroxypropoxy)-	1
1-Propene, 3-(2-cyclopentenyl)-2-methyl-1,1-diphenyl-	1
1s,4R,7R,11R-8-Hydroxy-1,3,4,7-tetramethyltricyclo[5.3.1.0(4,11)]undec-2-ene	1
1-Tritylhistamine	1
2(1H)-Pyridinone, 3-acetyl-4-hydroxy-1,6-dimethyl-	1
2(1H)-Pyridinone, 3-acetyl-4-hydroxy-6-methyl-	1
2(1H)-Quinolinone, 3-[(trifluoromethyl)thio]-4-methyl-	1
2-(1-Hydroxy-1-methylethyl)cyclohexanol	1
2-(1-Methylcyclopentyloxy)-tetrahydropyran	1
2-(2-Naphthyl)-2-propanol	1
2-(3à,5-Cyclo-6á-methoxynorcholanyl)-1,1-diphenylethylene	1
2(3H)-Furanone, 5-methyl-	1
2(3H)-Furanone, dihydro-5-(2-octenyl)-, (Z)-	1
2(4H)-Benzofuranone, 5,6,7,7a-tetrahydro-4,4,7a-trimethyl-, (R)-	1
2(5H)-Furanone	1
2-(Bromovinyl)trimethylsilane	1
2-(E)-Hexenoic acid, (4S)-amino-5-methyl-	1
2-(p-Fluorophenyl)-1-methylbenzimidazole	1
2,2,3,3,4,4-Hexamethyltetrahydrofuran	1
2,2-Bis(hydroxymethyl)-2,2',2"-nitrilotriethanol	1
2,2-Bis[(4-trimethylsiloxy)phenyl]propane	1
2,2-Diethyl-2-sila-1,3-dioxacyclohexane	1
2,2-Diisopropyl-1,3-dioxolane	1
2,2'-Trimethylenebis-1,3-dioxolane	1
2',3',4',5,7,8-Hexamethoxyflavone	1
2,3,4,6-Tetramethoxystyrene	1

2,3,5,6-Tetrafluoroanisole	1
2,3,5-Trimethyl-6-isopentylpyrazine	1
2,3-Benzofurandione	1
2,3-Butanediol, 2,3-dimethyl-	1
2,3-Dihydro-1-ethyl-1H-3-methylcyclopenta[b]quinoxaline	1
2,3-Dihydro-2-methyl-4-(4-methylphenyl)-1H-1,5-benzodiazepine	1
2,3-Dimethyl-5-(2,6,10-trimethylundecyl) furan	1
2,3-Di-O-methyl-D-xylopyranose	1
2,3-Disila-5-heptene, 2,2,3,3,4-pentamethyl-4-(phenylthio)-	1
2,4,6-Trimethylpropiophenone	1
2,4,6-Tris(1,1-dimethylethyl)-4-methylcyclohexa-2,5-dien-1-one	1
2,4-Diphenyl-4-methyl-2(E)-pentene	1
2,4-Pyrimidinediamine, 6-methyl-N4-phenyl-	1
2,5,10-Undecanetrione, 6,6-dimethyl-	1
2,5,5-Trimethyl-2-oxo-1,2,3,-dioxophosphorinane	1
2,5,6-Tri-O-acetyl-3,4-di-O-methyl-D-mannonitrile	1
2,5-Cyclohexadiene-1,4-dione, 2,5-bis(1,1-dimethylpropyl)-	1
2,5-Dimethoxymandelic acid, di-TMS	1
2,5-Dimethylbenzophenone	1
2,5-Dimethylpyrimidine	1
2,5-Furandione, 3-methyl-	1
2,5-Pyrrolidinedione	1
2,6-Bis(1,1-dimethylethyl)-4-(1-oxopropyl)phenol	1
2,6-Difluorobenzoic acid, 4-nitrophenyl ester	1
2,6-Pyridinedicarboxylic acid	1
2-[(2RS)-2-(2-Hydroxyethoxy)propyl]-2-methyl-1,3-dioxolane	1
2-[6-(1-Hydroxy-1-methylethyl)naphthalen-2-yl]propanoic acid	1
21.5553 ? Octadecanoic acid (ID#:57-11-4)	1
22,23-Dihydrospinasterone	1
24Xi-methylcholestane-3á,5à,6á-triol-3á,6á-diacetate	1
27-Norergosta-5,22-dien-3-ol, (3á,22Z)-	1
2-Acetyl-2-methyltetrahydrofuran	1
2-Acetyl-5-methylthiophene	1

2-Acetylmethylamino-4,5,6,7-tetrahydrobenzothiazol-7-one	1
2-Amino-4,6-dimethyl-5-iodopyrimidine	1
2-Amino-4-acetamino anisole	1
2-Amino-4-hydroxy-6,7-bis[3-phenylpropyl]pteridine	1
2-Amino-benzoic acid	1
2-Anilino-4-methylquinoline	1
2-Benzyl-6-methyl-4(3H)-pyrimidinone	1
2-Bromo-3-methyl-6-phenyl-thiazolo(3,2-b)-1,2,4-triazole	1
2-Butanamine, N,N-dimethyl-	1
2-Butanol, 3,3'-oxybis-	1
2-Butanone, 1-(4-tert-butyl-2,6-xylyl)-3-o-tolyl-	1
2-Butanone, 3-hydroxy-	1
2-Buten-1-one, 1-(2,6,6-trimethyl-2-cyclohexen-1-yl)-, (E)-	1
2-Butene, 1,4-diethoxy-	1
2-Carbomethoxy-8-methyl-8-azabicyclo[3.2.1]oct-2-ene	1
2-Chloroethyl benzoate	1
2-Chloroethyl methyl sulfide	1
2-Chloromethyl-1H-benzoimidazole-5-carboxylic acid	1
2-Cyano-2-isopropyl-3-methylbutanoic acid	1
2-Cyclobutyl-N-(4-iodo-phenyl)-acetamide	1
2-Cyclohexene-1-thione, 3,5,5-trimethyl-	1
2-Cyclopenten-1-one, 2-hydroxy-	1
2-Cyclopentene-1,4-dione	1
2-Dodecanol, 2-methyl-	1
2E,4E-Hexadiene, adduct with 4-methyl-1,2,4-triazolin-3,5-dione	1
2-Ethyl-3-hydroxypropionic acid, di-TMS	1
2-Ethylidenehydrazono-3-methyl-7-chloro-2,3-dihydrobenzothiazole	1
2-Ethylthio-7-methylthio-1,3,4-thiadiazolo(3,2-a)(1,3,5)triazine-5-one	1
2-Fluoro-4-bromobenzaldehyde	1
2-Fluorobenzylamine, N,N-dibutyl	1
2-Fluorobenzylamine, N,N-dioctyl	1
2H,8H-Benzo[1,2-b:5,4-b']dipyran-10-propanol, 5-methoxy-2,2,8,8-tetramethyl-	1
2H,8H-Benzo[1,2-b:5,4-b']dipyran-2-one, 5-methoxy-8,8-dimethyl-10-(3-methyl-2-butenyl)-	1

2H-[1,2,3]Triazole, 4-nitro-	1
2H-1-Benzopyran-2-one, 7-methoxy-6-(3-methyl-2-oxobutyl)-	1
2H-1-Benzopyran-5-carboxylic acid, 3,4-dihydro-2-methyl-4-oxo-	1
2H-Pyran, 2-[[(3á)-cholest-5-en-3-yl]oxy]tetrahydro-	1
2H-Pyran-2-one, tetrahydro-4-methyl-	1
2H-Tetrazole, 2-methyl-	1
2-Hydroxy-4,5-methylenedioxypropiophenone	1
2-Imidazolidinone, 1,3-dimethyl-	1
2-Isopropenyl-3,6-dimethylpyrazine	1
2-Methoxy-1,3-dioxolane	1
2-Methyl-1,1-bis(2,4-dimetoxyphenyl)propane	1
2-Methyl-2-propyl methylphosphonofluoridate	1
2-Methylheptanoic acid	1
2-Methylpropionic acid, 4-cyanophenyl ester	1
2-Monopalmitin	1
2-Naphthaleneacetic acid, 6-methoxy-à-methyl-	1
2-Norbornen-7-ol, 7-(p-methoxyphenyl)-, p-nitrobenzoate, anti-	1
2-Octanol, 2,6-dimethyl-	1
2-Octenoic acid	1
2-Oxetanone, 3,3-dimethyl-	1
2-Oxo-3-phenyl-2H-pyrane-6-carboxylic acid, ethyl ester	1
2-Oxo-5-benzyl-4,6-diphenyl-1,2-dihydropyrimidine	1
2-Pentenoic acid, 4-oxo-, methyl ester, (Z)-	1
2-Phenazinol, 6-amino-	1
2-Phenyl-2-trimethylsilyloxypropanoic acid, trimethylsilyl ester	1
2-Phenyl-8-methyl-4H-imidazo(2,1-c)(1,4)benzoxazine	1
2-Piperidinone	1
2-p-Nitrophenyl-5-isopropyloxy-oxadiazole-1,3,4	1
2-Propanol, 1,1'-[(1-methyl-1,2-ethanediyl)bis(oxy)]bis-	1
2-Propenamide, 3-methoxy-N-phenyl-, (E)-	1
2-Propenamide, N-(1-methylethyl)-N,3-diphenyl-	1
2-Propenoic acid, 3-(4-methoxyphenyl)-, 2-ethylhexyl ester	1
2-Propenoic acid, 3-(dimethylamino)-, methyl ester	1
2-Propenoic acid, 3-bromo-, methyl ester, (Z)-	1

2-Pyrazoline-1-carboxamide, 3-methyl-	1
2-pyrrolidinone	1
2-t-Butyl-1-methanesulfonyl-3-methyl-imidazolidin-4-one	1
2-t-Butyl-1-methyl-3-phenyl-imidazolidin-4-one	1
2-Thiazolamine, 5-nitro-	1
2-Thiazolidinone, 3-(1-methylethyl)-4-methyl-	1
2-Thioacetylimino-3-methyl-2,3-dihydrobenzothiazole	1
2-Thiophenecarboxylic acid, 4-nitrophenyl ester	1
2-Undecen-4-ol	1
2-Undecenoic acid, trimethylsilyl ester	1
3-(2'-Chloro-phenyl)-2-methyl-4(3H)-quinazolinone	1
3(2H)-Benzofuranone, 6-methoxy-2-[(2-methoxyphenyl)methylene]-, (E)-	1
3(2H)-Furanone, 5-methyl-2-octyl-	1
3(2H)-Isoquinolinone, octahydro-, (4ar-trans)-	1
3-(2-Methylphenyl)propionic acid	1
3-(2-t-Butoxyethyl)decahydroisoquinoline	1
3-(3-Hydroxyphenyl)-3-trifluoromethyl-3H-diazirine	1
3-(4-Fluorobenzoyl)-2(3H)-thioxo-4-thiazolyl 4-fluorobenzoate	1
3(4H)-Phenanthrenone, 4a,4b,5,6,7,8,8a,9,10,10a-decahydro-4b,8,8-trimethyl-, [4aS-(4aà,4bá,8aà,10aá)]-	1
3-(Dioxolan-2-yl)-1,1-dimethyl-2-phenylpropylhydroxylamine	1
3-(Fluorosulfonyl)benzoic acid	1
3(N,N-Dimethylmyristylammonio)propanesulfonate	1
3,3,5-Trichloro-2,4-dithiahexane 2,2,4,4-tetroxide	1
3,3-Dimethoxy-2-butanone	1
3,4-Dihydroxy-5-methoxybenzaldehyde	1
3,4-Dihydroxypropiophenone	1
3,4-Methylenedioxymandelic acid	1
3,5,6-Trimethoxyfurano-(7,8,2",3")-flavone	1
3,5-Dihydroxybenzamide	1
3,5-Dimethoxyphenethylamine	1
3,5-Dimethyl-1-dimethylphenylsilyloxybenzene	1
3,5-Dimethyl-1-dimethylvinylsilyloxybenzene	1
3,5-Dimethyl-2,4,6-trichlorophenol	1
3,5-di-tert-Butyl-4-hydroxybenzaldehyde	1

3,5-di-tert-Butyl-4-hydroxybenzyl alcohol	1
3,6,10-Trioxa-2,11-disiladodecane, 2,2,11,11-tetramethyl-	1
3,6,9,12-Tetraoxa-2,13-disilatetradecane, 2,2,13,13-tetramethyl-	1
3,6-Dioxa-2,4,5,7-tetrasilaoctane, 2,2,4,4,5,5,7,7-octamethyl-	1
3,6-Dioxa-2,7-disilaoctane, 2,2,4,7,7-pentamethyl-	1
3,6-Diphenyl-5-(2,4-dihydroxyphenyl)-1,2,4-triazine	1
3,7,11,15-Tetramethyl-2-hexadecen-1-ol	1
3,7a-Diazacyclohepta[jk]fluorene-5-acetaldehyde, à-ethylidene-1,2,3,3a,4,5,6,7-octahydro-7,10-	1
3á,16à,22á,30-Tetrahydroxy-13,28-epoxyoleanane	1
3-Amino-6-isobutylthieno[2,3-b]pyridine-2-carboxylic acid,phenylamide	1
3-Chloro.2,4-pentanedione	1
3-Chloro-benzo[b]thiophene-2-carboxylic acid [2-(4-methoxyphenoxy)-ethyl]-amide	1
3-Cyano-1,3-dimethyl-5,5-dimethoxycarbonylisoxazolidine	1
3-Cyano-5,5-dimethoxycarbonyl-N-methylisoxazolidine	1
3-Dodecanol, 3,7,11-trimethyl-	1
3-Ethoxy-2-bromo-1-propanol	1
3-Furan-2-yl-acrylic acid 4-[(2-chloro-benzoyl)-hydrazonomethyl]-phenyl ester	1
3-Furanmethanol	1
3-Hexanone, 2-methyl-	1
3-Hexen-1-ol, benzoate, (Z)-	1
3-Hexenamide, N,N,2-trimethyl-, (E)-(.+-.)-	1
3H-Pyrazolo[4,3-c]pyridazin-3-one, octahydro-7-hydroxy-6-methylene-2,5-diphenyl-	1
3-Hydroxyisoxazole-5-(N-isopropyl)carboxamide	1
3-Isopropoxy-1,1,1,7,7,7-hexamethyl-3,5,5-tris(trimethylsiloxy)tetrasiloxane	1
3-Isopropyl-4-methyl-dec-1-en-4-ol	1
3-Methanesulphonyl-thiophene-2-carboxamide	1
3-Methyl-1,2-diphenyl-3-(2-thienyl)cyclopropene	1
3'-Methyl-2-benzylidene-coumaran-3-one	1
3-Methyl-4-amino-4,5(1H)-dihydro-1,2,4-triazole-5-one	1
3-Methylbutyl N-(heptafluorobutyryl)leucinate	1

3-Methylbutyl N,O-bis(heptafluorobutyryl)hydroxyprolinate	1
3-Phenyl-2,9-dioxa-4-aza-fluoren-1-one	1
3-Pyridinecarbonitrile, 1,4-dihydro-1-methyl-	1
3-tert-Butyl-4-hydroxyanisole	1
4-(2-Chloroethoxy)-6-methoxy-N,N-dimethyl-1,3,5-triazin-2-amine	1
4-(2-t-Butyl-5-oxooxazolidine-3-carbonyl)-N,N-dimethylbenzamide	1
4-(4-Aminophenyl)-2,6-diphenyl pyrimidine	1
4-(4-Fluorophenyl)-2,3-dihydro-2-methyl-1H-1,5-benzodiazepine	1
4-(4-Methylbenzoylmethyl)-2H-1,4-benzoxazin-3(4H)-one	1
4-(9-Acridinyl)-N,N-diethylbenzenamine	1
4-(Hydroxymethyl)-1-phenyl-2-azetidinone	1
4-(m-Nitrophenyl)-2-thiazolamine	1
4-(Trifluoromethylsulfonyl)anisole	1
4,2-Cresotic acid, 6-methoxy-, methyl ester, 3,5-dichloro-4,6-dimethoxy-o-toluate	1
4,4'-(m-Phenylenedioxy)diphenol	1
4,5-Dihydro-4,4-diisopropyl-2-phenyl-1,3-oxazin-6-one	1
4,5-Dihydro-N-hydroxy-N-phenyl-3-furamide	1
4,6-Bis(isopropylamino)-1,3,5-triazine-2-carboxylic acid	1
4',6'-Dimethoxy-2',3'-dimethylacetophenone	1
4,6-Octadiyn-3-one, 2-methyl-	1
4,7-Methano-1H-inden-6-ol, 3a,4,5,6,7,7a-hexahydro-, acetate	1
4,9-Dimethyl-2-nitroanthra[2,1-b]furan	1
4-[4-Nitrophenyl]-2,4-dioxobutyric acid	1
4-Amino-2-methyl-5,6-trimethylenepyrimidine	1
4-Deoxypyridoxine	1
4'-Dimethylamino acetanilide	1
4-Ethoxy-N-(1H-[1,2,4]triazol-3-yl)-benzamide	1
4H-1,2,4-Triazol-4-amine	1
4H-1,3,5-Oxadiazine-4-carboxylic acid, 2-(dimethylamino)-6-(2-fluorophenyl)-4-(trifluoromethyl)-, ethyl ester	1
4H-1-Benzopyran-8-carboxylic acid, 3-methyl-4-oxo-2-phenyl-	1
4-Heptanol, 2,6-dimethyl-4-propyl-	1

4-Hexen-3-one	1
4H-Pyrido[1,2-a]pyrimidine-4-thione, 2-methyl-	1
4-Hydroxyanthraquinone-2-carboxylic acid, di-TMS	1
4-Iodoimidazole	1
4-Methyl itaconate	1
4-Methyl-2-(2-nitro-5-piperidin-1-yl-phenyl)-2H-phthalazin-1-one	1
4-Methyl-2-trimethylsilyloxy-acetophenone	1
4-Methylbenzene	1
4-Octen-3-one	1
4-Penten-2-ol, 1,1,1-trifluoro-2-(trifluoromethyl)-	1
4-Phenyldibenzofuran	1
4-Pyridinecarboxaldehyde	1
4-Pyridinol, 3,5-dichloro-2,6-diethyl-	1
4-Pyrimidinamine, 5-methyl-	1
4-t-Butyl-2-(4-methoxy-phenyl)-6-p-tolyl-pyridine	1
4-Trichloromethyl-3,4(1H)-dihydro-2,3-benzothiazine 2,2-dioxide	1
4-Vinylbenzoic acid	1
5-(2,4-Dimethylphenyl)-3-(5-nitrofuran-2-ylmethylene)-3H-furan-2-one	1
5-(4-Hexyloxybenzoyloxy)-2-(4-nitrophenyl)pyrimidine	1
5-(p-tert-Butylphenoxymethyl)-3-(1-naphthyl)-2-oxazolidone	1
5,7,4'-Trihydroxy-8-(3-hydroxy-3-methylbutyl)isoflavone	1
5,7-Dichloro-2-naphthylamine	1
5,8,11,14,17-Eicosapentaenoic acid, methyl ester, (all-Z)-	1
5-Amino-2-methoxyphenol	1
5-Amino-3-phenylpyrazole	1
5à-Pregnane-3á,20à-diamine, N3-isopropylidene-N20,N20-dimethyl-	1
5-Fluoro-2-hydroxyacetophenone	1
5-Hepten-3-one, 5-ethyl-2-methyl-	1
5-Iodo-2-trimethylsilyloxy-acetophenone	1
5-Methylenehydantoin	1
5-Nitro-3-phenyl-1H-indazole	1
5-Propoxy-2,2'-bipyridyl	1
5-Thiazoleethanol, 4-methyl-	1

6-[3,4-Dichlorophenyl]-N,N-dimethyl-1,2,4-triazin-3-amine	1
6H,12H-Indazolo[2,1-a]indazole-6,12-dione	1
6H-Dibenzo[b,d]pyran-1,9-diol, 6a,7,8,9,10,10a-hexahydro-6,6,9-trimethyl-3-pentyl-, [6aR-(6aà,9á,10aá)]-	1
6H-Dibenzo[b,d]pyran-6-one, 7,9-dihydroxy-3-methoxy-1-methyl-	1
6-Hydroxy-5-(3-methyl-butyl)-2-(2-morpholin-4-yl-ethylsulfanyl)-3-phenyl-3H-pyrimidin-4-one	1
6-Isoquinolinamine	1
6-Methoxycarbonyl-9-methyl-7-oxo-4,7-dihydro[1,2,4]-triazolo(3,4-c)[1,2,4]triazine	1
6-methylpyridine	1
6-Phenylisoquinoline	1
7,10-Methanofluoranthene, 8,9-dichloro-6b,7,8,9,10,10a-hexahydro-,(6bà,7á,8à,9á,10á,10aà)-	1
7,8-Dimethoxy-2-methyl-3H-pyrimido[4,5-b]quinolin-4-one	1
7á-Ethyl-8á-hydroxy-2,6-dimethylbicyclo[4.4.0]dec-1-ene	1
7-Azabicyclo[4,2,0]octan-8-one	1
7H-Benzo[c]furo[2,3-f][1]benzopyran, 2,7,7,10-tetramethyl-4-pentyl-	1
7-Methoxy-2,2,4,8-tetramethyltricyclo[5.3.1.0(4,11)]undecane	1
7-Propyl-cis-bicyclo[3.2.0]hept-6-en-2-one	1
8-C-á-d-[2-O-(E)-p-Coumaroyl]glucopyranosyl-2-[(R)-2-hydroxy]propyl-7-methoxy-5-methylchromone	1
8-Chloro-6-[2-piperidino-1-hydroxyethyl]-2-phenylquinoline	1
8-Methyl-5,6,7,8-tetrahydro-2,4-quinazolinedione	1
8-Phenylquinoline-6-carboxylic acid	1
9H-Carbazole, 9-ethyl-	1
9-Hexadecenoic acid, methyl ester, (Z)-	1
9H-Fluorene, 1,9-dimethyl-	1
9H-Purine	1
9-Octadecenamide, (Z)-	1
9-Octadecenoic acid, (E)-	1
à Isomethyl ionone	1
α,α,α',α'-Tetramethyl-1,4-benzenedimethanol	1
α,α-Methyl-2-deoxy-D-ribopyranoside	1
α-Alanine,N-hydroxy-N-[2,3-O-(1-methylethylidene)-5-O-	1

(triphenylmethyl)-α-d-ribofuranosyl]-, methyl ester	
Acetaldehyde, tetramer	1
Acetamide, N-(1-naphthyl)-2,2,2-trifluoro-	1
Acetamide, N-ethyl-	1
Acetic acid	1
Acetic acid, (2,4-dichlorophenoxy)-, 2-ethylhexyl ester	1
Acetic acid, (2,4-xylyl)-	1
Acetic acid, mercapto-, 2-methoxyethyl ester	1
Acetic acid, phenoxy-	1
Acetic acid, trichloro-, ethyl ester	1
Acetyl iodide	1
Adamantane-1-carboxamide, N-(4-amino-3-furazanyl)-	1
Adenosine	1
α-D-Glucopyranoside, 6-deoxy-à-Lmannopyranosyl	1
α-D-Glucopyranoside, methyl 2,3,4,6-tetra-O-methyl-	1
Alanine	1
Allyl dithioacetate	1
Allyl fluoride	1
Aluminum, tetraethylbis(æ-methylaminato)di-	1
Amine, N,N,N-tris(trimethylsiloxymethyl)-	1
Amitriptyline	1
Ammonium Chloride	1
Amphetamine PFP	1
Androstan-17-one, 3,16-bis(acetyloxy)-, (3α,5α,16α)-	1
Anthracen-9-one, 10-heptyl-10-hydroxy-	1
Azadirachtin, de[(E)-2-methyl-1-oxo-2-butenyl](1,2-dioxopropyl)dihydro-	1
Azetidine, 1-acetyl-2-methyl-	1
Benzaldehyde, 2,4-dihydroxy-6-methyl-	1
Benzaldehyde, 3-fluoro-4,5-dihydroxy-	1
Benzaldehyde, 4-benzyloxy-3-methoxy-2-nitro-	1
Benzamide, 4-allyloxy-N-(1-isochromenylmethyl)-	1
Benzamide, 4-fluoro-N-(3-ethylphenyl)-	1
Benzamide, 4-methyl-	1
Benzamide, N,N-diethyl-4-methyl-	1
Benzenamine, 2-iodo-	1
Benzene, (1-butylhexyl)-	1
Benzene, (1-propyldecyl)-	1

Benzene, (2,2-dimethylbutyl)-	1
Benzene, 1-(chloromethyl)-3-methoxy-	1
Benzene, 1-(chloromethyl)-4-methoxy-	1
Benzene,1,1'-(1,1,2,2,3,3-hexafluoro-1,3-propanediyl) bis[2,3,4,5,6-pentafluoro-	1
Benzene, 1,1'-(1,1,2,2-tetramethyl-1,2-ethanediyl)bis-	1
Benzene, 1,1'-(1-methylethylidene)bis[4-methoxy-	1
Benzene, 1,1'-sulfonylbis[2-methyl-	1
Benzene, 1,1'-thiobis[2,4,6-trinitro-	1
Benzene, 1,2,4-trimethyl-	1
Benzene, 1,3,5-trichloro-2,4,6-trimethyl-	1
Benzene, 1-bromo-2-methoxy- (2-Bromoanisole)	1
Benzene, 1-chloro-2-dimethoxymethyl-	1
Benzene, 1-fluoro-4-(2-methoxyethenyl)-, (Z)-	1
Benzene, 1-methoxy-4-(phenylethynyl)-	1
Benzene, 1-methyl-4-propyl-	1
Benzene, iodo-	1
Benzeneacetic acid, 4-(1,1-dimethylethyl)-	1
Benzeneacetic acid, 4-methoxy	1
Benzeneacetic acid, α-methyl-, methyl ester	1
Benzeneacetonitrile, 4-(1,2,3,6-tetrahydro-4-pyridinyl)-	1
Benzenebutanoic acid, 2,5-dimethyl-	1
Benzenecarbothioic acid,S-propyl ester	1
Benzeneethanol, α-bromo-	1
Benzenemethanamine, N-(phenylmethyl)-	1
Benzenemethanol, α-[1-(methylamino)ethyl]-	1
Benzenemethanol, α-methyl-à-(1-methyl-2-propenyl)-	1
Benzenemethanol, α-phenyl-	1
Benzenepropanoic acid, 2-pentyl ester	1
Benzenesulfin-p-anisidide	1
Benzenethiol, 2-(phenylamino)-	1
Benzenetridecanoic acid, 3-chloro-4-methoxy-, 2-decyl-3-methoxy-5-pentylphenyl ester	1
Benzhydrazide, 3-methyl-N2-[1-methyl-2-(5-methyl-3-nitro-1-pyrazolyl)ethylideno]-	1
Benzhydrazide, 4-[4-(4-methoxyphenyl)-5-methylthiazol-2-ylamino]-	1
Benzo[1,2-b:5,4-b']difuran-4,8-dione, 5-methyl-2-(1-	1

methylethenyl)-	
Benzo[b][1,5]-naphthyridine, 4-chloro-	1
Benzo[b]1,4-dioxine-6,7-diamine, 2,3-dihydro-	1
Benzofuran, 2,3-dihydro-	1
Benzofuran, 4,5,6,7-tetrahydro-3,6-dimethyl-	1
Benzoic acid, 1-methylethyl ester	1
Benzoic acid, 2-(6-phenanthridinyl)-, methyl ester	1
Benzoic acid, 2-(acetyloxy)-, methyl ester	1
Benzoic acid, 2,3,4,5-tetrafluoro-, methyl ester	1
Benzoic acid, 2,6-bis(trimethylsiloxy)-, methyl ester	1
Benzoic acid, 2,6-dichloro-	1
Benzoic acid, 2-amino-, ethyl ester	1
Benzoic acid, 2-amino-, methyl ester	1
Benzoic acid, 2-benzoyl-	1
Benzoic acid, 2-ethyl-6-hydroxy-, methyl ester	1
Benzoic acid, 2-methoxy-	1
Benzoic acid, 3-(5-chloro-2-methoxybenzoyl)-4-hydroxy-	1
Benzoic acid, 3,5-dichloro-2,4-dihydroxy-6-pentyl-, 4-carboxy-3-methoxy-5-pentylphenyl ester	1
Benzoic acid, 4-(1-methylethyl)-	1
Benzoic acid, 4-(4-butylcyclohexyl)-, 2,3-dicyano-4-ethoxyphenyl ester	1
Benzoic acid, 4-(4-pentylcyclohexyl)-, 4'-cyano[1,1'-biphenyl]-4-yl ester	1
Benzoic acid, 4-(4-propylcyclohexyl)-, 4'-cyano[1,1'-biphenyl]-4-yl	1
Benzoic acid, 4-fluoro-, 2-oxo-2-phenylethyl ester	1
Benzoic acid, 4-methyl-	1
Benzoic acid, methyl ester	1
Benzoic,acid,thio-,S-(2-methoxy-ethyl)ester	1
Benzothiazole, 2-(methylthio)-	1
Benzyl butyl phthalate	1
Benzyl chloride	1
Bicyclo[2.2.2]oct-2-ene, 1,2,4,5,5,6,6-heptafluoro-3-methoxy-	1
Bicyclo[3.2.0]hepta-2,6-diene, 5-chloro-	1
Bis(3-chloro-1-propyl)(1-chloro-2-propyl)phosphate	1
Bis(N-methoxy-N-methylamino)methane	1

Bis(trifluoromethyl)fluorophosphine	1
Bismuthine, tripropyl-	1
Bis-S-triazolo[4,3-b,3',4'-f]pyridazine, 3,3'-dimethyl	1
Borane, methanetetrayltetrakis[difluoro-	1
Boric acid, triphenyl ester	1
Butabarbital	1
Butanal	1
Butanamide	1
Butane, 1,2,4-trimethoxy-	1
Butanoic acid	1
Butanoic acid, 2-(pentafluoropropionylamino)-, isopropyl ester, L-	1
Butanoic acid, 2-ethyl-, 1,2,3-propanetriyl ester	1
Butanoic acid, tributylsilyl ester	1
Caffeine	1
Capparisinine	1
Caprolactam	1
Carbamazepine-10,11-dibromo-	1
Carbamic acid, methyl ester	1
Carbamodithioic acid, dimethyl-, bis(anhydrosulfide) with methylarsonodithious acid	1
Carbomethoxysulfenyl ethyltrithiocarbonate	1
Carbon dioxide	1
Carbonic acid, 3-hexenyl methyl ester, (Z)-	1
Carbonic acid, phenyl ester, ester with methyl p-hydroxybenzoate	1
Carbonodithioic acid, S,S'-(diphenylmethylene) O,O'-diethyl ester	1
Carbonotrithioic acid, bis(trifluoromethyl) ester	1
Carbonotrithioic acid, diethyl ester	1
Carbostyril, 3-ethyl-4-hydroxy-7-methoxy-	1
Cherylline, 2-(p-bromobenzoyl)-2-demethyl-O,O-dimethyl-	1
Chirald	1
Cholest-5-en-3-ol (3α)-	1
Cholest-5-en-3-ol (3α)-, trifluoroacetate	1
Cholesta-4,6-dien-3-ol, (3α)-	1
Cholestan-3-one, (5α)-	1
Cholesterol	1

Chromium, bis[(1,2,3,4,5,6-ü)-1,1'-biphenyl]-	1
Cinoxate	1
cis-9,10-Epoxyoctadecanamide	1
Clorophene	1
Clozapine	1
Cobalt, (ü5-2,4-cyclopentadiene-1-yl)[(1,2,3,3a,7a-ü)-1H-inden-1-yl]-	1
Cobalt, cyclopentadienyl-(cyclopenta-1,3-diene)	1
Cobalt, di-æ-chlorotetranitrosyldi-	1
Cocaine	1
Crotonic acid, o-formylphenyl ester	1
Cyanogen chloride	1
Cyclic octaatomic sulfur	1
Cyclizine	1
Cyclobuta[1,2-d:3,4-d']bis[1,3]dioxole, tetrahydro-, (3aα,3bβ,6aα,6bβ)-	1
Cyclobuta[de]naphthalene	1
Cyclobutanecarboxylic acid, 2-tetrahydrofurylmethyl ester	1
Cyclobutanone, 2,3,3-trimethyl-	1
Cyclobutanone, 2-tetradecyl-	1
Cyclohexane, decyl-	1
Cyclohexanecarboxylic acid, 1-amino-	1
Cyclohexanemethanol, α,α,4-trimethyl-, cis-	1
Cyclohexanone, 2-(2-chlorophenyl)-2-(methylamino)-, (ñ)-	1
Cyclohexene, 3,3,5,5-tetramethyl-1-(trimethylsilyloxy)-	1
Cyclohexene, 3-methyl-6-(1-methylethylidene)-	1
Cyclopentane-1,2-dicarboxylic acid dipiperidide	1
Cyclopentaneacetic acid, 3-oxo-2-pentyl-, methyl ester	1
Cyclopropene, 1-chloro-2,3,3-trifluoro-	1
Decanoic acid, 2,2-bis[[(1-oxodecyl)oxy]methyl]-1,3-propanediyl ester	1
Decanoic acid, 4-oxo-	1
Dehydroacetic Acid	1
Desmethyltramadol, O-	1
Dextrorphan	1
D-Glucopyranoside, 4-O-decyl-	1
D-Glucose, 3-O-[6-deoxy-α-Lmannopyranosyl]-	1
Di(pentamethylphenyl)ketone	1

Dibutyl phthalate	1
Dichlorophenoxy methyl acetate, 2,4-	1
Diclofenac	1
Diethylene glycol dibenzoate	1
Diethylene glycol monododecyl ether	1
Diethyltoluamide	1
Difluorophosphoric acid	1
Dihydrocodeine Bitartrate	1
Dimethyl trimethylsilylmethylphosphonate	1
Dimethyl Sulfone	1
Dimethyl-(allyl)-silyloxybenzene	1
Dimethylphosphinic fluoride	1
di-p-Tolyl sulfone	1
Dipyrrolo[1,2-a:-1',2'-d]pyrazine-5,10-dione, octahydro-2,7-dihydroxy-	1
Disilane, hexakis(4-methylphenyl)-	1
Dixyrazine	1
dl-2-Benzylaminooctanol	1
dl-7-Azatryptophan	1
Dodecanamide	1
Dodecanamide (Lauramide)	1
Dodecanoic acid, 3-hydroxypropyl ester	1
Dodecanoic acid, ethenyl ester	1
Dodecanoic acid, methyl ester	1
Dothiepin	1
d-Ribo-tetrofuranose, 4-c-cyclopropyl-1,2-O-isopropylidene-, àα-	1
Epicholestanol	1
Ergosta-5,24-dien-3-ol, acetate, (3α)-	1
Ethane, 1,1,2,2-tetrafluoro-	1
Ethane-1,1-diol dibutanoate	1
Ethaneperoxoic acid, 1-cyano-1,4-diphenylpentyl ester	1
Ethanol, 1-(2-butoxyethoxy)-	1
Ethanol, 1-(2-methyl-2H-tetrazol-5-yl)-2-[(thiophen-2-ylmethyl)amino]-	1
Ethanol, 2-(2-butoxyethoxy)-	1
Ethanol, 2-(2-ethoxyethoxy)-	1
Ethanol, 2-(2-methoxyethoxy)-	1

Ethanol, 2-(dibutylamino)-	1
Ethanol, 2-(dodecyloxy)-	1
Ethanol, 2-butoxy-	1
Ethanone, 1-(2,4,6-trihydroxyphenyl)-	1
Ethanone, 1-(2,6-dihydroxy-4-methoxyphenyl)-	1
Ethanone, 1-(5,6,7,8-tetrahydro-3,5,5,6,8,8-hexamethyl-2-naphthalenyl)- (Tonalide)	1
Ethanone, 1-(5-methoxy-2-methyl-3(1H)-indolyl)-	1
Ethanone, 1,1'-(1,4-phenylene)bis-	1
Ethanone, 1,1'-(6-methoxy-2,5-benzofurandiyl)bis-	1
Ethanone, 1-[4-(1,1-dimethylethyl)phenyl]-	1
Ethenetricarbonitrile, (2,4,6-trimethylanilino)-	1
Ethenetricarbonitrile, 3,4-xylidino-	1
Ether, α,α-dimethylbenzyl bis(trifluoromethyl)methyl	1
Ethyl 2-isocyanatopropionate	1
Ethyl 4-(ethyloxy)-2-oxobut-3-enoate	1
Ethyl N-tert-butylformimidate	1
Ethyl Vanillin	1
Ethylamine, 2-((p-bromo-α-methyl-α-phenylbenzyl)oxy)-N,N-dimethyl-	1
Ethylamine, N,N-bis(trifluoromethyl)-2-(trifluorosilyl)-	1
Ethylamine, N,N-dinonyl-2-(2-thiophenyl)-	1
Ethylamine, N-heptyl-N-octyl-2-(2-thiophenyl)-	1
Ethylene brassylate	1
Ethylene glycol monoisobutyl ether	1
Ethylene oxide	1
Ethylenediamine, N-(p-fluorophenyl)-N,N'-dimethyl-N'-phenyl-	1
Ethylheptavinyloctasilsesquioxane	1
Ethylvinyl sulfide	1
Formamide	1
Formamide, N,N-diethyl-	1
Formamide, N-methyl-	1
Fosfosal	1
Fumaric Acid	1
Furan, 2-(methoxymethyl)-	1
Furan, 2,2'-[1,2-ethanediylbis(oxy)]bis[tetrahydro-5-(2-methoxy-4-methylphenyl)-5-methyl-	1

Furan-2-carboxamide, N-(2-fluorophenyl)-	1
Furo[2,3-b]quinolin-4(9H)-one, 7,8-dimethoxy-9-methyl-	1
Glucose propylglycoside tetraacetate	1
Glycerol tricaprylate	1
Guaifenesin di-tms derivative	1
Guanidine, N-(4-fluorophenyl)-	1
Guanidine, N,N-dimethyl-	1
Heptyl ethylphosphonofluoridate	1
Hexadecanamide	1
Hexadecanoic acid propyl ester	1
Hexadecanoic acid, methyl ester	1
Hexadecanoic acid, methyl ester	1
Hexanamide (Caproamide)	1
Hexanedioic acid, bis(2-ethylhexyl) ester	1
Hexanedioic acid, bis(2-methylpropyl) ester	1
Hexanedioic acid, dicyclohexyl ester	1
Hexanedioic acid, mono(2-ethylhexyl)ester	1
Hexanoic acid, 2-ethyl-, ethyl ester	1
Hexanoic acid, 4-methyl-	1
Homosalate	1
Hydrazine, 1,1-diethyl-2-(1-methylpropyl)-	1
Hydrazine, 1,2-dibutyl-	1
Hydrazine, 2-[fluorobis(1-methylpropyl)silyl]-1,1-dimethyl-	1
Hydrocodone	1
Hydroxymethyl 2-hydroxy-2-methylpropionate	1
Ibuprofen	1
Imidazo[2,1-a]isoquinoline	1
Imidazo[2,1-c]1,2,4-triazine, 1,4-dihydro-3-(4-methylphenyl)-6,7-diphenyl-	1
Imidazo[4,5-e][1,4]diazepine-5,8-dione, 1,4,6,7-tetrahydro-	1
Imidazolidine, 1,3-dimethyl-2-(4-pyridyl)-	1
Indeno[3a,4-b]oxiren-2-ol, octahydro-4a-methyl-5-[(tetrahydro-2H-pyran-2-yl)oxy]-, (1aα,2α,4aα,5α,7aS*)-	1
Indole	1
Iodoacetylene	1
Iridium, [2-(diphenylphosphino)phenyl-C,P]bis(triphenylphosphine)-,	1

Isobutyric acid 3,5-dichloro-2,6-dimethyl-4-pyridyl ester	1
Isoparvifuran	1
iso-Pentanal N-methyl-N-formylhydrazone	1
Isopropyl Myristate	1
Isopropyl stearate	1
Isothiourea, 2-methyl-1-(2,4-dimethylphenyl)-3-(1,1-dimethyl-2-propynyl)-	1
Isoxazolo[4,3-a]phenazine, 1-phenyl-	1
Ketone, methyl 2-methyl-1,3-oxothiolan-2-yl	1
L-Glucose, 6-deoxy-3-O-methyl-	1
Lilial	1
L-Valine	1
Malonamide, 2-(propylamino)-N,N'-diheptyl-N,N'-dimethyl-	1
Malononitrile, 2-phenylazo-	1
m-Aminophenylacetylene	1
Mequinol	1
Metacetamol	1
Methadone N-oxide	1
Methanamine	1
Methane, dimethoxy-	1
Methane, isocyanato-	1
Methane, trimethoxy-	1
Methanesulfonic anhydride	1
Methanethiol	1
Methanol, (1-ethyl-2-benzimidazolyl)(2-methoxyphenyl)-	1
Methanol, chloro-, acetate	1
Methanone, (4,5-dihydro-3,5-diphenyl-4-isoxazolyl)phenyl-	1
Methyl 2,3,4-tri-O-methyl-6-deoxy-α-D-mannopyranoside	1
Methyl 2-[2-(4-chlorophenyl)-5-methyl-1H-imidazol-1-yl]dithiobenzoate	1
Methyl 2α-carboxymethyl-3α-hydroxy-nor-A(1)-lup-20(29)-en-28-oate	1
Methyl 2-ethyl hexylphthalate	1
Methyl 2-ethyldecanoate	1
Methyl 4,4-dichlorobutanoate	1
Methyl 4-methyl-4-nitroso-2-trimethylsiloxy-pentanoate	1
Methyl N-(thioformyl)dithiocarbamate	1
Methyl n-hexyl ketone-1-phenyl-1,2-ethanediol ketal 1	1

Methyl salicylate	1
Methyl(methyl-4-deoxy-2,3-di-O-methylαl-threo-hex-4-enopyranosid)uronate	1
Methyl(methyl-4-deoxy-2-O-methylαl-threo-hex-4-enolpyranosid)uronate	1
Methyl(methyl-4-deoxyαl-threo-hex-4-enopyranosid)uronate	1
Methylene fluoride	1
Methylglyoxal	1
Methyltris(trimethylsiloxy)silane	1
Mirtazapine	1
m-Methoxybenzoic acid, hexadecyl ester	1
morpholine	1
Morpholine, 4-(3-methylcyclohex-1-enyl)-	1
Myristic acid, 2,3-bis(trimethylsiloxy)propyl ester	1
N-(1,1-Dimethyl-2-propynyl)-N,N-dimethylamine	1
N-(2,3,4,5,6-Pentafluorobenzyl)piperidine	1
N-(4-Aminophenyl)-N'-phenyl-urea	1
N-(5-Oxo-6-trifluoromethyl-2,3,5,6-tetrahydro-imidazo[2,1-b]thiazol-6-yl)-2-phenyl-acetamide	1
N,3-Diethyl-3-nonanamine	1
N,N',N'',N'''-Tetrakis(trifluoroacetyl)arginine	1
N,N-Dimethyl-1-propanamine	1
N,N'-Dimethyl-N,N'-dioctadecyl-ethane-1,2-diamine	1
N-[2-(4-Methylphenylthio)ethyl]alanine	1
N-[4-Methoxy-3-methoxycarbonyl)benzoyloxy]succininide	1
N-Acetyl-d-threo-O-methylthreonine	1
Naphthalen-1,4-imine-2,3-dicarboxylic acid, 5,6,7,8-tetrachloro-9-(1,1-dimethylethyl)-1,4-dihydro-, dimethyl ester	1
Naphthalene, 1,2-dihydro-1,1,6-trimethyl-	1
Naphthalene, 1,7-dimethoxy-	1
Naphthalene, 1-isothiocyanato-	1
Naphtho[1,2-b]furan-2,6(3H,4H)-dione, 3a,5,5a,9,9a,9b-hexahydro-9-hydroxy-3,5a,9-trimethyl-	1
Naphtho[1,2-b]furan-2,8(3H,4H)-dione, octahydro-3,5a,9-trimethyl-, [3S-(3α,3aα,5aα,9α,9aα,9bα)]-	1
Naphtho[2,1-b]furan-2(1H)-one, decahydro-3a,6,6,9a-	1

tetramethyl-, [3ar-(3aα,5aα,9aα,9bα)]-	
N-Ethyl-4-hydroxypiperidine	1
n-Hexadecanoic acid (Palmitic acid)	1
n-Hexyl-6-methoxy-4-methyl-8-quinolinamine	1
Nickel tetracarbonyl	1
N-Methylpyrrole-2-carboxylic acid	1
N-Nitroso diethanolamine	1
Nonane, 1-iodo-	1
Norvenlafaxine	1
n-Pentanal N-methyl-N-formylhydrazone	1
n-Propyl benzoate	1
O-Acetylprzewaquinone b	1
Obtusenol	1
Octadecanamide	1
Octadecanenitrile	1
Octadecanoic acid (Stearic acid)	1
Octadecanoic acid, methyl ester	1
Octane, 2,7-dimethyl-	1
Octanoic acid, 4-nitrophenyl ester	1
Octanoic acid, 5-(acetyloxy)-, ethyl ester	1
Octyldimethylsilyloxybenzene	1
O-Methyl,bis(O-1,2,2-trimethylpropyl) phosphate	1
Oxalic acid, monoamide, N-(2-ethylphenyl)-, heptyl ester	1
Oxamide, N-(3-methoxypropyl)-N'-cycloheptylidenamino-	1
oxyoctanoic acid	1
p-((Dimethylcarbamoylmethyl)amino)-N,N-dimethylbenzamide	1
Pempidine	1
Pent-1-en-3-one, 1-amino-4,4-dimethyl-1-(3-pyridyl)-	1
Pentanamide, 2-(dimethylamino)-3-methyl-N-[3-(1-methylethyl)-7-(2-methylpropyl)-5,8-dioxo-2-oxa-6,9-diazabicyclo[10.2.2]hexadeca-10,12,14,15-tetraen-4-yl]-, [3R-[3R*,4S*(2S*,3S*),7S*]]-	1
Pentane, 1-bromo-5-methoxy-	1
Pentane,-2,2-bis(2-[5-methylfuryl-])-5-nitro-	1
Pentanedioic acid, (2,4-di-t-butylphenyl) mono-ester	1
Pentanedioic acid, dimethyl ester	1
Pentanoic acid, 2-acetyl-4-methyl-, methyl ester	1

Pentanoic acid, 4-oxo-,	1
Pentanoic acid, 5-hydroxy-, 2,4-di-t-butylphenyl esters	1
Pentasiloxane, dodecamethyl-	1
Perfluoropropane	1
Perhydro-histrionicotoxin, 1-methyl-2-depentyl-, acetate	1
Phenanthrene, 3,6-dimethoxy-9,10-dimethyl-	1
Phenol, 2,4-bis(1-methyl-1-phenylethyl)-	1
Phenol, 2,6-bis(1,1-dimethylethyl)-	1
Phenol, 2,6-dimethoxy-4-(2-propenyl)-	1
Phenol, 2-bromo-4-(1,1-dimethylethyl)-	1
Phenol, 2-methoxy-	1
Phenol, 3,4-dimethyl-	1
Phenol, 4-amino-2,5-dimethyl-	1
Phenol, 4-bromo-	1
Phenol, 4-ethyl-2-methoxy-	1
Phenol, p-(2-methyl-4-thiazolyl)-	1
Phenylethyl Alcohol	1
Phenytoin	1
Phosphine, 1,2-ethanediylbis[dicyclohexyl-	1
Phosphinic acid, diethyl-, methyl ester	1
Phosphonic acid, methyl-, dipentyl ester	1
Phosphonic acid, pentyl-, diethyl ester	1
Phosphonofluoridothioic hydrazide, P-ethyl-2,2-dimethyl-	1
Phosphoric acid, 2-chloroethenyl dimethyl ester	1
Phosphoric acid, bis(trimethylsilyl)monomethyl ester	1
Phosphoric acid, diethyl pentyl ester	1
Phosphoric acid, isodecyl diphenyl ester	1
Phosphoric acid, tris(2-ethylhexyl) ester	1
Phosphorochloridic acid, dimethyl ester	1
Phthalic acid, decyl 2-pentyl ester	1
Phthalic acid, di(3-chlorophenyl) ester	1
Phthalic acid, monoamide, N-ethyl-N-(3-methylphenyl)-, heptyl ester	1
Phthalic acid, nonyl 4-octyl ester	1
Phthalic anhydride	1
Piperidin-2-one-5-carboxylic acid, 5,6-didehydro-, methyl(ester)	1
Piperidine	1

Piperidine, 1,2-dimethyl-	1
Piperidine-2,5-dione	1
Pregn-16-en-20-one, 3,18-bis(acetyloxy)-14,15-epoxy-, (3α,5α,14α,15α)-	1
Primidone	1
Proline, 3-hydroxy-4-methyl-	1
Propan-2-one, 1-(3-nitro-[1,2,4]-triazolo[3,2,-c][1,2,4]-triazol-1-yl)-	1
Propan-2-one, 1-(4-isopropoxy-3-methoxyphenyl)-	1
Propanal, butylhydrazone	1
Propanamide, N-(4-ethoxyphenyl)-	1
Propane, 1-(chloromethoxy)-2-methyl-	1
Propane, 1,1,3,3-tetramethoxy-	1
Propanedioic acid, dimethyl ester	1
Propanoic acid, 2-(4-chloro-2-methylphenoxy)- (Mecoprop)	1
Propanoic acid, 2-methyl-	1
Propanoic acid, 2-methyl-, 2,2-dimethyl-1-(2-hydroxy-1-methylethyl)propyl ester	1
Propanoic acid, 2-methyl-, 2-ethyl-3-hydroxyhexyl ester	1
Propanoic acid, 2-methyl-, 3-hydroxy-2,4,4-trimethylpentyl ester	1
Propanoic acid, 2-methyl-, methyl ester	1
Propenoic acid, 3-[3,5-di-t-butyl-4-hydroxyphenyl]-	1
Propionic acid, 3-(butylthio)-, methyl ester	1
Propylhexadrine, n-heptafluorobutyryl deriv.	1
Protriptyline, N-acetyl-	1
p-tert-Butyl cyclohexyl-acetate cis	1
Pyridine, 2,5-dimethyl-	1
Pyridine, 3-(ethylthio)-	1
Pyridine, 3-[1-(2-propynyl)-2-piperidino]-	1
Pyridine, 3-methoxy-	1
Pyridine, 3-trimethylsiloxy-	1
Pyridine-3-carboxamidoxime	1
Pyrido[1,2-a]benzimidazolium, 1,2,3,4-tetrahydro-5-(1,2,3,4-tetrahydro-6-hydroxy-1,3-dimethyl-2,4-dioxo-5-pyrimidinyl)-, hydroxide, inner salt	1
Pyrido[2,3-d]pyridazine-5(6H)-thione	1
Pyrilamine	1

Pyrimido[1,6-a]indole, 7-chloro-1,2,3,4-tetrahydro-2,5-dimethyl-	1
Pyrolo[3,2-d]pyrimidin-2,4(1H,3H)-dione	1
Pyrrole	1
Pyrrolidine, 1,1'-methylenebis-	1
Pyrrolo[3,4-f]isoindole-1,3,5,7-tetraone, 2,6-di(pyridin-4-yl)-	1
Quinoline, 4-(2-hydroxy-2-methoxy-1-thioxoethyl)-2-phenyl-	1
Quinoxaline, 5,8-dimethoxy-6-((2-(dimethylamino)ethyl)amino)-	1
Salsalate	1
Sarin	1
S-Ethyl S-(2-diisopropylaminoethyl) methylphosphonodithioate	1
Silabenzene,1-methyl-	1
Silacyclopen-2-ene, 1,1-difluoro-	1
Silanamine, N-[2,6-dimethyl-phenyl]-1,1,1-trimethyl-	1
Silane, (1,1-dimethylethyl)(hexadecyloxy)dimethyl-	1
Silane, (diphenylmethoxy)trimethyl-	1
Silane, (diphenylmethyl)trimethyl-	1
Silane, [(3,7,11,15-tetramethyl-2-hexadecenyl)oxy]trimethyl-	1
Silane, [(dimethylsilyl)methyl]trimethyl-	1
Silane, [[(3α,5α)-cholestan-3-yl]oxy]trimethyl-	1
Silane, [[(3α,5α,20S)-pregnane-3,20-diyl]bis(oxy)]bis[tripropyl-	1
Silane, [[4-(7-methoxyheptyl)-5-(3-methyl-2-butenyl)-1,3-cyclopentanediyl]bis(oxy)]bis[trimethyl-, (1α,3α,4α,5α)-	1
Silane, [1,4-phenylenebis(oxy)]bis[trimethyl-	1
Silane, 1,3-decadiynyltrimethyl-	1
Silane, dimethyl(octadecyloxy)propyl-	1
Silane, methoxytrimethyl-	1
Silane, methylenebis[dimethyl-	1
Silane, trimethyl(2-methyl-2,4-cyclopentadien-1-yl)-	1
Silane, trimethyl(3-methyl-1-butynyl)-	1
Silanol, allyldimethyl-	1
Silanol, trimethyl-	1

Silanol, trimethyl-, 2-aminobenzoate	1
Silicic acid, diethyl ester	1
Stearyltrimethylammonium chloride	1
s-Triazine, 2-amino-4-(morpholinomethyl)-6-piperidino-	1
S-Triazolo(1,5-a)pyrimidine, 5-methyl-7-ethylamino-	1
Sulfonyl-bis[8-methylthiophylline	1
Sulfoximine, S-methyl-S-(1-oxohexyl)-S-phenyl-	1
t-Butyldiphenyl(prop-2-ynyloxy)silane	1
Tetracosanoic acid, methyl ester	1
Tetradecanoic acid, tetradecyl ester (Myristyl Palmitate)	1
Tetrakis(pentafluorobenzoyl)-hydrazine	1
Tetrasulfide, dimethyl	1
Thiazolidine-4-carboxylic acid	1
Thiophene, 2-hexyl-	1
Thiophene, 3-(1,1-dimethylethyl)-	1
Thiophenetetracarbonitrile	1
Thiosalicylic acid	1
Thiourea, N,N'-dimethyl-	1
Thorium, tetrakis(2,4-pentanedionato-O,O')-, (SA-8-11''11''1'1'''1'1''')-	1
threo-2,5-Dimethyl-2-(2-methyl-2-tetrahydrofuryl)tetrahydrofuran	1
Tocopherol-ç-tms-derivative (high mass adjustment=100%)	1
Tributyl acetylcitrate	1
Tricosanoic acid, tert-butyldimethylsilyl ester	1
Tricyclo[4.4.0.0(2,5)]dec-8-ene, 1,2,3,3,4,4,5,6-octafluoro-	1
Triethyl phosphate	1
Triethylene glycol monododecyl ether	1
Trifluoromethyldisulfane	1
Triisopropylsilyloxycyclobutane	1
Trimethyl(4-tert.-butylphenoxy)silane	1
Trimethylene oxide	1
Trimethylsilyloxycyclobutane	1
Trisiloxane, octamethyl-	1
Tritriacontan-3-one	1
Urea, ethyl-	1
Vanillin	1
Xanthene, 9,9-dimethyl-	1

xanthine, 1,3,7,8-tetramethyl- (Methylcaffeine)	1
Zirconium, tetrakis(2,4-pentanedionato-O,O')-	1